The Geology of New Mexico, A Geologic History, New Mexico Geological Society, p. 203–248.

Ken - Best wishes. Steve

LARAMIDE OROGENY IN CENTRAL AND NORTHERN NEW MEXICO AND SOUTHERN COLORADO

STEVEN M. CATHER
New Mexico Bureau of Geology and Mineral Resources
New Mexico Institute of Mining and Technology
Socorro, NM 87801; *steve@gis.nmt.edu*

INTRODUCTION

The Laramide orogeny was a profound tectonic episode that produced varying degrees of structural disruption throughout the Rocky Mountain-Colorado Plateau area during late Campanian through Eocene time. The stratigraphy of Laramide intraforeland basins and the structure of intervening uplifts have been studied for more than a century. With the advent of seismic reflection profiling and widespread deep drilling during the past several decades, the data base for interpretation of Laramide deformational processes and basin evolution has improved markedly, especially in the Wyoming region. Knowledge of the nature of deformation in the southern Rocky Mountains, however, has lagged behind that of other areas of the Laramide foreland, primarily due to relatively less petroleum exploration (except in the San Juan Basin) and to the complicating effects of middle to late Tertiary volcanism and rifting.

This chapter is an appraisal of our state of knowledge about the Laramide orogeny in central and northern New Mexico and southern Colorado. I will attempt to synthesize the Laramide stratigraphic and structural development of this region, at the same time pointing out topics in need of further study and those whose interpretation remains controversial. The main goals of this paper are: (1) summarize the inception and evolution of Laramide basins in the study area, (2) describe the timing and style of deformation of Laramide uplifts, (3) outline major ongoing controversies regarding the roles of strike-slip faulting and slip partitioning in Laramide deformation, and (4) synthesize the Laramide tectonostratigraphic evolution of central and northern New Mexico and southern Colorado.

LARAMIDE BASIN EVOLUTION

Six basins of Laramide age occur within the study area. These are the San Juan, Raton, Galisteo-El Rito, Baca, Carthage-La Joya and Sierra Blanca Basins (Figs. 1, 2). A thorough discussion of the stratigraphy of each basin is beyond the scope of this report, except where it is necessary to clarify varying use of nomenclature among workers. As will be described below, the Laramide stratigraphic successions in northern and central New Mexico consist of three parts that are separated from one another by regional unconformities. The first two episodes of sedimentation (middle Campanian-early Maastrichtian and latest Maastrichtian-middle Paleocene) occurred only in the San Juan and Raton Basins. The final phase of Laramide sedimentation (Eocene) is represented in all the basins of the study area. Episodes of Laramide sedimentation are inferred to result mostly from tectonism because the duration of individual episodes is far longer than would be expectable in Milankovitch-type climatic cycles, the thickness of resultant deposits greatly exceeds that which might result from eustatic base-level changes, and basins show syntectonic relationships to adjacent uplifts.

To illustrate the episodic nature of Laramide sedimentation, I have used well data to calculate rates of stratal accumulation for areas at or near the depositional axis of the Raton and San Juan Basins (Fig. 3). Note that these stratal accumulation curves reflect present-day stratal thicknesses and have not been corrected for compaction. Compaction calculations require data concerning the thickness of overburden that has been removed from the basins during middle and late Tertiary erosion; these values are presently poorly constrained. One previously published well log was chosen from the axial part of each basin, and formation tops were picked by the writer and B. S. Brister using geophysical logs. Our picks are substantially the same as those of earlier researchers. For the San Juan Basin, we examined electric logs from the Aztec Oil and Gas Company Trail Canyon No. 1 well (Table 1; well 114 of Molenaar, 1983); for the Raton Basin, we utilized the Odessa Natural Corporation-Maguire Oil Co. W. S. Ranch well No. 2 (Table 2; Woodward, 1984).

To calculate stratal accumulation rates, we identified geophysically distinct strata in these wells to which age determinations could be assigned (Tables 1, 2). Particularly useful were the $^{40}Ar/^{39}Ar$ age determinations for biozones in Upper Cretaceous marine strata by Obradovich (1993). Because high-precision dates from bentonites and dated biozones are available for Turonian through Campanian strata, stratal accumulation rates calculated for Upper Cretaceous units are generally better constrained than those for Paleogene continental successions.

San Juan Basin

Today, the San Juan Basin has the form of an asymmetrical syncline with an arcuate axis that is bowed to the north (Fig. 4). It has abrupt structural margins on the northwest (Hogback monocline), northeast (southwest limb of the Archuleta Anticlinorium) and east (Nacimiento Uplift). The southern part of the basin is a gentle north-dipping structural incline, the Chaco homocline (Chaco slope of previous workers). The Chaco homocline adjoins the north flank of the Zuni uplift (Fig. 1), which bounds the basin on the south. The toe of the Chaco homocline is a faulted hingeline (Ayers et al., 1994) that separates the homocline from the gently folded, relatively flat-lying floor of the basin.

Inception and early phase of subsidence

From Turonian to early Campanian time (~95–80 Ma), the San Juan Basin occupied a small part of the Western Interior Basin, a broad foreland basin that, in part, subsided in response to the effects of tectonic loading in the Cordilleran thrust belt to the west (e.g., Lawton, 1988). During this time interval, stratal accumulation rates for the Mancos Shale, Point Lookout Sandstone, and Menefee Formation in the axial part of the San Juan Basin ranged from ~26–60 m/m.y. (Fig. 3). The thickness of the Mancos Shale in the axial part of the San Juan Basin (643 m; Table 1) is closely similar to the Mancos thickness near Mesa Verde National Park (682 m; Leckie et al., 1997), nearby to the northwest of the basin

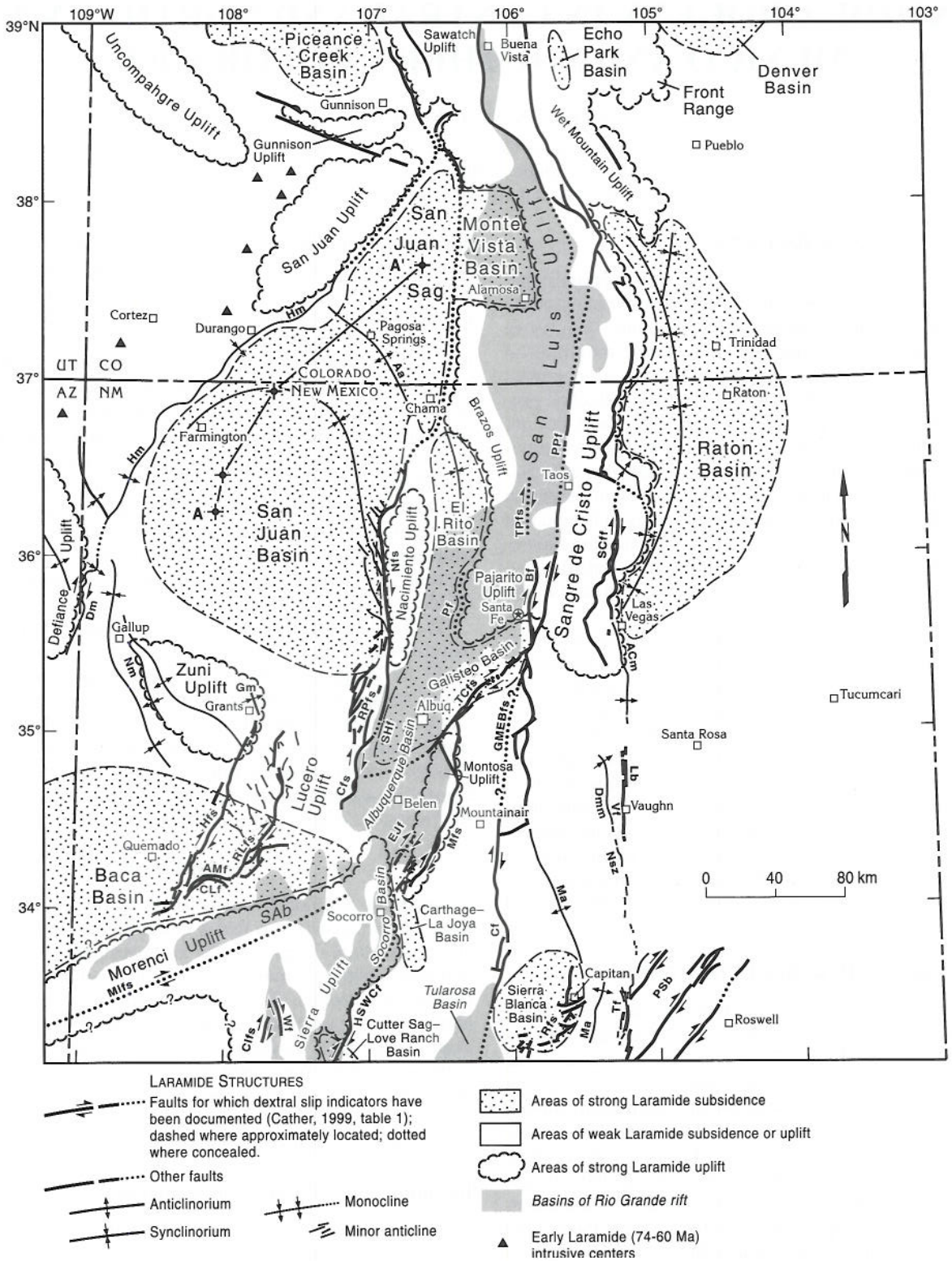

FIGURE 1. Map showing Laramide uplifts, basins, and selected structures, and Rio Grande rift basins. Laramide structures are: **Aa**, Archuleta Anticlinorium; **AMf**, Alegres Mountain fault; **ACm**, Anton Chico monocline; **Bf**, Borrego fault; **Clfs**, Chloride fault system; **Cf**, Chupadera fault; **Cfs**, Comanche fault system; **CLf**, Cox Lake fault; **Dm**, Defiance monocline; **Dmm**, Derramadera monocline; **EJf**, East Joyita fault; **GMEBfs**, Glorieta Mesa-Estancia Basin fault system; **Gm**, Grants monocline; **Hfs**, Hickman fault system; **Hm**, Hogback monocline; **HSWCf**, Hot Springs-Walnut Canyon fault; **Lb**, Leon buckle; **Ma**, Mescalero arch; **Mfs**, Montosa fault system; **Mlfs**, Morenci lineament fault system; **Nfs**, Nacimiento fault system; **Nsz**, Nalda shear zone; **Nm**, Nutria monocline; **Pf**, Pajarito fault; **PSb**, Pecos Slope buckles; **PPf**, Picuris-Pecos fault; **RLfs**, Red Lake fault system; **RPfs**, Rio Puerco fault system; **Rfs**, Ruidoso fault system; **SHf**, Sand Hill fault; **SCff**, Sangre de Cristo frontal faults; **TCfs**, Tijeras-Cañoncito fault system; **Tf**, Tinnie fold belt; **TPfs**, Tusas-Picuris fault system; **Vf**, Vaughn fault; **Wf**, Winston fault; **A–A'** is line of section for Figure 5; **Sab**, San Agustin Basin of Rio Grande rift. Map has not been restored palinspastically. Evidence for oblique-slip on structures is summarized by Cather (1999a, table 1).

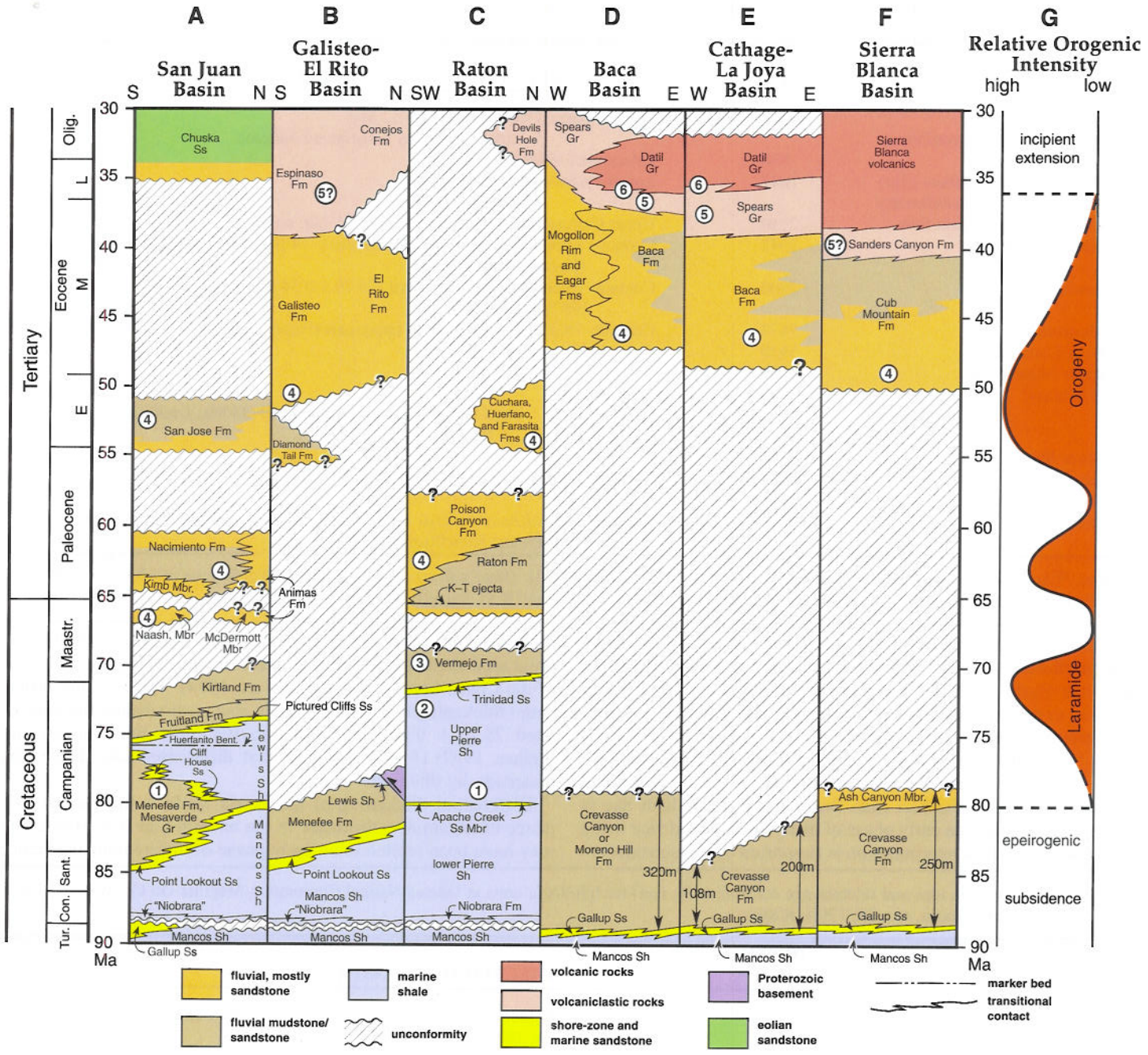

FIGURE 2. Stratigraphic columns and interpreted relative orogenic activity for Laramide basins in central and northern New Mexico and southern Colorado during late Turonian through early Oligocene (90–30 Ma). **A**, San Juan Basin. Abbreviations are: **Naash. Mbr**, Naashoibito Member of Ojo Alamo Sandstone and equivalent units (Unit B of Baltz, 1967, and Smith, 1992a; pre-Ojo Alamo sandstone of Ayers et al., 1994, fig. 2.4) (note that Fassett et al., 2002, consider this unit to be Paleocene); **Kimb. Mbr**, Kimbeto Member of Ojo Alamo Sandstone; **Huerfanito Bent.**, Huerfanito Bentonite Bed of Lewis Shale; **B**, Galisteo-El Rito Basin; **C**, Raton Basin; **D**, Baca Basin; **E**, Carthage-La Joya Basin; **F**, Sierra Blanca Basin; **G**, relative orogenic intensity for three phases of Laramide basin subidence (see text). Circled numerals correspond to uplift stages in Figure 15. Approximate thicknesses of Upper Cretaceous strata between top of Gallup Sandstone and base of Eocene are depicted in columns D, E, and F.

(Fig. 4). These relationships indicate that differential subsidence had not begun in the San Juan Basin prior to ~80 Ma. In this paper, the onset of disruption of the foreland basin to form a mosaic of smaller intraforeland basins and uplifts is considered to define the beginning of the Laramide orogeny. As will be discussed below, initial Laramide deformation began in northern New Mexico and southern Colorado between about 80 and 75 Ma.

Approximately synchronous with the beginning of the final marine transgression (Cliff House Sandstone) in the San Juan Basin, stratal accumulation rates in the axial part of the basin more than doubled to ~150 m/m.y. (Table 1, Fig. 3) during deposition of the Lewis Shale. The Lewis Shale attains its maximum thickness in the northern San Juan Basin and thins landward (southwest) to a pinchout in the southern part of the basin, as has been documented in the detailed regional cross sections of Molenaar (1983). Recent drilling in the San Juan Sag (Gries et al., 1997), however, has

TABLE 1. Formation tops and selected age constraints (in feet) for lithologic units in Aztec Oil and Gas Company Trail Canyon No. 1 (San Juan Basin, sec. 21, T32N, R8W).

UNIT	DEPTH (FT)	SELECTED AGE CONSTRAINTS
San Jose Fm	collar	Lower Eocene (Wasatchian, ~55–52 Ma)
unconformity		Lacuna of poorly constrained duration
Nacimiento Fm	830	Paleocene (~64.5–61 Ma)
Ojo Alamo Ss (Kimbeto Mbr)	1647	Lower Paleocene (~65–64.5 Ma)
unconformity		Lacuna ~6 m.y.
Kirtland and Fruitland Fms	2110	Upper Campanian (~74 Ma to ~71.5 or 71 Ma, see text)
Pictured Cliffs Ss	3542	Contains zone of *Didymoceras cheyennese* [~74 Ma] near this well (Fassett, 2000, fig. 14)
Lewis Sh	3600	Contains Huerfanito Bentonite Bed (75.76 ± 0.34 Ma; Fassett et al., 1997) at 4404 ft
Mesaverde Gr	5674	Contains 78.22 ± 0.26 Ma ash in upper part (Peters, 2001)
Point Lookout Ss	5938	
upper Mancos Sh	6060	
"Niobrara"	7380	
disconformity		Basal Niobrara disconformity (~89–88 Ma; Leckie et al., 1997, fig. 29)
lower Mancos Sh	8065	
Greenhorn Ls	8000	Contains zone of *Mammites nodosoides* [93 Ma]
lower Mancos Sh	8065	
Dakota Ss	8170	Contains zone of *Acanthoceras amphibolum* [94.93 ± 0.53 Ma] in upper part (Roberts and Kirschbaum, 1995)

Note: $^{40}Ar/^{39}Ar$ age constraints in brackets [ ] are from Obradovich (1993). Other age constraints are from Woodburne and Swisher (1995), Williamson and Lucas (1992), Hunt and Lucas (1992), Williamson (1996), and S. G. Lucas (2001, oral commun.).

demonstrated that the Lewis Shale also thins in the *seaward* direction (northeast) from its maximum thickness near the axis of the San Juan Basin (Fig. 5). Such seaward thinning is diametrically opposed to the expected seaward thickening that should result from the time-transgressive stratigraphic rise of the regressive Pictured Cliffs Sandstone that bounds the top of the Lewis Shale in both areas. The approximately two-fold thinning of the Lewis Shale between the axis of the San Juan Basin and the San Juan Sag is interpreted to reflect an early phase of differential subsidence in the San Juan Basin. This interpretation is supported by the subsidence-induced reorientation of upper Lewis-Pictured Cliffs shoreline as it prograded northeastward across the structural hingeline at the toe of the Chaco homocline (Ayers et al., 1994). The fact that differential thickening of the Lewis Shale also occurs below the intercalated 75.76 ± 0.45 Ma Huerfanito Bentonite Bed (Fassett and Steiner, 1997) (Fig. 5) suggests that differential subsidence was underway by this time.

Differential thickening of the Lewis Shale is the earliest evidence of Laramide subsidence in the nascent San Juan Basin, and may have been related to an early phase of differential subsidence

TABLE 2. Formation tops and selected age constraints (in feet) for lithologic units in Odessa Natural Corporation-Maguire Oil Co. W. S. Ranch Well No. 2 (Raton Basin, sec. 30, T30N, R20E).

UNIT	DEPTH (FT)	SELECTED AGE CONSTRAINTS
Raton Fm	collar	K-T boundary [65.4 ± 0.1] ~265 ft above base in nearby well (Pillmore and Flores, 1987)
unconformity		Lacuna of unknown duration
Vermejo Fm	1035	
Trinidad Ss	1195	Estimated by W. A. Cobban (written commun. *in* Fassett, 1976) to contain the zone of *Baculites eliasi* or *B. baculus* [~71 Ma]
upper Pierre Sh	1350	Contains Campanian-Maastrichtian boundary [71.3 ± 0.5 Ma] in upper transition zone ~100–150 ft below Trinidad Ss (Flores, 1987).
Apache Creek Ss Mbr	3791	Contains *Baculites* sp. (weakly ribbed) [~80 Ma] (Cobban, 1956; Scott and Cobban, 1963).
lower Pierre Sh	3812	
Smoky Hill Mbr, Niobrara Fm	4245	
Fort Hays Mbr, Niobrara Fm	4493	
unconformity		Basal Niobrara disconformity (~88–89 Ma)
Carlisle Sh	4526	
Greenhorn Ls	4700	Contains zone of *Mammites nodosoides* [~92 Ma]
Graneros Sh	4764	
Dakota Ss	4842	Contains zone of *Acanthoceras amphibolum* [94.93 ± 0.53 Ma] in upper part (Roberts and Kirschbaum, 1995).

Note: $^{40}Ar/^{39}Ar$ age constraints in brackets [ ] are from Obradovich (1993).

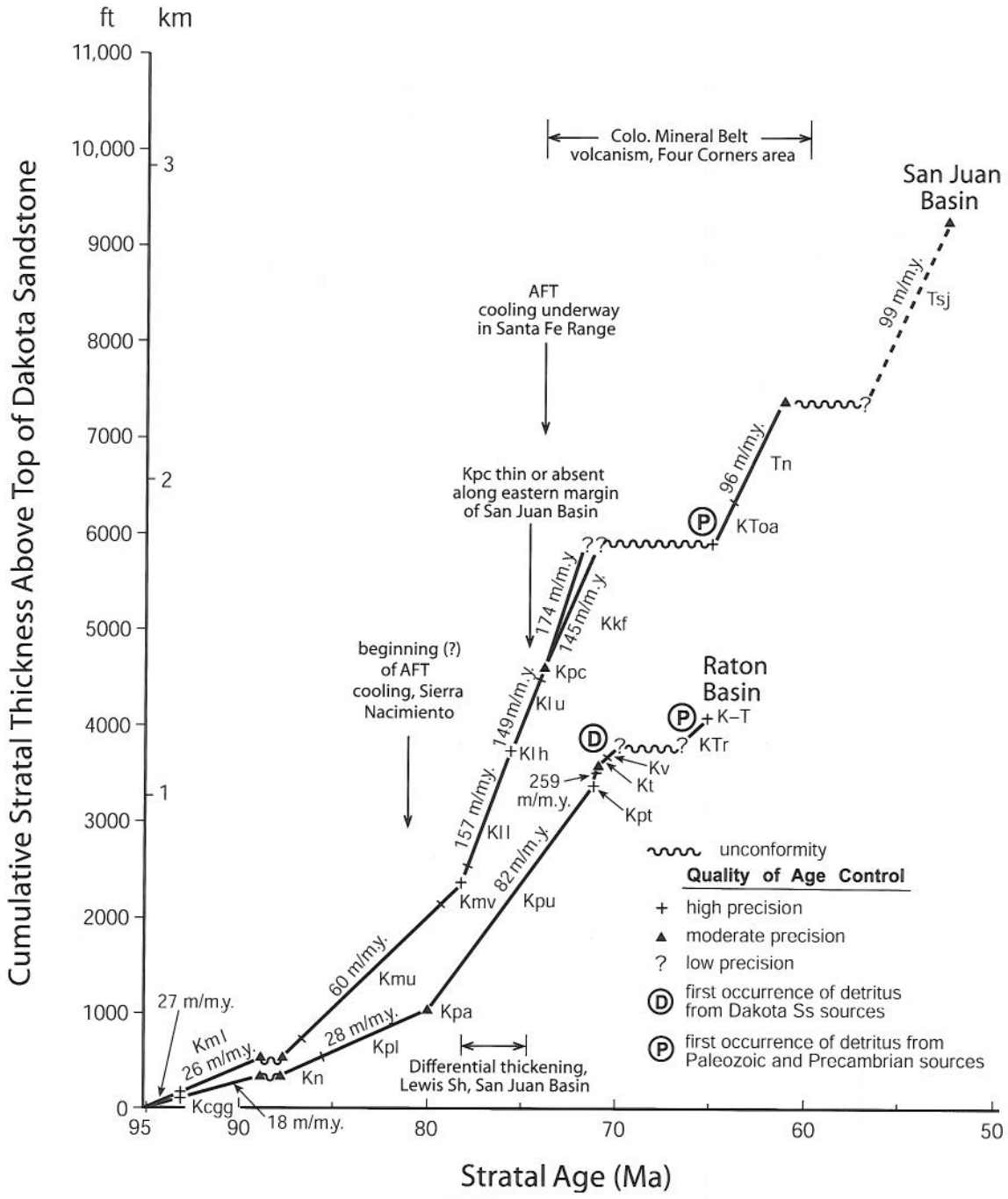

FIGURE 3. Graph of cumulative stratal thickness above top of Dakota Sandsone vs. stratal age for selected wells from the axial parts of the San Juan Basin (Aztec Oil and Gas Company Trail Canyon No. 1; Table 1) and the Raton Basin (Odessa Natural Corporation-Maguire Oil Co. W. S. Ranch well no. 2; Table 2) showing stratal accumulation rates and unconformities. Note that thicknesses have not been decompacted. San Juan Basin units are: **Kml**, lower Mancos Shale; **Kn**, "Niobrara"; **Kmu**, upper Mancos Shale; **Kmv**, Mesaverde Group; **Kll**, lower Lewis Shale; **Klh**, Huerfanito Bentonite Bed; **Klu**, upper Lewis Shale; **Kpc**, Pictured Cliffs Sandstone; **Kkf**, Fruitland and Kirtland Formations; **KToa**, Ojo Alamo Sandstone; **Tn**, Nacimiento Formation; **Tsj**, San Jose Formation. Note that the well is collared in the lower part of the San Jose Formation (Table 1), and for that reason the stratal accumulation rate (dashed line) for the San Jose is derived from age-thickness relationships in the Tertiary depocentral area in the northeast part of the San Juan Basin (see text). Raton Basin units are: **Kggc**, Graneros Shale, Greenhorn Formation and Carlisle Shale; **Kn**, Niobrara Formation; **Kpl**, lower Pierre Shale; **Kpa**, Apache Creek Sandstone Member of Pierre Shale; **Kpu**, upper Pierre Shale; **Kpt**, transitional beds at top of Pierre Shale; **Kt**, Trinidad Sandstone; **Kv**, Vermejo Formation; **KTr**, Raton Formation; **K-T**, Cretaceous-Tertiary boundary layer in Raton Formation. See Tables 1 and 2 for age constraints. Also shown is beginning of apatite fission-track (AFT) cooling in Nacimiento Uplift and Santa Fe Range (Kelley et al., 1992), timing of differential thickening of Lewis Shale (see text), timing of non-deposition or erosion of Pictured Cliffs Sandstone along evolving range-front of Nacimiento Uplift (Baltz, 1967; Fassett and Hinds, 1971), and age range of volcanism in Colorado Mineral Belt in the Four Corners area (Mutschler et al., 1987; Semken and McIntosh, 1997). Time scale after Obradovich (1993) and Woodburne and Swisher (1995).

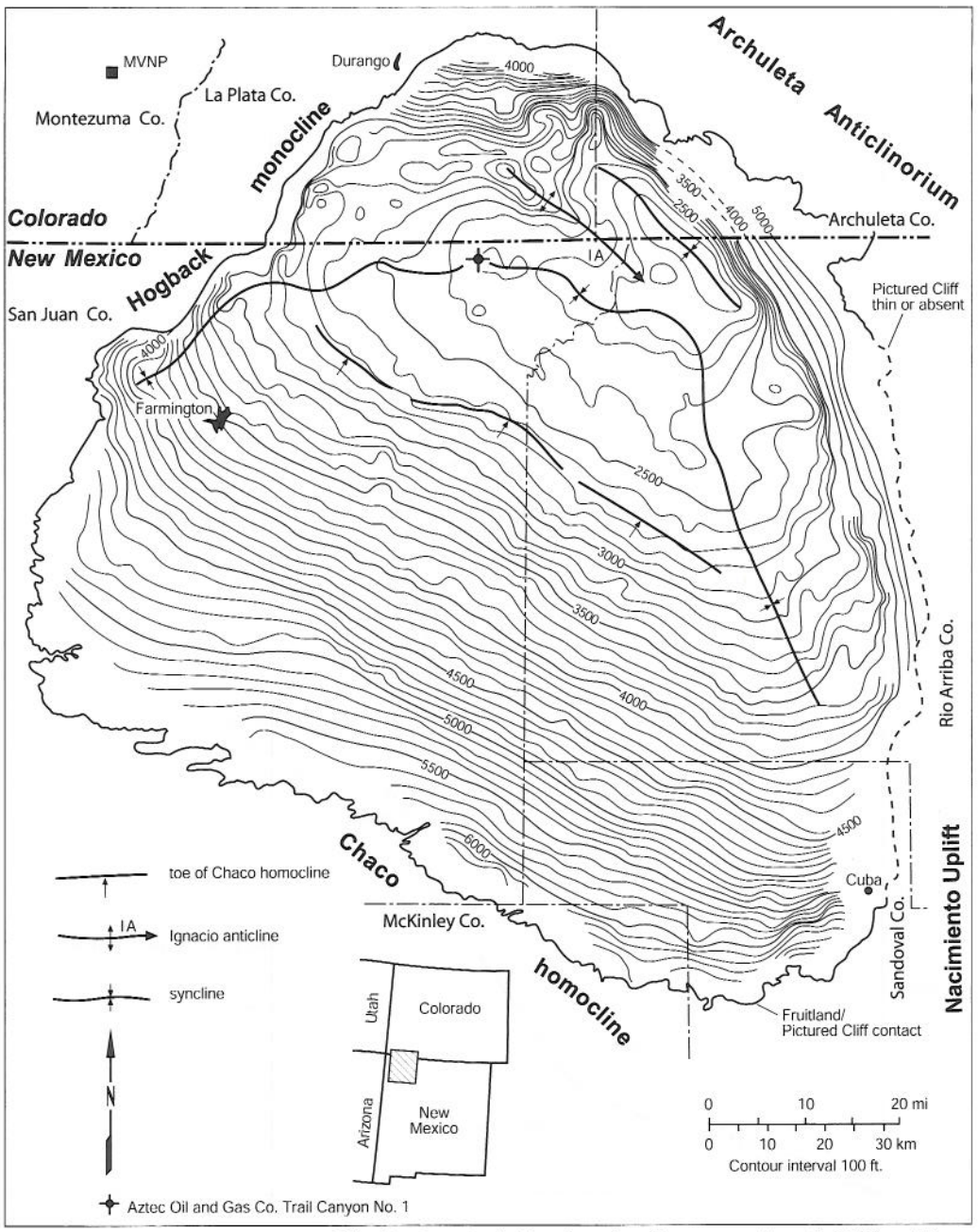

FIGURE 4. Structure-contour map of the San Juan Basin based on data from approximately 2500 well logs, contoured on the Huerfanito Bentonite Bed. Note location of Aztec Oil and Gas Co. Trail Canyon No. 1, utilized in Table 1 and Figure 3. **IA**, Ignacio anticline. **MVNP**, Mesa Verde National Park. Modified from Ayers et al. (1994, fig. 2.5)

in the northeastern part of the basin (Ayers et al., 1994; note, however, that this conclusion was challenged by Fassett, 2000, who interpreted piston-like subsidence for the entire basin during Lewis and Pictured Cliffs deposition). The Archuleta Anticlinorium, which divides the San Juan Basin from the San Juan Sag, attained most of its structural relief in Paleogene time (see below), but must have been active also during Lewis time (middle to late Campanian) to account for the seaward thinning of the Lewis Shale. Late Campanian (~75 Ma) deformation also occurred along the eastern margin of the San Juan Basin, as is indicated by the thinness or local absence of the Pictured Cliffs Sandstone (Baltz, 1967; Fassett and Hinds, 1971; Woodward, 1987). Stratigraphic thinning or omission of the Pictured Cliffs is restricted to a narrow zone along the flank of the Nacimiento Uplift and the southern part of the Archuleta Anticlinorium, and is indicative of an early phase of activity on these structures.

The Pictured Cliffs Sandstone consists of shore-zone deposits related to the final (R-5) regression of the Late Cretaceous sea from northwestern New Mexico (Fassett and Hinds, 1971; Molenaar, 1983). The Pictured Cliffs shoreline prograded northeastward or north-northeastward. The shoreline was relatively linear, suggesting wave reworking and multiple deltaic sources of sediment (Flores and Erpenbeck, 1981; Ayers et al., 1994). The Pictured Cliffs regression occurred in response to increased sediment supply from volcanism and tectonism in southern Arizona (Cumella, 1983), and was markedly time transgressive (Fassett, 2000, figs.

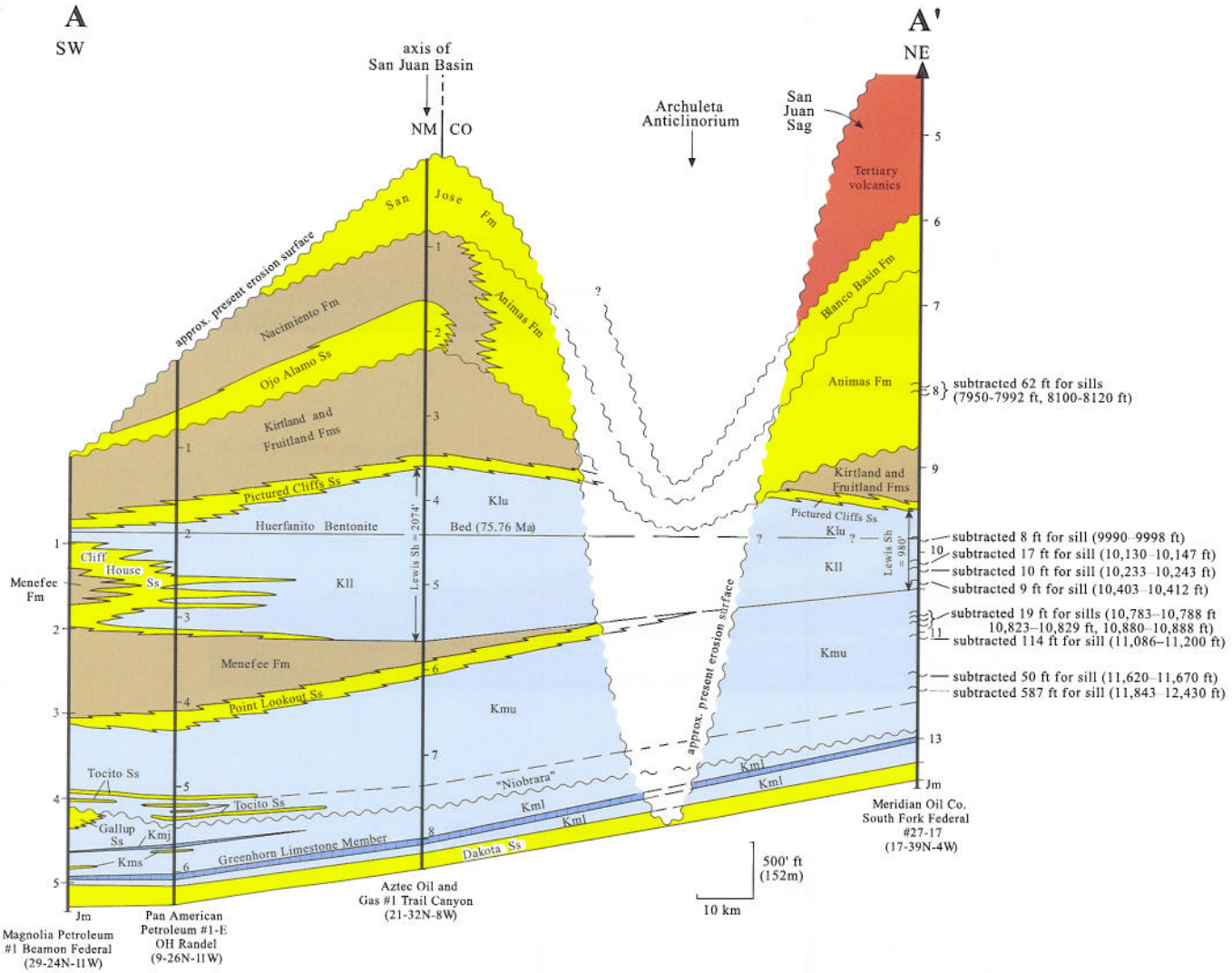

FIGURE 5. Cross section of Upper Cretaceous and Tertiary strata in San Juan Basin-Archuleta Anticlinorium-San Juan Sag area (line of section shown in Figure 1). Data for selected wells in San Juan Basin are modified slightly from Molenaar (1983, fig. 3, his wells 107, 109, and 114). Well in San Juan Sag is modified from Gries et al. (1997); note that thickness of Tertiary sills have been subtracted. Formation tops were picked by the author and B. S. Brister. Datum is Huerfanito Bentonite Bed. Unit abbreviations are: **Kml**, lower Mancos Shale; **Kms**, Semilla Sandstone Lentil; **Kmu**, upper Mancos Shale; **Kll**, lower Lewis Shale; **Klu**, upper Lewis Shale. Well near axis of San Juan Basin (Aztec Oil and Gas No. 1 Trail Canyon) is same as that utilized in Figure 3 and Table 1. Note approximate two-fold seaward thinning of Lewis Shale from axial part of San Juan Basin to the San Juan Sag.

14, 18). Pronounced stratigraphic rise of the Pictured Cliffs Sandstone occurred near the synclinal axis of the San Juan Basin. This has been attributed to active basin subsidence (Ayers et al., 1994) or to decreased sediment supply (Fassett and Hinds, 1971).

Following the northeastward retreat of the Lewis sea and the regressive Pictured Cliffs shoreline, coal-bearing coastal plain deposits of the Fruitland Formation accumulated in the San Juan Basin and San Juan Sag. These deposits interfinger with the uppermost beds of the Pictured Cliffs Sandstone, and attain a maximum thickness of ~183 m in the northwestern San Juan Basin near Durango, Colorado (Ayers et al., 1991, fig. 14). Paleoflow was toward the northeast or north-northeast, as shown by sandstone isolith patterns in the Fruitland (Ayers et al., 1994). The thickness of the Fruitland Formation decreases to the southeast, at least in part due to syndepositional thinning (Hunt and Lucas, 1992).

The Kirtland Formation transitionally overlies the coal-bearing Fruitland Formation and was deposited in an alluvial plain environment. Depositional systems and direction of sediment transport for the Kirtland Formation, however, have only locally been adequately studied. Stratigraphic studies of the Kirtland Formation and overlying Ojo Alamo Sandstone have led to varied stratigraphic nomenclature for these rocks (e.g., Bauer, 1916; Reeside, 1924; Baltz, 1967; Fassett and Hinds, 1971; Powell, 1973; Klute, 1986; Hunt and Lucas, 1992). In this study, I adopt the terminology of Hunt and Lucas (1992), although I herein regard the Naashoibito Member of Baltz et al. (1966) as the lower member of the Ojo Alamo Sandstone (e.g., Powell, 1973, Lucas and Sullivan, 2000, p. 100) (Fig. 6).

Distinct thickening of the Kirtland-Fruitland interval (Fig. 7) suggests the existence of a Kirtland depocenter in the northwestern San Juan Basin, as was first noted by Caswell Silver (1950, 1951) and subsequently by other workers (Dilworth, 1960; Klute, 1986; Hunt and Lucas, 1992). Much of the northwestward thickening of the Kirtland-Fruitland interval may be due to syndepositional thickening of the Farmington Sandstone Member (Hunt and Lucas, 1992). As opposed to the relatively uniform northeastward paleo-

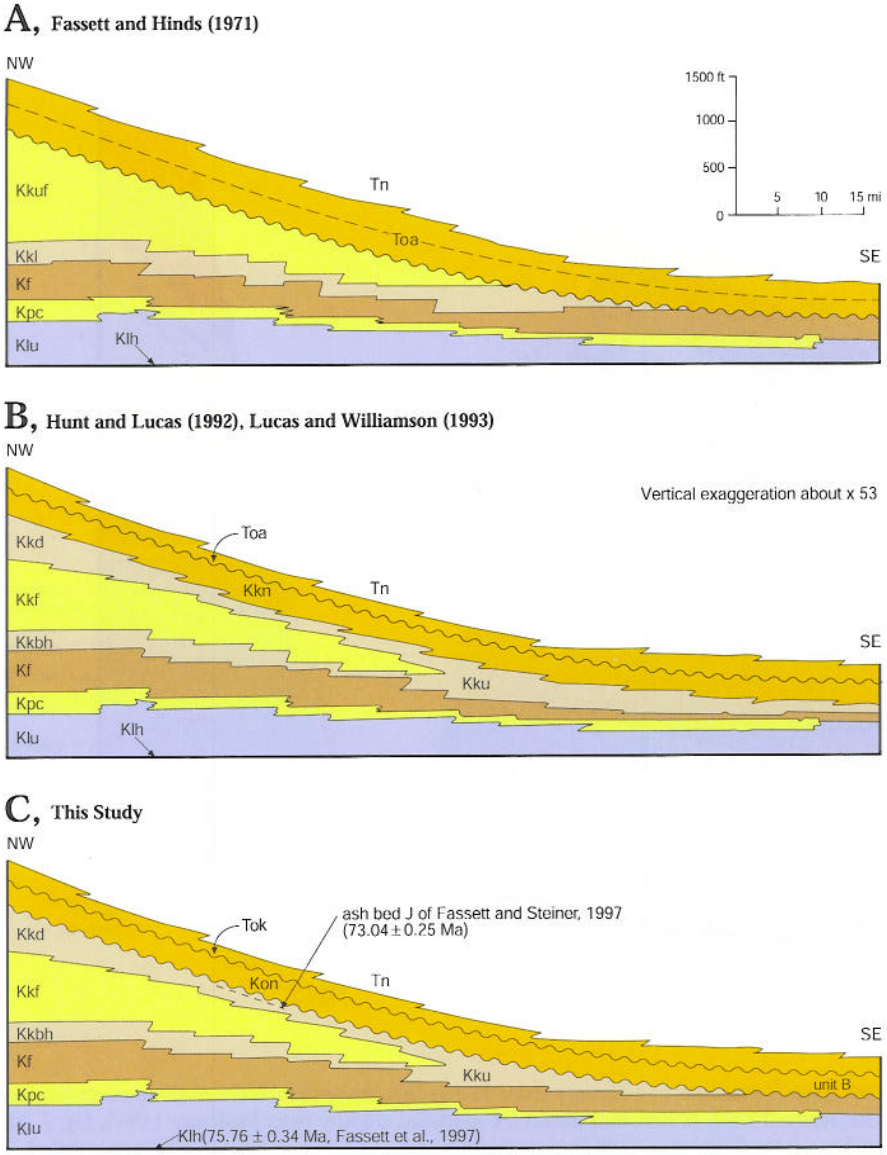

FIGURE 6. Schematic cross sections of San Juan Basin from northwest to southeast, showing varying use of nomenclature and differing placement of regional unconformities. **A,** Modified from Fassett and Hinds (1971, plate 2). Ojo Alamo Sandstone (**Toa**) is used in the broad sense first proposed by Bauer (1916). Southeastward thinning of underlying Kirtland Formation is related to pre-Ojo Alamo tilting and erosion. Following Bauer (1916) and Reeside (1924), the Kirtland Formation consists of three members: the upper shale member and Farmington Sandstone Member (**Kkuf**) and the lower shale member (**Kkl**). Baltz (1967) and Fassett and Hinds (1971) also noted that the Pictured Cliffs Sandstone (**Kpc**) is thin or absent in a narrow zone adjacent to the Nacimiento Uplift (see also Woodward, 1987). There the Fruitland Formation (**Kf**) locally disconformably overlies the upper Lewis Shale (**Klu**). **B**, Modified from Hunt and Lucas (1992) and Lucas and Williamson (1993). Following Baltz et al. (1966), Hunt and Lucas (1992) restricted the Ojo Alamo Sandstone to the Tertiary upper part of the original unit that interfingers with the overlying Nacimiento Formation (**Tn**), and relegated the lower part of Bauer's (1916) Ojo Alamo Sandstone to the Naashoibito Member of the Kirtland Formation (Kkn). They regarded the Naashoibito to be conformable with the underlying upper shale member, which they renamed De-na-zin Member. Baltz et al. (1966) inferred that an unconformity divides the Ojo Alamo Sandstone from the Naashoibito Member. Hunt and Lucas (1992) and Lucas and Williamson (1993a) argued that this unconformity represents a lacuna of 2–3 m.y. or less. Hunt and Lucas (1992) regarded the southeastward thinning of the Kirtland to be syndepositional, largely related to the pinchout of the Farmington Sandstone Member. Southeast of the pinchout, the De-na-zin Member (**Kkd**) merges with the Bisti Member and Hunter Wash Member (**Kkbh**, formerly lower shale member) to form the Kirtland Formation undivided (**Kku**). **C**, This study. Dated ash located 4.9 m below the Naashoibito Member (73.04 ± 0.25 Ma; Fassett and Steiner, 1997) indicates the upper part of the De-na-zin Member is late Campanian, significantly older than the overlying Naashoibito Member. These relationships support the existence of a major (~6 m.y.) unconformity between these units, as noted previously by Fassett and Hinds (1971). For this reason and for reasons of lithologic similarity, I follow Powell (1973 and Lucas and Sullivan (2000, p. 100) in assigning the Maastrichtian Naashoibito Member (**Kon**) to the Ojo Alamo Sandstone (note that Fassett et al., 2002, consider the Naashoibito to be Tertiary). The Kimbeto Member (**Tok**) disconformably overlies the Naashoibito and constitutes the upper part of the Ojo Alamo. In areas of the San Juan Basin where the Naashoibito Member has been eroded prior to deposition of the Kimbeto Member, the unconformity beneath the Ojo Alamo thus may represent as much as 8 m.y. of missing stratigraphic record. The Naashoibito Member may be equivalent to "unit B" of Baltz (1967) and Smith (1992a) in the southeastern San Juan Basin, and with the "pre-Ojo Alamo" sandstone of Ayers et al. (1994, fig. 2.4). In this model, the southeastward thinning of the Kirtland Formation is due to both syndepositional processes (~74–71 Ma) and post-depositional erosion (~72–67 Ma), although the relative importance of these factors is undetermined.

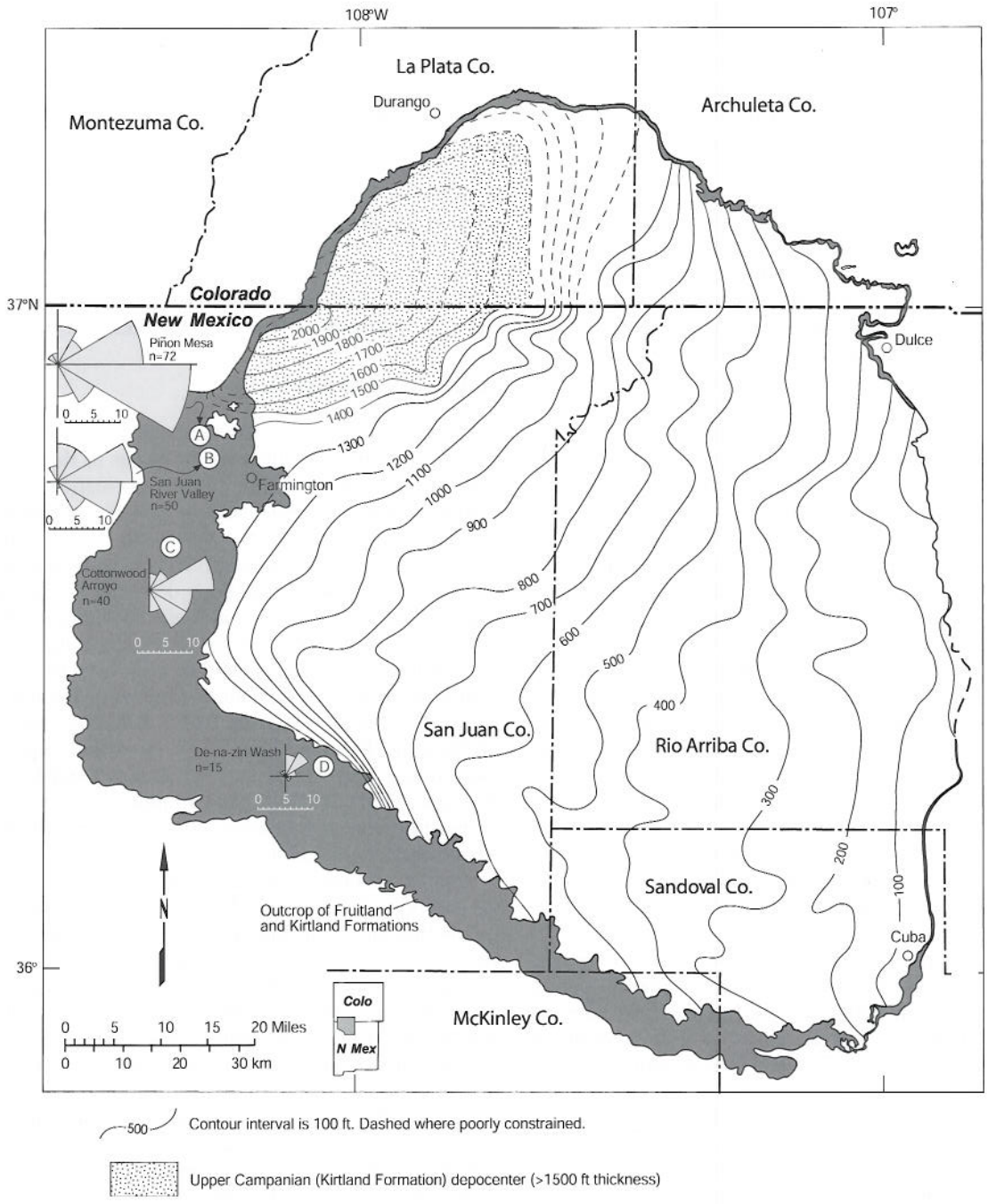

FIGURE 7. Isopach map of Fruitland and Kirtland Formations, San Juan Basin. Isopach contours are dashed where poorly constrained due to absence of overlying Ojo Alamo Sandstone. Paleocurrent data (based on cross bedding, parting lineation, and pebble imbrication) are for Farmington Sandstone Member of Kirtland Formation and were collected by the author. Scales show number of paleocurrent measurements. Paleocurrent localities are: **A**, Piñon Mesa; **B**, San Juan River Valley; **C**, Cottonwood Spring area; **D**, De-na-zin Wash. Modified from Fassett and Hinds (1971, fig. 11).

flow of the underlying Fruitland Formation, paleocurrent directions during deposition of the Farmington Sandstone Member (Fig. 7) were more varied (cf. Dilworth, 1960). Paleocurrents during Kirtland Formation deposition near De-na-zin Wash in the southwestern San Juan Basin were northeastward, similar to those in the underlying Fruitland Formation (Fig. 7). In contrast, paleocurrents near the Kirtland depocentral area in the northwest part of the basin were easterly, nearly orthogonal to the adjoining Hogback monocline. These easterly paleocurrents imply a syntectonic relationship between the Kirtland depocenter and the Hogback monocline. An unresolved part of the southeastward thinning of the Kirtland, however, may be the result of latest Campanian-early Maastrichtian (~72–67 Ma) erosional beveling prior to deposition of the Naashoibito Member of Ojo Alamo Sandstone (Baltz et al., 1966; Fassett, 1985; Ayers et al., 1994).

The thickening of the Kirtland and Fruitland Formations in the Farmington-Durango area suggests that the northwestern structural margin of the San Juan Basin (the Hogback monocline) was

active during late Campanian-early Maastrichtian time. Thick coal deposits and northeast-trending net-coal isopach lines for the Fruitland Formation near the Hogback monocline (Fassett, 2000, fig. 28) suggest that deformation on the monocline may have been initiated during Fruitland deposition. Adjacent to the Hogback monocline near Farmington, New Mexico, the Farmington Sandstone Member of the Kirtland Formation contains numerous 1–8 cm clasts of light-gray sandstone. These clasts consist of sandstone that is better sorted and more quartzose than sandstone of the Kirtland Formation, and thus were not derived intraformationally. These clasts probably were derived from the texturally and mineralogically more mature Pictured Cliffs Sandstone. This, in turn, implies the Pictured Cliffs Sandstone was exposed by uplift and erosion along the Hogback monocline during the late Campanian.

Stratal accumulation rates for the northwest-thickening Kirtland-Fruitland interval are not precisely constrained throughout most of the basin because of uncertainty about the effects of syndepositional differential subsidence versus post-Kirtland erosional beveling. For this reason, a range of stratal accumulation rates (~145–174 m/m.y.) is depicted in Figure 3. The lower rate represents the stratal accumulation rate (~140 m/m.y.) determined for the Kirtland-Fruitland interval in the southwest part of the basin by Fassett (2000, fig. 17) and corresponds to the end-member case where basin-wide sedimentation rates were constant and all of the northwestward thickening resulted from subsequent beveling. [Note that such post-depositional erosion predicts that the top of the Kirtland Formation is significantly younger to the northwest.] The higher stratal accumulation rate assumes a constant time interval for Kirtland-Fruitland deposition (~2.5 m.y.; Fassett, 2000, fig. 17) and represents the end-member case where northwestward thickening is entirely syndepositional and accumulation rates vary as a function of Kirtland-Fruitland thickness (174 m/m.y. in the well depicted in Figure 3; note that the corresponding stratal accumulation rate in the northwestern depocenter would be ~243 m/m.y.). The truth probably lies somewhere between these end-members.

Kirtland-Fruitland stratal accumulation rates equal or exceed those for continental deposits in other Laramide basins during Campanian-Eocene time in northern New Mexico. The Kirtland Formation attains thicknesses of as much as 460 m north of Farmington (Fassett and Hinds, 1971), and thus accounts for nearly half of the potential sedimentary accommodation related to the structural relief of the Hogback monocline in that area (~1070 m; Craigg et al., 1989). If decompacted using the parameters defined by Fassett (2000, fig. 7), the Kirtland may account for about three-quarters of this potential sedimentary accommodation.

Erslev (1997) and Ruf (2000) analyzed minor faults in the vicinity of Durango, Colorado, and argued for sequential northeast, northwest, and north-northeast σ_1 orientations during Tertiary time. The northwest σ_1 orientation is orthogonal to the trend of the Hogback monocline (Ruf, 2000, p. 94), and is interpreted here to be related to development of the monocline during late Campanian-early Maastrichtian time. This suggests the age of the northwest σ_1 orientation of Erslev (1997) and Ruf (2000) to be ~74–67 Ma, and not Paleogene as inferred by Ruf (2000, fig. 7.1). A pre-Tertiary age for most of the structural relief of the Hogback monocline is indicated also by stratigraphic relationships in southwestern Colorado (Baltz et al., 1966, fig. 5).

In this chapter, I limit the term Hogback to the monocline that forms the northwest boundary of the San Juan Basin and, possibly, the San Juan Sag (Figs. 1, 4). Many previous workers have also applied the name Hogback to the steep southwest limb of the Archuleta Anticlinorium that bounds the northeast side of the San Juan Basin. As will be shown below, the Archuleta Anticlinorium is mostly younger (Paleogene) and is nearly orthogonal to the trend of the Hogback monocline. Because of differences in the age and orientation of these structures, I reserve usage of the term Hogback monocline for the northwest basin-boundary structure. The Hogback monocline may continue on trend to the northeast to form the northwest boundary of the San Juan Sag (Fig. 1). Constraints in this latter region, however, are very poor due to limited drilling and cover by volcanic rocks of the San Juan field. Although Kirtland/Fruitland strata are present in the San Juan Sag (Brister and Chapin, 1994; Gries et al., 1997), it is not known if they thicken to the northwest as they do in the San Juan Basin.

Middle phase of subsidence

The middle phase of tectonic subsidence and associated sedimentation in the San Juan Basin began in the latest Cretaceous with the deposition of the Animas Formation in the north and northwest part of the basin and the Ojo Alamo Sandstone throughout the basin except in the northwest. The Animas Formation ranges from Late Cretaceous to Paleocene in age (Reeside, 1924; Lehman, 1985; Fassett and Hinds, 1971) and contains considerable andesitic detritus. The volcaniclastic McDermott Member constitutes the basal 30–100 m of the formation in the northwest part of the San Juan Basin, and is overlain with local unconformity by the drab beds of the Nacimiento Formation or the upper member of Animas Formation (Reeside, 1924; Lehman, 1985, fig. 21). The McDermott Member may be a proximal equivalent of the Naashoibito Member of the Ojo Alamo Sandstone to the south (Reeside, 1924), although the two units are now disjunct because of incision prior to deposition of the Kimbeto Member of the Ojo Alamo Sandstone (Lehman, 1985).

A significant unconformity divides the Kirtland Formation from the overlying Naashoibito Member of the Ojo Alamo Sandstone in the southwestern San Juan Basin. The unconformity occurs 4.9 m above a volcanic ash bed in the upper part of the Kirtland Formation (De-na-zin Member of Hunt and Lucas, 1992) that has been dated at 73.04 ± 0.25 Ma by the $^{40}Ar/^{39}Ar$ technique (Fassett and Steiner, 1997). The upper constraint on the duration of the lacuna represented by the unconformity is given by probable late Maastrichtian (Lancian) dinosaur bones and fossil mammals from the Naashoibito Member (Lehman, 1985, Hunt and Lucas, 1992) which are approximately 67 Ma (S. G. Lucas, oral commun., 2001; note that Fassett et al., 2002, considered these dinosaur fossils to be Paleocene). These relations indicate a lacuna of at least ~6 m.y. duration that encompassed at least latest Campanian and early Maastrichtian time in the southwestern San Juan Basin.

The Naashoibito Member is locally conglomeratic and is generally less than about 30 m thick. Paleocurrent directions in the Naashoibito have not been adequately studied. Powell (1972) reported south-southwest paleoflow for the unit, but did not present his data or describe the locations of his measurements. The Naashoibito Member is not everywhere present in the San Juan Basin, locally having been either not deposited or erosionally removed prior to deposition of the Kimbeto Member of the Ojo Alamo Sandstone (Lehman, 1985; Smith, 1992a; Ayers et al., 1994). The overlying Kimbeto Member (also locally conglomeratic) is early Paleocene in age (~65 Ma; Fassett and Lucas, 2000) because of intertonguing with the overlying Nacimiento Formation (Baltz et al., 1966). The unconformity between the Kimbeto Member and the Naashoibito Member may contain the Cretaceous-

Tertiary boundary (Baltz et al., 1966; Hunt and Lucas, 1992; cf. Fassett et al., 2002) and encompasses no more than about 2–3 m.y. of missing stratigraphic record (Hunt and Lucas, 1992, p. 235; Lucas and Williamson, 1993a), perhaps far less. Where the Naashoibito is missing, however, the basal Ojo Alamo unconformity may represent a lacuna of as much as 6–8 m.y.

Stratal accumulation rates in the southwestern San Juan Basin were very low during the time interval between the end of deposition of the Kirtland Formation (73.04 ± 0.25 Ma in the southwest part of the basin) and initial deposition of the Kimbeto Member of the Ojo Alamo Sandstone (~65 Ma). Most of this time interval is represented by unconformities or possibly cryptic condensed sections; only deposition of the thin Naashoibito Member locally interrupted this period of non-deposition and/or erosion. These low stratal accumulation rates (Fig. 3) mark the interval between the first and second of the phases of Laramide subsidence and sedimentation in the San Juan Basin.

The Ojo Alamo Sandstone exhibits paleocurrent and provenance evidence for derivation from source regions northwest of the basin (Powell, 1973; Lehman, 1985; Klute, 1986; S. M. Cather, *unpubl.*). Citing evidence for southeasterly paleoflow and the presence of clasts derived from Paleozoic, Precambrian and Laramide volcanic sources, the Ojo Alamo Sandstone has been interpreted by some workers to record the local beginning of the Laramide orogeny during late Maastrichtian-early Paleocene time (e.g., Fassett, 1985; Lehman, 1985). The data presented above, however, support an entirely different scenario: the initiation of Laramide tectonism and rapid subsidence in the San Juan Basin preceded deposition of the conglomeratic sediments of the Ojo Alamo by approximately 10 m.y., and deposition of these coarse-grained units occurred during and immediately following a *lull* in subsidence and accommodation (Fig. 3). The association of the coarse-grained deposits of the Naashoibito and Kimbeto Members of the Ojo Alamo with an episode of low accommodation implies that these coarse-grained, sheet-like units were unable to spread southeastward until late Campanian-early Maastrichtian rapid basin subsidence had ceased. The existence of such "antitectonic" (Paola et al., 1992) conglomeratic sequences has been supported both by theory (Leeder and Gawthorpe, 1987; Blair and Bilodeau, 1988) and by stratigraphic analysis of other Laramide basins (Beck et al., 1988).

The second phase of Laramide subsidence and sedimentation in the San Juan Basin began with deposition of the Kimbeto Member of the Ojo Alamo Sandstone shortly after the Cretaceous-Tertiary boundary. The Kimbeto Member consists of sandstone, pebbly sandstone, and conglomerate that were deposited by generally southeast-flowing braided streams (Powell, 1973; Klute; 1986; S. M. Cather, *unpubl.*; cf. Sikkink, 1987, who interpreted generally southward paleoflow). The Kimbeto Member is as much as ~120 m thick and is present throughout the basin, except in its northwest part where it grades laterally into fine-grained deposits of the Nacimiento Formation (Baltz et al., 1966; Lehman, 1985). Elsewhere in the basin, the Kimbeto Member grades upward into the Nacimiento Formation. Although the Kimbeto Member appears to be entirely of early Paleocene age, it contains dinosaur bones that have been variously interpreted to be reworked (Lucas and Williamson, 1993a) or to represent dinosaurs that survived the terminal K-T event (Fassett and Lucas, 2000).

The bulk of the medial Laramide phase of sedimentation in the San Juan Basin is represented by the Nacimiento Formation and its northern lateral equivalent, the upper member of the Animas Formation. Consisting largely of mudstone and fine sandstone, the Nacimiento is as much as 500 m thick and was deposited during the early to early late Paleocene in the southern part of the basin (~64.5–61 Ma; Williamson and Lucas, 1992; Williamson, 1996). The age range of the upper member of the Animas Formation is imprecisely known, but includes beds of late Paleocene (Tiffanian) age (Simpson, 1935).

The stratal accumulation rate for the Nacimiento Formation near the basin axis in the northern part of the basin is ~96 m/m.y. (Fig. 3, Table 1). This is comparable to the range of stratal accumulation rates (63–116 m/m.y., not decompacted) estimated for the main body of the Nacimiento in the southern part of the basin (Williamson, 1996, fig. 16). The upper ~20–80 m of the Nacimiento Formation consists of the sandstone-dominated (locally pebbly) Escavada Member (Williamson and Lucas, 1992) that contains numerous silcretes and exhibits markedly lower stratal accumulation rates (11–25 m/m.y.) than subjacent parts of the formation (Williamson, 1996). The genetic stratigraphy and sediment-dispersal systems of the Nacimiento Formation have not yet been adequately studied.

Late phase of subsidence

Throughout much of the periphery of the San Juan Basin, outcrops of the Nacimiento Formation and correlative upper Animas Formation are overlain by pebbly sandstones of the Cuba Mesa Member of the Eocene San Jose Formation with disconformity or slight angular unconformity (Baltz et al., 1966; Baltz, 1967). The duration of the lacuna represented by this unconformity is imprecisely known because of poor biostratigraphic control in the Cuba Mesa Member. Smith and Lucas (1991) and Smith (1992b) argued that the unconformity beneath the Cuba Mesa Member gives way to a conformable sequence of fine-grained deposits toward the area of maximum Tertiary subsidence in the northeast part of the basin. In this area, the San Jose-Nacimiento contact is purported to be mudstone on mudstone. Such a scenario would suggest that unconformity development in peripheral areas occurred in response to increased tectonic subsidence and accommodation (relative to sediment supply) that temporarily focused sedimentation near the basin center (Smith, 1992b).

To further evaluate the nature of the San Jose-Nacimiento contact, electric logs for representative wells in two east-west transects, one in T32N and one in T30N, were examined by the writer and B. S. Brister. These transects encompassed the area within which the basal Cuba Mesa Member of the San Jose Formation was interpreted to be absent by Smith and Lucas (1991) and Smith (1992b). Our analysis indicates the presence of sandstone of the Cuba Mesa Member throughout this area. Furthermore, the San Jose-Nacimiento contact is sharp and resembles electric-log response elsewhere in the southern part of the basin where the contact is known to be unconformable. Based on these observations, we infer that the San Jose-Nacimiento contact may be everywhere disconformable, and that the previous interpretation of a conformable contact relationship near the basin axis is possibly the result of miscorrelation.

Unconformity development as a result of *decreased* tectonic subsidence and resultant decreased accommodation, as proposed above for the unconformities beneath the Ojo Alamo Sandstone, is an alternative mechanism by which the San Jose-Nacimiento unconformity may have developed. If tectonic subsidence and accommodation peaked during deposition of the fine-grained deposits of the lower Nacimiento Formation and subsequently decreased to zero by the end of deposition of the Escavada Member, an explanation would be provided for the silcretes and

diminished strata accumulation rates of the Escavada as well as for a possible basin-wide surface of non-deposition or erosion that caps it. More work on the nature of the San Jose-Nacimiento contact in the San Juan Basin is needed.

The San Jose Formation represents the final preserved episode of Laramide sedimentary aggradation in the San Juan Basin. The San Jose is as much as 550 m thick and contains early Eocene (Wasatchian) fossil vertebrates in its middle and upper parts (Smith and Lucas, 1991; Smith, 1992b; Lucas and Williamson, 1993b). Stratal accumulation rates for the San Jose Formation, estimated from thicknesses and age relations in the Eocene depocenter in the northeast part of the San Juan Basin, are ~99 m/m.y. (Fig. 3). Note, however, that these rates are imprecise because of age uncertainty for the Cuba Mesa Member, only the upper part of which has been dated by interfingering with the Wasatchian Regina Member of the San Jose Formation.

Largely fluvial in origin, the San Jose Formation shows evidence for southwesterly to southeasterly paleoflow (Smith and Lucas, 1991). A major belt of south-flowing channels developed parallel to, and west of, the rising Nacimiento Uplift (Smith, 1992b). The Blanco Basin Formation of the San Juan Sag is a piedmont deposit that may be equivalent to the San Jose Formation (Lucas, 1984; Brister, 1992), although poor age constraints and geographic isolation of the Blanco Basin Formation preclude precise correlation. Early Eocene fluvial systems exited the southeastern San Juan Basin and flowed east into the Galisteo Basin (Cather, 1992). As shown by stratigraphic relationships in the Chuska Mountains, nearly one kilometer of post-San Jose Formation sediments may have been deposited in the San Juan Basin during middle Eocene-early Oligocene time (Fassett, 1985; Cather et al., *in press*). These sediments were subsequently stripped by erosion, probably during the middle and late Tertiary.

San Juan Basin summary

Isopach patterns and structure contour maps document that the Laramide evolution of the San Juan Basin was complex. As described previously, late Campanian sedimentation was focused in the northwest part of the basin (Fig. 7). By early Tertiary time, the depocenter had shifted to the northeast part of the basin. A structure contour map (Fig. 8) of the base of the Tertiary (base of the Kimbeto Member of the Ojo Alamo Sandstone) reveals a north-northwest trending asymmetrical syncline with about 900 m of structural relief. The steep northeast limb of the syncline is contiguous with the southwest limb of the Archuleta Anticlinorium. The axial area of the syncline approximately corresponds to the area of greatest thickness of Tertiary sediments in the San Juan Basin (Fig. 9), although interpretation of this isopach map is complicated by the fact that the upper surface of the isopach interval is modern topography. The relative importance of Paleocene versus Eocene structural development in the northeast part of the basin is not yet well documented.

An isopach map of the stratigraphic interval between the Huerfanito Bentonite Bed and the base of the Kimbeto Member of the Ojo Alamo Sandstone (Fig. 10) provides an interesting comparison with Figure 8. If one makes the simplifying assumption that the base of the Kimbeto Member was horizontal instead of dipping gently to the southeast as shown by paleocurrent analysis (Powell, 1973; Klute, 1986), then Figure 10 may be viewed as an approximate paleo-structure contour map on the Huerfanito Bentonite Bed at the beginning of Tertiary time. Note that the contours in Figures 8 and 10 are mutually nearly orthogonal, and imply that the San Juan Basin subsided in an oblique, seesaw fashion.

The northwest thickening of the Huerfanito-Kimbeto isopach interval depicted in Figure 10 represents the combined effects of at least three processes: (1) northeastward (basinward) thickening of the Pictured Cliffs Sandstone (Fassett and Hinds, 1971; Ayers et al., 1991) and the upper Lewis Shale; (2) northwest syndepositional thickening during late Campanian time of the Kirtland Formation (Silver, 1951; Dilworth, 1960; Hunt and Lucas, 1992); and (3) southeastward erosional beveling during Maastrichtian time of the Kirtland and Fruitland Formations prior to deposition of the Ojo Alamo Sandstone (Fassett and Hinds, 1971; Smith, 1992a; Ayers et al., 1994). The latter two processes probably accompanied shortening of the Hogback monocline, as would be implied by the isostatic constraints of paired uplift and subsidence. By similar reasoning, subsequent major Paleogene subsidence in the northeast part of the basin was probably driven by shortening and tectonic loading in the Archuleta Anticlinorium, which, in turn, implies that the anticlinorium formed largely during Paleocene and Eocene time. Initial structural development of the anticlinorium, however, occurred earlier, during deposition of the Lewis Shale and Pictured Cliffs Sandstone.

A Paleogene age is also indicated for the Ignacio anticline (Fig. 4), a major, southeast-plunging anticline in the northern part of the basin that is subparallel with, and probably related to, the nearby Archuleta Anticlinorium. The Ignacio anticline is not manifested by stratal thinning on the Huerfanito-Ojo Alamo isopach map (Fig. 10), but is visible on the Ojo Alamo structure contour map (Fig. 8).

Stratigraphic relationships thus indicate that Laramide subsidence in the San Juan Basin was polygenetic. Initial subsidence occurred in the northeast part of the basin ~78–75 Ma. This was followed by northwest tilting and subsidence ~74–67 Ma, and then a return to major subsidence in the northeast part of the basin in the early Tertiary. It thus seems likely that the arcuate axis of the San Juan Basin that is apparent in structure contour maps of the Huerfanito Bentonite Bed (Fig. 4) and older units (e.g., Craigg et al., 1989) is the result of the superposition of spatially and temporally distinct phases of subsidence. An analogous model of diachronous, seesaw subsidence and sedimentation has been proposed for the Laramide Green River Basin (Beck et al., 1988).

The three diachronous subsidence events outlined above for the San Juan Basin may correspond to the sequential northeast, northwest, and north-northeast σ_1 orientations documented by Ruf (2000) in the Durango area. If so, then these relationships indicate that patterns of Laramide shortening in northern New Mexico were complex and not regionally synchronous. For example, subsidence patterns and growth-fold relationships in the northeastern and eastern San Juan Basin indicate the late phase of northeast shortening began in the early Paleocene or possibly the Late Cretaceous (Baltz, 1967, p. 85), whereas similar northeast shortening east of the Rio Grande rift began later, in the late Paleocene or early Eocene (Erslev, 2001). The pre-Eocene phases of northeast and northwest shortening near Durango (Ruf, 2000) may correspond temporally to east-northeast shortening east of the Rio Grande (Erslev, 2001).

The end of Laramide subsidence in the San Juan Basin occurred prior to deposition of the Chuska Sandstone in the southwest part of the basin. The base of the Chuska Sandstone overlies a low-relief erosion surface that beveled tilted Mesozoic strata along the Defiance monocline (Wright, 1956). The lower, fluvial part of the Chuska Sandstone contains an ash that has been dated at 34.75 ± 0.20 Ma (late Eocene) (Cather et al., *in press*). Thse fluvial beds

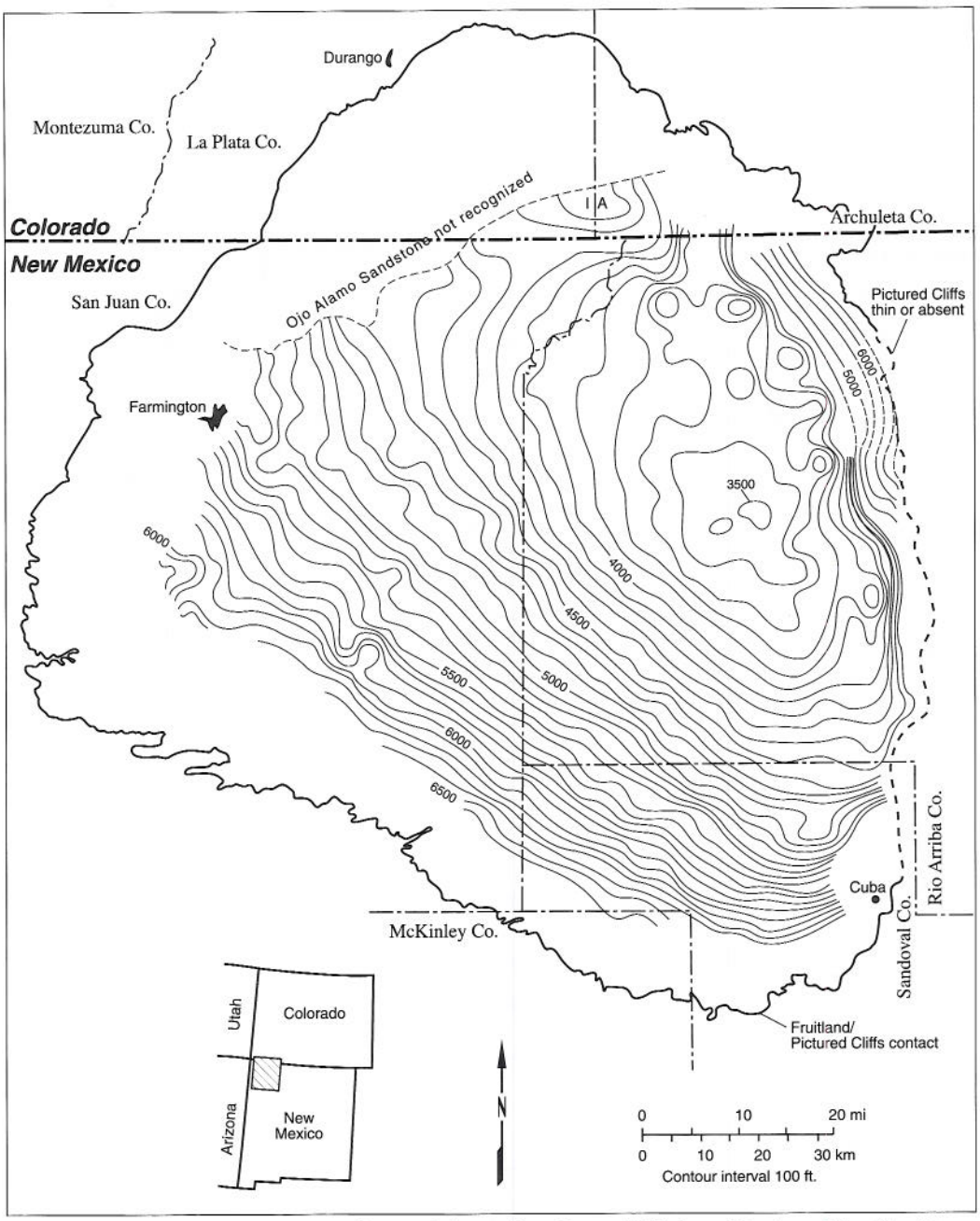

FIGURE 8. Structure contour map of base of the Tertiary (base of Kimbeto Member of the Ojo Alamo Sandstone), San Juan Basin. **IA**, Ignacio anticline. Modified from Ayers et al. (1991, fig. 7).

consist mostly of distal piedmont deposits that prograded south-southwestward from the San Juan Uplift following the cessation of Laramide subsidence in the San Juan Basin (Cather et al., *in press*).

Raton Basin

The Raton Basin of northeastern New Mexico and adjacent Colorado is a north-trending asymmetrical syncline that flanks the Sangre de Cristo Mountains on the east (Fig. 11). Structural relief on Proterozoic basement along the steep, western limb of the basin may be as much as 3.7–4.6 km, although a significant part of this relief is attributable to late Paleozoic tectonism (Baltz, 1965; Baltz and Myers, 1999). The synclinal axis of the basin extends southward to near Las Vegas, New Mexico (Fig. 1). Laramide deposits are preserved mostly in the northern part of the basin, north of Cimarron.

Inception and early subsidence

Prior to about 80 Ma, stratal accumulation rates in the axial portion of the basin in northeastern New Mexico were low, ~18–28 m/m.y. (Fig. 3, Table 2). Following approximately the deposition of the Apache Creek Sandstone Member of the Pierre Shale (~80 Ma), stratal accumulation rates in the Raton Basin tripled to ~82 m/m.y. (note that because of few age constraints in this part of the section, the actual age of the rate increase is not precisely known). Rates further increased to ~259 m/m.y. during deposition of the uppermost Pierre Shale and the regressive Trinidad Sandstone (~72–71 Ma). Part of this increase, however, may be related to a temporary increase in the rate of sedimentation due to passage of

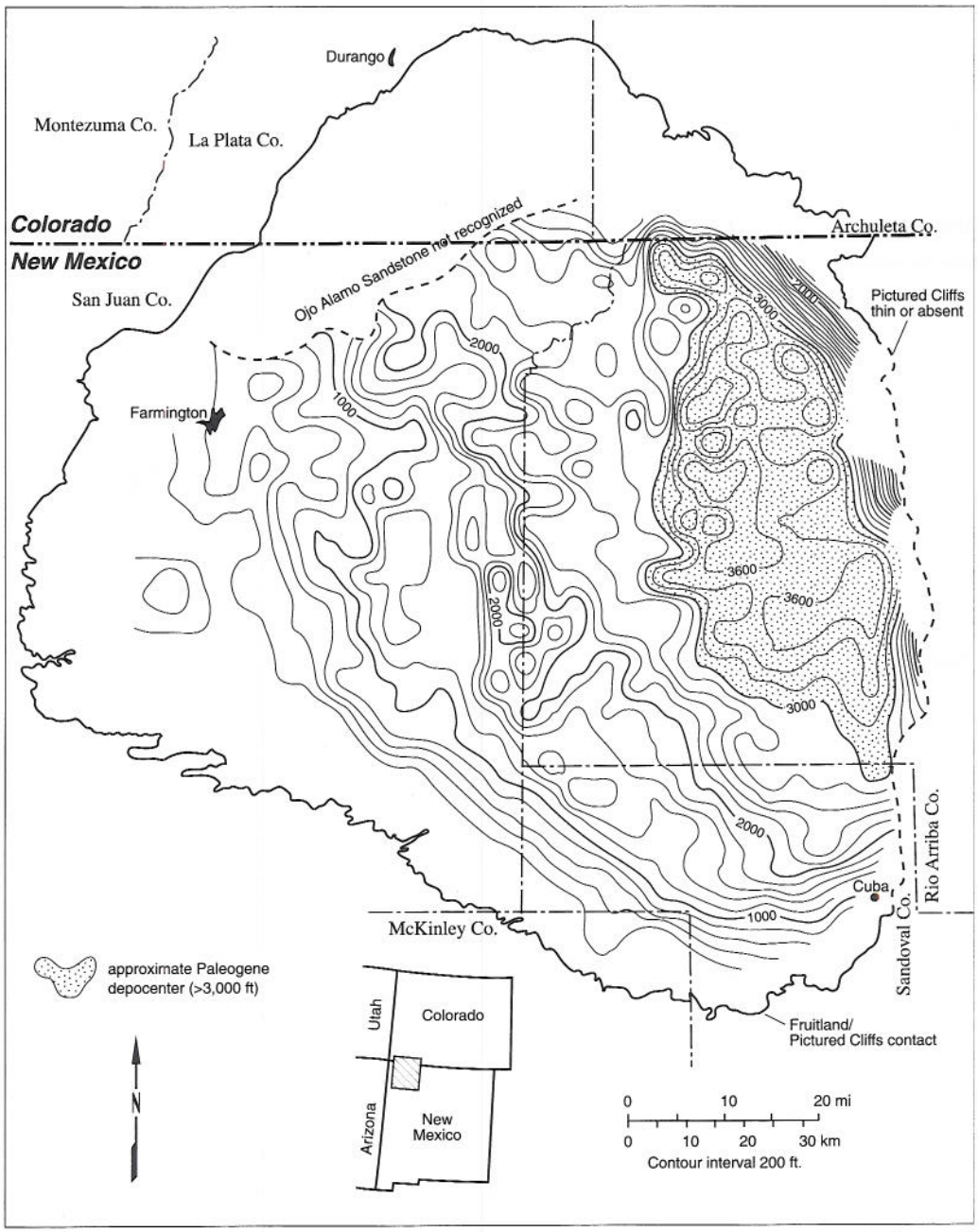

FIGURE 9. Isopach map of Tertiary strata (Kimbeto Member of the Ojo Alamo Sandstone, Nacimiento and San Jose Formations) in San Juan Basin. Note that upper surface of the isopach interval is modern topography. Modified from Ayers et al. (1991, fig. 18).

the shelf-margin clinoform as it prograded through the basin–axis area.

The Trinidad Sandstone consists of shore-zone deposits that record the final withdrawal of the Late Cretaceous epeiric seaway from northeastern New Mexico. It is correlative with the Pictured Cliffs Sandstone of the San Juan Basin and the Fox Hills Sandstone of the Denver Basin. The Trinidad Sandstone prograded as the result of sediment supply to a large deltaic center near Trinidad, Colorado (Flores and Tur, 1982). Deltaic sediments were redistributed by wave action to form strike-fed barrier-island coastlines to the north and south (Flores, 1987; Tyler et al., 1995). Episodes of vertical aggradation of the barrier-bar system induced by relative sea-level rise or decreased sediment supply produced elongate, thickened areas in the Trinidad Sandstone (Fig. 12). The northwest trend of these thickened zones in Colorado has long been recognized (Matuszczak, 1969; Dolly and Meissner, 1977), but the northeast trends in New Mexico have been recognized only recently (Tyler et al., 1995). The net sandstone map (Fig. 12) indicates that the shoreline prograded eastward during the final regression in the Raton Basin, not northeastward as in the San Juan Basin. The arcuate pattern apparent in Figure 12 suggests a point-source of sediment supply to the deltaic depocenter near Trinidad, Colorado, and that wave reworking and longshore transport were major processes in the adjacent barred coastlines.

Coal-bearing coastal plain deposits of the Vermejo Formation overlie and interfinger with the Trinidad Sandstone. The Vermejo is as much as 115 m thick. Coal beds in the Vermejo Formation formed predominantly in coastal swamps landward of Trinidad

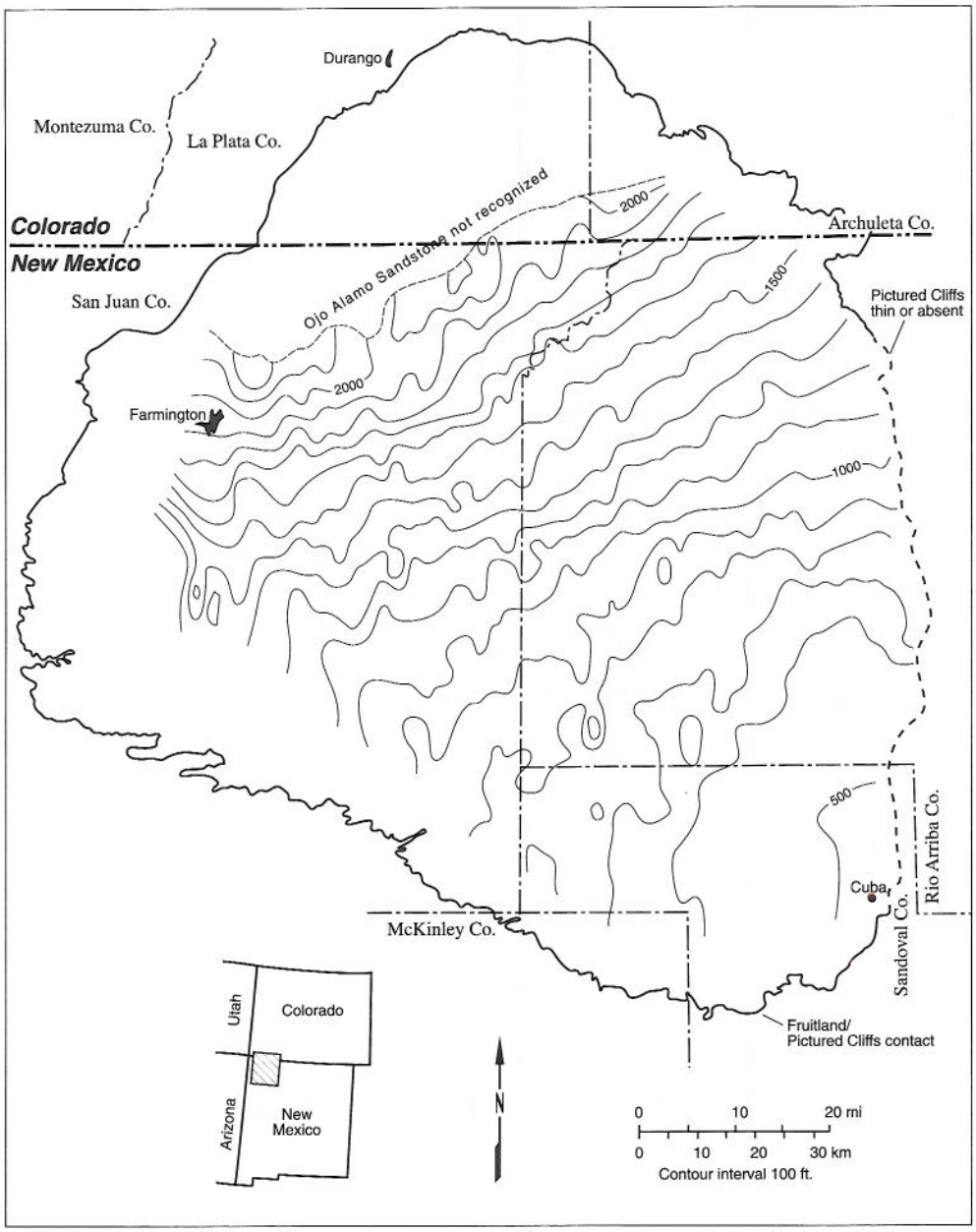

FIGURE 10. Isopach map of the stratigraphic interval between the Huerfanito Bentonite Bed and the base of the Paleocene Kimbeto Member of the Ojo Alamo Sandstone in the San Juan Basin. Note that if the slight southeastward depositional dip of the Kimbeto Member is neglected, this map approximates a structure contour map on the Huerfanito Bentonite Bed during earliest Tertiary time. Modified from Ayers et al. (1994, fig. 2.12).

barrier islands (Pillmore, 1969, 1976; Tyler et al., 1995). Net coal thicknesses in the Vermejo Formation (Fig. 13) form an arcuate map pattern similar to that of the underlying Trinidad Sandstone (Fig. 12), but one displaced slightly to the north.

Medial phase of subsidence

An unconformity representing a lacuna of poorly constrained duration separates the Vermejo Formation from the overlying Upper Cretaceous and Tertiary Raton Formation, and marks the end of the early phase of Laramide sedimentation in the Raton Basin and the beginning of the medial phase. Regardless of the magnitude of this unconformity, it is clear from Figure 3 that a substantial decrease in the net stratal accumulation rate must have occurred shortly after 71 Ma because the control point for the Cretaceous-Tertiary (K-T) boundary in the basal Raton Formation lies off the trend defined by the upper Pierre-Trinidad-Vermejo stratal accumulation rates. Thus this lower rate is, at least in part, accounted for by non-deposition or erosion. The sharpness of the Vermejo-Raton contact in the subsurface near the basin axis (Table 2) suggests that there the contact is also an unconformity, as has been interpreted in nearby outcrops (e.g., Pillmore and Flores, 1987; Speer, 1976). In contrast to the interpretations of some previous workers, the unconformity does not appear to record the beginning of Laramide deformation, but rather a quiescent interlude (zero accommodation) between two subsidence events. During this interlude the basin became overfull and a mildly erosive regime of across-basin-axis sedimentary transport prevailed. It

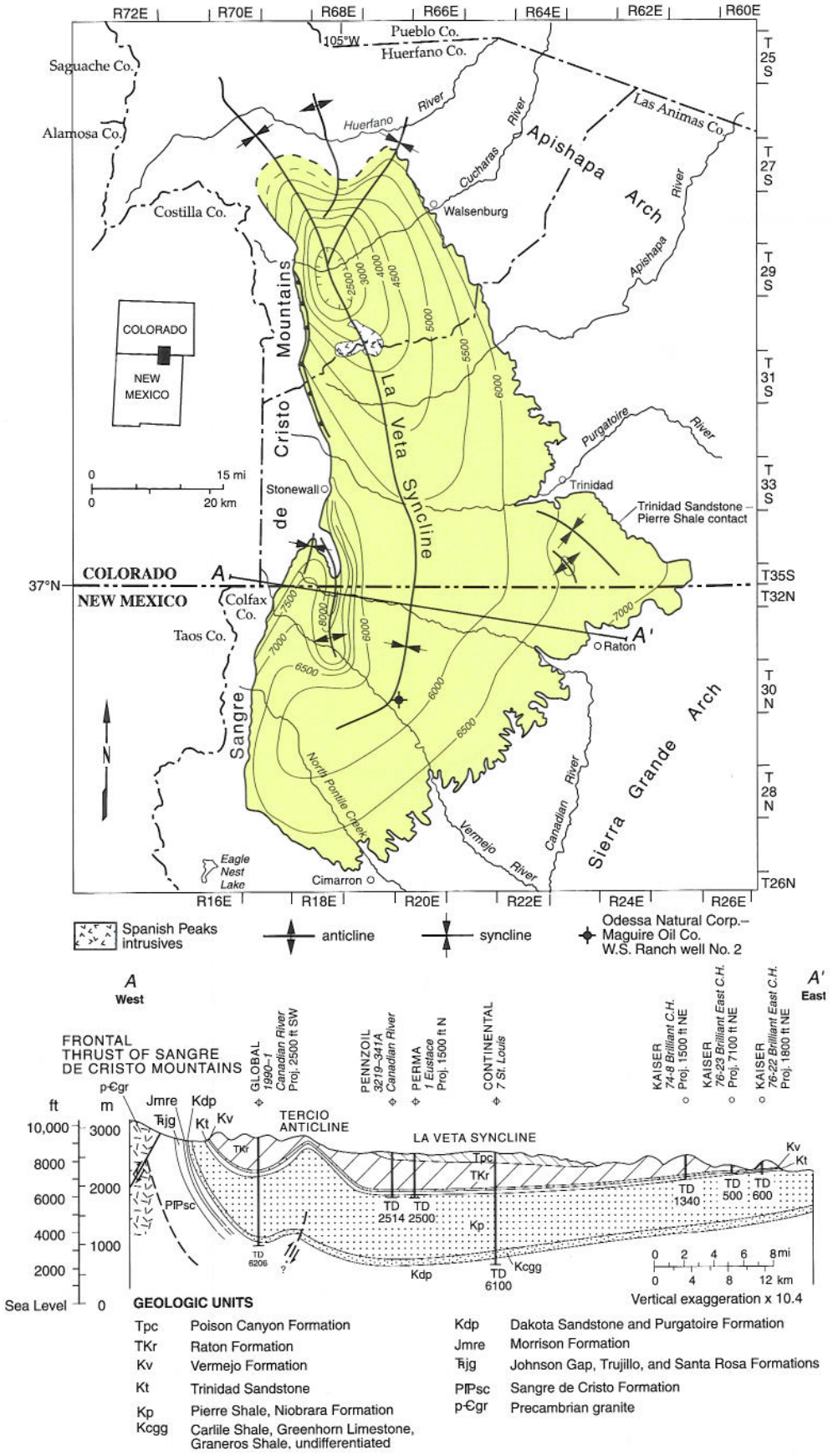

FIGURE 11. Structure contour map on the top of the Trinidad Sandstone, and cross section of Raton Basin. Note location of Odessa Natural Corporation-Maguire Oil Co. W. S. Ranch well No. 2, utilized in Table 2 and Figure 3. Modified from Tyler et al. (1995).

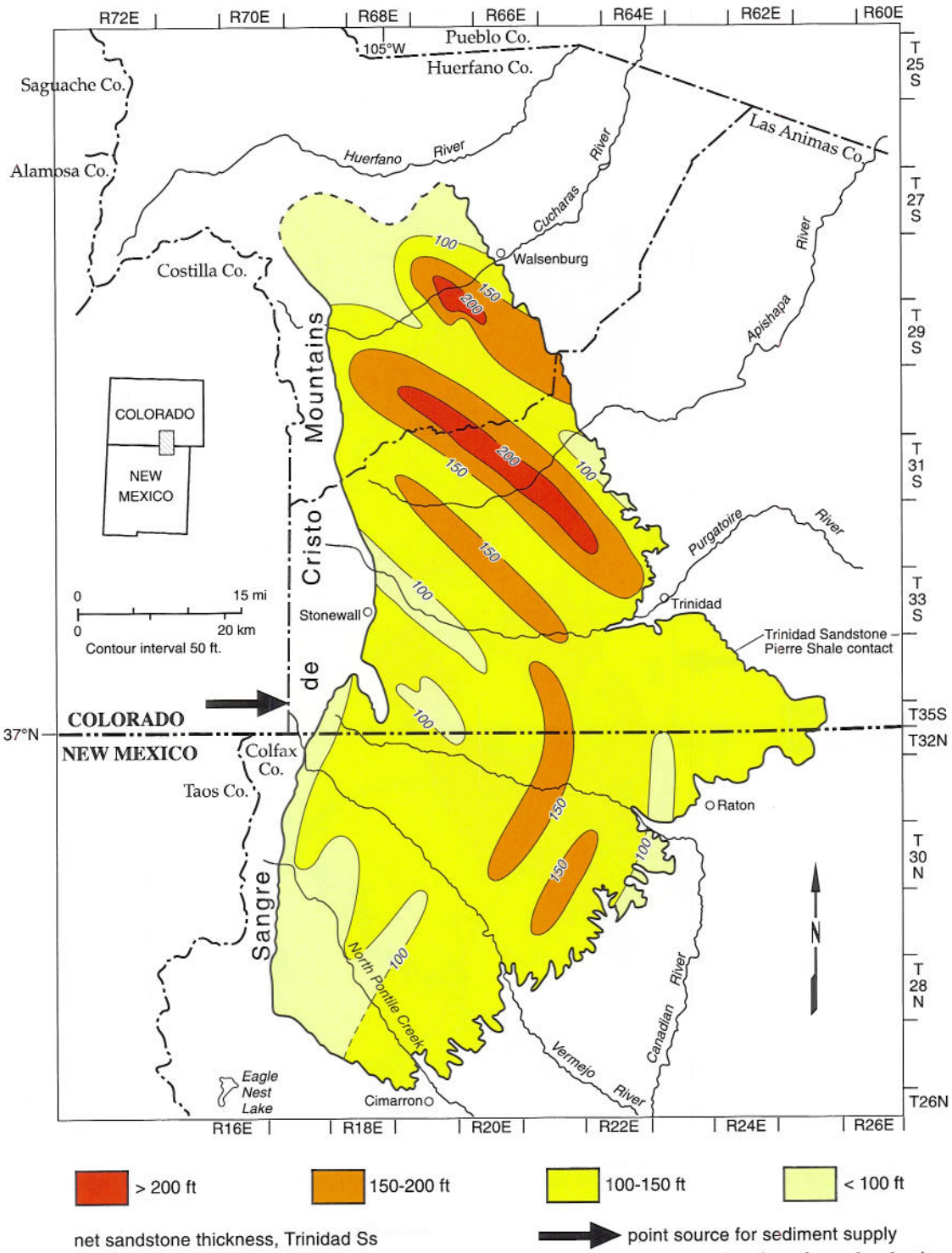

FIGURE 12. Net sandstone thickness map for Trinidad Sandstone, Raton Basin. Note location of postulated point source for sediment supply. Modified from Tyler et al. (1995, fig. 119).

is notable that, within geochronological constraints, the lacuna represented by the Vermejo-Raton unconformity (bracketed ~71–65.4 Ma) in the Raton Basin must be at least in part contemporaneous with that related to the Kirtland–Naashoibito (73.04–67 Ma) unconformity and/or Naashoibito–Kimbeto (~67–65 Ma) unconformity/condensed section in the San Juan Basin (Fig. 2A, C).

The Raton Formation consists in most places of a basal siliceous-pebble conglomerate with overlying sandstones and mudstones that are locally associated with coal beds (Flores and Pillmore, 1987). The K-T boundary and its associated iridium anomaly are present 81 m above the base of the Raton Formation in drill holes at York Canyon near the basin axis (Tschudy, 1973; Pillmore et al., 1984; Shoemaker et al., 1987). The K-T boundary (65.4 ± 0.1 Ma; Obradovich, 1993) is the only precise age constraint for uppermost Cretaceous through Paleocene strata in the Raton Basin; other, less precise constraints are derived from fossil floras in the Vermejo and Raton Formations (Ash and Tidwell, 1976) and palynomorphs (Tschudy, 1973; Newman, 1987).

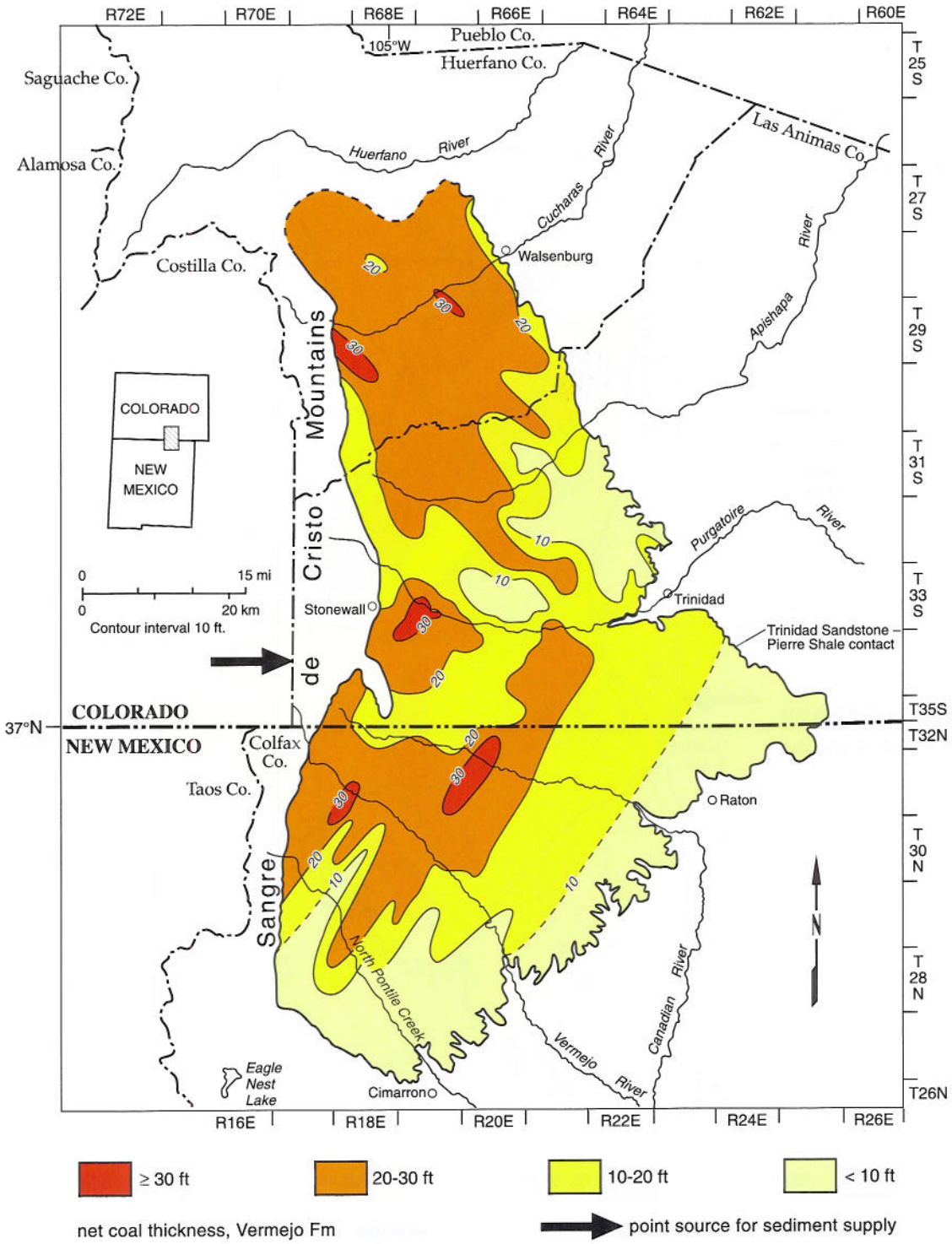

FIGURE 13. Net coal thickness map for Vermejo Formation, Raton Basin. Note location of postulated point source for sediment supply. Modified from Tyler et al. (1995, fig. 121).

The Poison Canyon Formation is an arkosic, coarse-grained, oxidized piedmont deposit that is in part laterally equivalent to, and overlies, the finer-grained, carbonaceous beds of the Raton Formation (Pillmore and Flores, 1990) (Fig. 2C). In the Huerfano Park area in the northernmost Raton Basin, a local erosion surface at the base of the Poison Canyon Formation bevels rocks as old as the Pierre Shale and Niobrara Formation (Johnson and Wood, 1956; Johnson, 1959). Largely Paleocene in age as shown by its intertonguing with the Raton Formation, the Poison Canyon thickens to the west at the expense of the Raton. It interfingers with the basal Raton Formation in the western part of the basin. There, the lower Poison Canyon Formation may be as old as Maastrichtian (Johnson and Wood, 1956; Pillmore and Flores, 1990). In a sense, the basal conglomerate of the Raton Formation is lithogenetically part of the Poison Canyon Formation lithosome. Because of its thin and discontinuous nature, however, it is mapped as part of the Raton Formation.

An unconformity divides the Poison Canyon Formation from

the overlying conglomerate, sandstone and mudstone of the Cuchara and Huerfano Formations, and is exposed even in the area of Eocene maximum subsidence near Spanish Peaks (Robinson, 1966; Johnson and Wood, 1956). This suggests the unconformity is basin-wide and is not restricted to areas peripheral to the area of maximum subsidence. The lacuna represented by the unconformity is poorly constrained due to lack of precise age control in the Poison Canyon Formation, but includes earliest Eocene and (possibly) late Paleocene time (Robinson, 1966). The pre-Cuchara unconformity in the Raton Basin is thus approximately correlative with the pre-San Jose unconformity in the San Juan Basin (Fig. 2A, C).

The combined Raton-Poison Canyon sequence comprises the medial phase (late Maastrichtian-Paleocene) of Laramide subsidence and accommodation in the Raton Basin. Because of poor age constraints, a detailed analysis of the relationships between tectonism, subsidence, and sedimentation is not yet possible. Based on relationships inferred for unconformities and associated conglomeratic strata at the base and top of the Raton-Poison Canyon sequence, the following hypothesis is proposed. After a period of non-accommodation and unconformity development that marked the top of the Vermejo Formation, a second phase of Laramide tectonic subsidence began in late Maastrichtian time. Initial accommodation was weak, resulting in slow accumulation of the widespread basal conglomerate of the Raton Formation. As accommodation increased and culminated relative to sediment supply, coarse-grained piedmont deposits (Poison Canyon Formation) became restricted to a narrow zone in the western part of the basin, proximal to the Sangre de Cristo Uplift. Fine-grained, locally carbonaceous sediments of the Raton Formation accumulated contemporaneously in the axial and eastern part of the Raton Basin. As rapid subsidence and accommodation waned, coarse-grained sediments (upper Poison Canyon Formation) were again able to prograde eastward across the basin. Development of a basin-wide unconformity at the top of Poison Canyon may reflect a cessation of accommodation that marked the end of the medial phase of Laramide subsidence in the Raton Basin.

Late phase of subsidence

The Eocene Cuchara, Huerfano and Farisita Formations represent the final phase of Laramide subsidence and sedimentary accommodation in the northern Raton Basin. With an aggregate thickness of more than 1500 m, these units have been variously interpreted to be superposed (Johnson and Wood, 1956; Johnson, 1959) or to be lateral facies equivalents (Briggs and Goddard, 1956; Robinson, 1966). The Cuchara and Farisita are commonly conglomeratic and locally contain clasts of basement-derived detritus more than one meter in length. The Huerfano and Farisita Formations have yielded vertebrate fossils of late Wasatchian and early Bridgerian age (Robinson, 1966) (~53–49 Ma; Woodburne and Swisher, 1995).

The locus of deposition in the Raton Basin migrated northward in a systematic fashion during Late Cretaceous-Paleogene time (Fig. 14). This migration has been attributed to diachronous thrust-sheet emplacement in the Culebra Range of the Sangre de Cristo Mountains by Lindsay (1998), although apatite fission-track cooling in the Culebra Range and elsewhere in the Sangre de Cristo Uplift (Kelley and Chapin, 1995) significantly post-dates the sedimentary fill of the Raton Basin. Alternatively, it is proposed here that a late Campanian-early Maastrichtian fluvial system was superimposed on the rising San Luis Uplift (west of the Picuris-Pecos fault) and initially provided a point-source of sediment supply for the regressive Trinidad Sandstone. This fluvial system would have cut a major paleocanyon as uplift proceeded, and this paleocanyon may have localized subsequent sediment supply as it was carried northward by Laramide dextral slip on the Picuris-Pecos fault. There is presently ~37 km of dextral separation of Proterozoic rocks and structures on the Picuris-Pecos fault, although how much of this is Laramide remains a contentious problem.

Galisteo-El Rito Basin

The late Laramide Galisteo-El Rito Basin lies between Chama, New Mexico, and the Albuquerque-Santa Fe area. Its fill comprises the Diamond Tail and Galisteo Formations in the south and the El Rito Formation and possibly parts of the Blanco Basin Formation in the north (Fig. 2B). The central part of the Galisteo-El Rito Basin is obscured by Neogene rift-related sedimentary rocks in the northern Albuquerque and Santo Domingo Basins and by Miocene-Pleistocene volcanic and volcaniclastic rocks of the Jemez volcanic field. The paleocontinuity of the Laramide basin beneath this covered region has been inferred by many workers (Spiegel, 1961; Baltz, 1978; Logsdon, 1981; Chapin and Cather, 1981; Lucas, 1984; Cather, 1992).

The Galisteo Formation (Stearns, 1943) in its original usage encompassed all of the strata above the Menefee Formation and below the volcaniclastic beds of the Espinaso Formation. Gorham (1979) and Gorham and Ingersoll (1979) subdivided the Galisteo into several informal members. The two lowermost of these (lower buff-pebbly sandstone and lower buff-sandstone and mudstone members) were subsequently recognized as an unconformity-bounded unit (Abbott et al., 1995) and renamed the Diamond Tail Formation (Lucas et al., 1997). The term Galisteo Formation was thereby restricted to the red-bed sequence that unconformably overlies the Diamond Tail Formation (Lucas et al., 1997).

The Diamond Tail Formation consists of a mostly drab sequence of sandstone, mudstone, and pebbly sandstone that ranges from a thin edge to 442 m thick at its type section near the ghost town of Hagan, New Mexico, about 40 km northeast of Albuquerque (Lucas et al., 1997). The Diamond Tail Formation is entirely fluviatile, and contains thick (5–10 m) channel sandstones that represent the deposits of major, probably extrabasinal, rivers. It rests with profound unconformity on the lower Campanian Menefee Formation. The Diamond Tail Formation thins markedly to the northwest, due both to syndepositional, southeastward thickening toward the intrabasin Tijeras-Cañoncito fault system and to northwestward erosional beveling prior to deposition of the Galisteo Formation (Abbott et al., 1995; Lucas et al., 1997). Paleocurrent directions have been variously interpreted to be south or southwestward (Gorham and Ingersoll, 1979) or northeastward (Cather et al., 2000; Cather et al., 2002). The only direct age constraint from the Diamond Tail Formation is a dentary fragment of *Hyracotherium* sp. (Lucas et al., 1997). This fossil indicates an early Eocene (Wasatchian) age for the upper part of the unit; the lower part of the Diamond Tail Formation is possibly as old as late Paleocene. The Diamond Tail Formation has been tentatively correlated with the Cuba Mesa and Regina Members of the San Jose Formation (Lucas et al., 1997).

The Galisteo Formation (*sensu* Lucas et al., 1997) is a variegated red-bed sequence of sandstone, mudstone, and conglomerate that is as much as 850 m thick at its depocenter near Hagan. It consists mostly of alluvial deposits that were derived from surround-

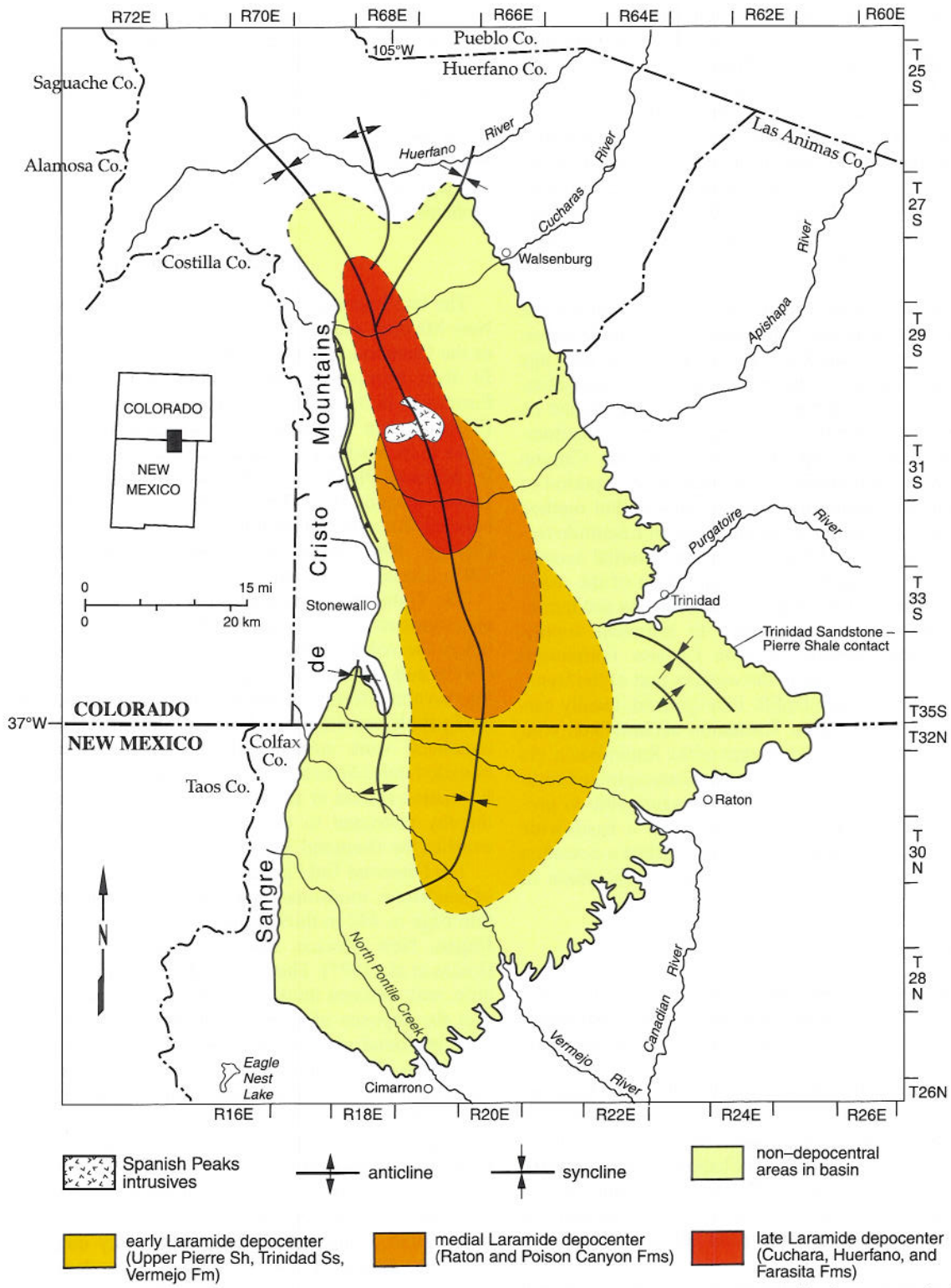

FIGURE 14. Map showing northward migration of approximate early, medial, and late Laramide depocenters in the Raton Basin. Modified from Lindsay (1998).

ing uplifts. The Galisteo overlies the Diamond Tail Formation with slight regional angular unconformity. The age of the Galisteo is Wasatchian-Duchesnian (Lucas, 1982; Lucas and Williamson, 1993); its deposition thus spanned most of the Eocene epoch. The lacuna represented by the Galisteo-Diamond Tail unconformity must be less than the duration of the Wasatchian land-mammal age (~6 m.y.; Woodburne and Swisher, 1995), as Wasatchian fossil mammals are present above and below the unconformity. The upper contact of the Galisteo Formation is gradational with the overlying volcaniclastic strata of the Espinaso Formation (upper middle Eocene-Oligocene; Gorham, 1979; Lucas, 1982). The age of this transition has been estimated using magnetic polarity stratigraphy to be about 38 Ma (Prothero and Lucas, 1996). The Espinaso Formation has yielded $^{40}Ar/^{39}Ar$ ages ranging from ~36

Ma to ~30 Ma (preliminary results reported by R. Esser, 2002, written commun.).

The Galisteo Formation in the Hagan area thins to the northwest by both syndepositional thickening and the effects of northwestward basal onlap (e.g., Gorham and Ingersoll, 1979, fig. 2; Lucas and Williamson, 1993, fig. 3). Paleoflow was generally toward the southwest, south, or southeast (Gorham and Ingersoll, 1979; Cather, 1992; Cather et al., 2000; 2002), although Galisteo Formation exposures near the Tijeras-Cañoncito fault system show evidence of fault-parallel (northeast or southwest) paleoflow (Abbott et al., 1995).

At the depocenter near Hagan, New Mexico, the combined thickness of the Diamond Tail and Galisteo Formations is approximately 1300 m (Gorham and Ingersoll, 1979). This thickness exceeds that of any other Paleogene depocenter in New Mexico [note, however, that the thickness of Paleogene strata in the northern Raton Basin near Spanish Peaks in Colorado (~1900 m) significantly exceeds that of the combined Diamond Tail-Galisteo interval]. Assuming that deposition of the Diamond Tail Formation began at about the Paleocene-Eocene boundary and neglecting the short but unknown hiatus represented by the unconformable Diamond Tail-Galisteo contact, then deposition of the Diamond Tail and Galisteo Formations occurred ~54–38 Ma. This corresponds to a stratal accumulation rate of ~81 m/m.y., comparable to the net Paleogene stratal accumulation rates in the San Juan Basin (~96–99 m/m.y.) but significantly less than latest Campanian-early Maastrichtian rates in the San Juan and Raton Basins (Fig. 3).

The southeast margin of the depocenter of the Galisteo Basin is marked by the Tijeras-Cañoncito fault system (Fig. 1; Ingersoll et al., 1990; Cather, 1992; Abbott et al., 1995) and, less certainly, by the southwest continuation of this fault system beneath the Albuquerque Basin of the Rio Grande rift (Cather, 1992). Both normal and reverse separation occurs locally on individual faults of the Tijeras-Cañoncito system, although normal separation seems to dominate in the northeast part of the fault system (Stearns, 1953, p. 491). Structural relationships and fault-kinematic data suggest that dextral oblique slip occurred on the Tijeras-Cañoncito fault system during the Laramide (Lisenbee, 1979, p. 96; Abbott et al., 1995; *in press*; Abbott, 1995). The Galisteo Basin has been interpreted to have formed as a southeast-tilted, transtensional half graben in a right-stepping releasing bend during late Laramide dextral wrenching along the eastern Colorado Plateau boundary (Cather, 1992; Abbott et al., 1995) or as part of a synclinal sag between paired thrust and back-thrust faults (Yin and Ingersoll, 1997).

An isolated outcrop of Galisteo Formation is exposed near St. Peter's Dome in the footwall of the Pajarito fault south of Los Alamos, New Mexico (Smith et al., 1970; Goff et al., 1990; Cather, 1992). It consists of an upward-coarsening redbed sequence of sandstone, mudstone and conglomerate that is as much as 630 m thick. The upper contact is an angular unconformity beneath middle Miocene beds of the Santa Fe Group; the lower contact is unexposed. The Galisteo Formation near St. Peter's Dome has not been directly dated. Paleocurrent measurements vary with stratigraphic position; they are generally southerly with the exception of those in the middle part of the unit which indicate northwest paleoflow (Cather, 1992, fig. 3). Large clasts of Proterozoic granite-gneiss in the upper part of the Galisteo Formation at St. Peter's Dome were interpreted by Cather (1992) to have been derived from a nearby Laramide uplift (Pajarito Uplift, Fig. 1) that was subsequently tectonically inverted to form the Española Basin of the Rio Grande rift.

The El Rito Formation was deposited in an elongate, north-south structural basin (El Rito Basin or Chama Basin) that developed between the Laramide Brazos Uplift on the east and the Nacimiento Uplift-Archuleta Anticlinorium on the west. The El Rito Basin appears to have been contiguous with the Laramide Galisteo Basin to the south. The El Rito Formation is a red-bed sequence of sandstone, conglomerate, and mudstone as much as 120 m thick (Smith, 1938; Bingler, 1968; Muehlberger, 1967). It unconformably overlies rocks as young as the Campanian Lewis Shale and as old as Proterozoic where it laps onto the Brazos Uplift. The El Rito Formation is disconformably overlain by the upper Eocene-Oligocene Conejos Formation and, to the south, the Miocene Abiquiu Formation. There are no direct age constraints or fossils known in the El Rito Formation. The El Rito shows evidence of generally southward paleoflow (Logsdon, 1981, Brister, 1992).

Using circumstantial evidence, Lucas (1984) argued that the El Rito Formation is middle Eocene, and that the Blanco Basin Formation nearby to the north is older and correlates with the lower Eocene San Jose Formation of the San Juan Basin. Brister (1992; see also Muehlberger, 1967, 1968), however, noted the possibility of correlation between the upper conglomerate of the Blanco Basin Formation and the El Rito Formation. An added complication is the interpretation of Baltz (1967, p. 51–52) and Smith (1992b, fig. 15B) that metaquartzite detritus in the San Jose Formation was derived from the Proterozoic rocks in the Brazos Uplift and subsequently transported westward across what is now the northern part of the El Rito Basin. No evidence for such westward paleoflow has been noted in the El Rito Formation (Logsdon, 1981; Brister, 1992), suggesting that an erosional regime of westward paleotransport may have predated El Rito aggradation. By the beginning of El Rito deposition, the divide between the San Juan and Galisteo drainage basins had shifted northward from near the latitude of Española, New Mexico, (Smith, 1992b, fig. 15) to near Chama, New Mexico (Brister, 1992). This shift presumably resulted from increased tectonic activity along the Nacimiento Uplift-Archuleta Anticlinorium and the Salado-Cumbres discontinuity of Baltz (1967) (see below). More work is needed on the Laramide structural and stratigraphic development of this critical area.

Baca Basin

The Baca Basin (Fig. 1) is a broad, shallow structural depression that formed in the southeast part of the Colorado Plateau late in the Laramide orogeny. It is bounded on the north by the Zuni Uplift, on the east by the Sierra Uplift, on the southeast by the Morenci Uplift, and on the southwest by the Mogollon Highland and Apache Uplift (Cather and Johnson, 1984; 1986). Basin-fill deposits are red beds that include (from west to east) the Mogollon Rim Formation (or gravels; Peirce et al., 1979; Potochnik, 1989, 2001), the Eagar Formation (Sirrine, 1956), and the Baca Formation (Wilpolt et al., 1946; Johnson, 1978; Cather, 1980). The nomenclature and geographic distribution of these units are discussed in Cather et al. (1994).

Although generally less than about 300 m thick, the fill of the Baca Basin is as much as 580 m thick in an area of intrabasin subsidence between the Hickman and Red Lake fault systems in west-central New Mexico (Fig. 1). Deposits of meandering streams in the basin fill were restricted to this actively subsiding area (Cather and Johnson, 1984; 1986). The remainder of the basin fill was largely deposited by braided streams, although a closed lacustrine system was present at times near the east end of the basin (Cather, 1983a). Paleoflow was generally eastward throughout the outcrop

areas of the Mogollon Rim, Eagar, and Baca Formations (Cather and Johnson, 1984; 1986).

The Baca Formation has produced middle to late Eocene vertebrate fossils of Bridgerian, Uintan, and Duchesnean age (Lucas, 1990; Lucas and Williamson, 1993). The lower contact of the basin-fill is a profound unconformity. In most places the subcrop is the Crevasse Canyon Formation or the Moreno Hill Formation, both of broadly constrained Late Cretaceous age (Fig. 2D). The regressive Gallup Sandstone (upper Turonian), the youngest well-dated unit below the unconformity, is about 320 m stratigraphically beneath the basal Eocene in the eastern Baca Basin (Tonking, 1957). Where basin-fill deposits onlapped the Mogollon Highland and the Sierra Uplift, underlying strata are as old as Pennsylvanian (Cather and Johnson, 1984; Potochnik, 1989). The upper contact of the basin-fill in the eastern Baca Basin is gradational with the overlying volcaniclastic strata of the upper middle Eocene-Oligocene Spears Group (Potochnik, 1989; Cather et al., 1994), which have yielded K–Ar ages as old as 39.6 ± 1.5 Ma and $^{40}Ar/^{39}Ar$ ages as old as 37.02 ± 0.15 Ma (Cather et al., 1987). Volcanic ashes from the upper part of the Mogollon Rim Formation, however, have yielded $^{40}Ar/^{39}Ar$ ages of about 33 Ma (Potochnik, 2001). These dates indicate that the age of top of the pre-volcanic section in the Baca Basin may be significantly younger to the west.

Carthage-La Joya Basin

The Carthage-La Joya Basin (Fig. 1) is a north-northwest-trending structural basin of late Laramide age that is bounded on the west by the Sierra Uplift (Cather, 1983b) and on the northeast by the Montosa Uplift (Cather, 1992). The basin is defined by scattered outcrops of Eocene red beds to the northeast, east, and southeast of Socorro, New Mexico (Johnson, 1978; Cather, 1980; Chapin and Cather, 1981; Cather and Johnson, 1984; 1986). Sediments were derived from rocks of Proterozoic and Paleozoic age exposed on the Sierra Uplift, now structurally inverted to form the Socorro Basin of the Rio Grande rift (Cather, 1983b).

The deposits of the Carthage-La Joya Basin have been assigned to the Baca Formation by most workers (Wilpolt et al., 1946; Johnson, 1978; Cather, 1980; Cather and Johnson, 1984; 1986; Spradlin, 1976; Beck and Chapin, 1994). Lucas and Williamson (1993), however, proposed the term Hart Mine Formation for the Eocene non-volcanic strata of the Carthage-La Joya Basin, based on the provenance of the sediments (mostly Paleozoic limestone and Proterozoic granite) and the paleogeographic separation of these strata from contemporaneous deposits of the Baca Basin. Cather et al. (1994) argued for abandonment of the Hart Mine terminology and retention of the Baca Formation because (1) the geographic limits of the Carthage-La Joya Basin are not well known due to effects of late Tertiary volcanism, erosion, and rifting, and (2) granite- and limestone-clast conglomerates are also present in the eastern part of the Baca Basin.

Fill of the Carthage-La Joya Basin is a red bed sequence of sandstone, conglomerate, and mudstone typically less than about 300 m thick. Deposition was by braided streams and aggrading arroyos; paleocurrents were generally eastward (Cather, 1983c; Cather and Johnson, 1984; 1986). The Baca Formation unconformably overlies Upper Cretaceous strata about 108–200 m above the upper Turonian Gallup Sandstone in the eastern Baca Basin and the Carthage-La Joya Basin. The Baca Formation is transitionally overlain by the upper middle Eocene-Oligocene Spears Group (Fig. 2E). The presence of Bridgerian fossils in the lower part of the basin fill (Lucas and Williamson, 1993) and the gradational contact relations with overlying volcaniclastic strata indicate the deposits of the Carthage-La Joya Basin are middle Eocene.

Sierra Blanca Basin

The least studied of the late Laramide basins of central and northern New Mexico is the Sierra Blanca Basin (Fig. 1). The fill of the Sierra Blanca Basin is the red beds of the Cub Mountain Formation, which crop out discontinuously mostly in the western and northern part of the basin. The Cub Mountain Formation (Bodine, 1956; Weber, 1964) as originally construed included all siliciclastic and volcaniclastic strata between the Mesaverde Group and the Sierra Blanca Volcanics. Cather (1991) restricted the term Cub Mountain to the lower, non-volcaniclastic part of the original unit and named the upper volcaniclastic strata the Sanders Canyon Formation (Fig. 2F).

The Cub Mountain Formation consists of about 760 m of sandstone, mudstone, and conglomerate at its type section in the western Sierra Blanca Basin. Entirely fluvial in origin, the Cub Mountain Formation shows evidence of northeastward paleoflow (Cather, 1991). Vertebrate remains from the lower part of the formation are Eocene, probably late Wasatchian or early Bridgerian (Lucas et al., 1989). The upper part of the Cub Mountain Formation grades into the overlying volcaniclastics of the Sanders Canyon Formation. The Sanders Canyon Formation has not been directly dated, but may be a distal equivalent of the upper middle Eocene Rubio Peak Formation (40–43 Ma, Seager and Clemons, 1975). The Cub Mountain Formation disconformably overlies the Upper Cretaceous Ash Canyon Member of the Crevasse Canyon Formation (Cather, 1991), about 250 m above the upper Turonian Gallup Sandstone.

LARAMIDE UPLIFT EVOLUTION

The record of orogeny that may be derived from uplifts is inherently different from that contained in associated basins. The stratigraphic record present in basins allows relatively precise ages and magnitudes to be assigned to subsidence events, and paleocurrent information faithfully records paleoslope orientations. In contrast, the dominance of erosional processes on uplifts progressively cannibalizes landscapes developed during earlier phases of uplift growth. In general, only the relative timing of faulting and folding events in an uplift is discernible, based largely on cross-cutting relationships. Consequently, much of the information about the absolute timing of uplift events is derived from adjoining basins. A technique that provides an exception to this rule is apatite fission-track (AFT) thermochronology, which can evaluate the approximate timing and rate of uplift independent of the stratigraphic record in adjacent basins. AFT ages can be thought of as the time of cooling through ~80–120°C. Given likely geothermal gradients, this represents the time the sampled volume of rock passed upward through ~3–5 km paleodepth. The AFT method has not yet been applied to all uplifts, however, and interpretation may be complicated by the effects of subsequent reheating. Furthermore, if erosion is sufficiently deep, the cooling record of an earlier uplift event may be removed.

To systematically evaluate the evolution of Laramide uplifts in southern Colorado and central and northern New Mexico, I have compiled a list of criteria that correspond to sequential stages of modeled, progressive uplift development (Fig. 15). Note that the six stages delineated in Figure 15 do not correspond in a simple way to the three phases of basin subsidence described previously. Diagnostic criteria for each stage of uplift are listed; most criteria

Diagnostic Criteria for Stages of Laramide Uplift Development

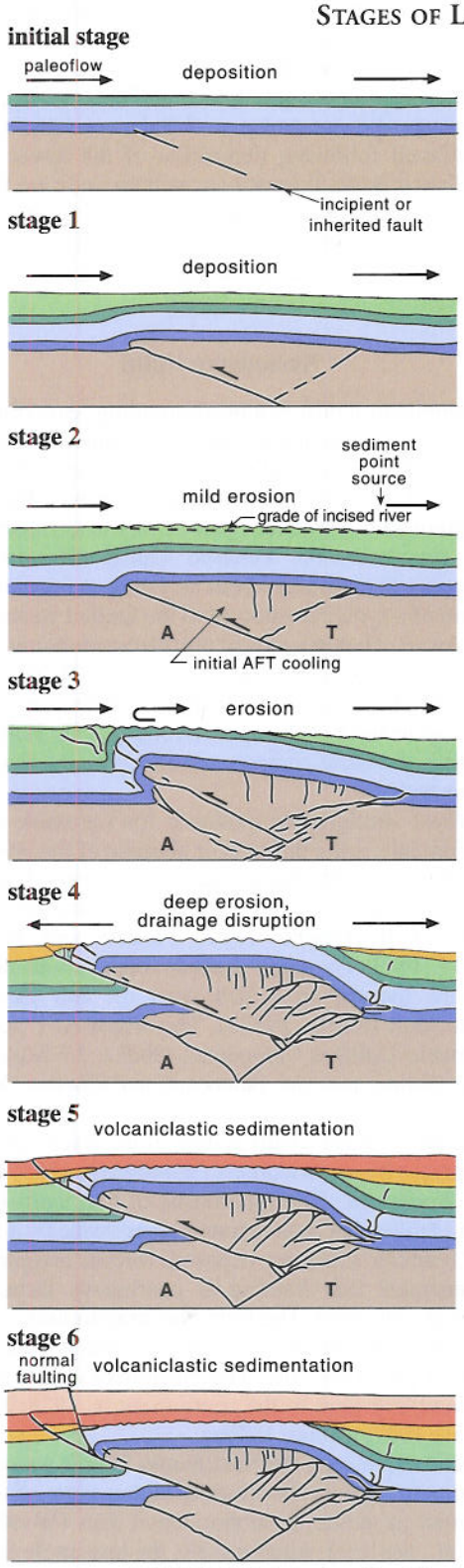

Initial Stage—Sedimentary aggradation related to regional foreland subsidence driven by thrust loading in areas to west. Sediment derived from distant thrust-related orogenic highlands. Sediment dispersal patterns determined by location of orogenic highlands relative to Late Cretaceous epeiric seaway.
EXAMPLE: Strata of Cenomanian through early Campanian age (~95–78 Ma) in northern New Mexico *(see text)*.

Stage 1—Incipient Laramide intraforeland deformation causes local variations in sedimentary accumulation rates within a regime of net aggradation. Sediment supply and transport determined by earlier foreland geometries.
EXAMPLES: Increased sedimentation rates during Campanian time (~78–71 Ma) in axial parts of San Juan and Raton Basins (Lewis Shale and upper Pierre Shale, respectively); NE thinning of Lewis Shale between northwestern New Mexico and southwestern Colorado *(see text)*.

Stage 2—Continued deformation results in areas of mild erosion over nascent Laramide uplifts and initial AFT cooling. Erosion and incision are sufficient to fix the position of paleorivers over rising uplifts, producing sedimentary point-sources where paleorivers pass downstream into adjacent basins. Sediment supply dominantly from distant Cordilleran sources with minor contribution of petrologically nondistinct detritus by recycling of earlier foreland–basin deposits (Mesaverde, Mancos) from local uplifts.
EXAMPLE: Point-sourced deposition of Trinidad Sandstone and Vermejo Formation in Raton Basin (~72–67 Ma) *(see text)*; initial AFT cooling (>74 Ma) of uplifted San Luis block west of Picuris–Pecos fault; (Kelley et al., 1992).

Stage 3—Continued rise of Laramide uplifts begins to expose older strata that contribute petrologically distinctive, locally derived detritus to adjacent basins. Beginning of local disruption of foreland sediment-dispersal patterns by rising intraforeland uplifts.
EXAMPLES: Quartzitic sand and chert pebbles recycled from Dakota Sandstone (?) in Vermejo and basal Raton Formations (uppermost Cretaceous) of the Raton Basin (Flores and Tur, 1981, p. 36; Flores, 1987, p. 263; Flores and Pillmore, 1987, p. 311).

Stage 4—Culminal phase of Laramide orogeny, characterized by widespread erosion of Paleozoic and Precambrian rocks from uplifted areas and rapid deposition of locally sourced clastics in intraforeland basins. Tectonic disruption of regional foreland sediment-dispersal patterns forms centripetal, locally closed drainages by Eocene time, following a pulse of deformation in early to middle Eocene.
EXAMPLES: Paleogene successions in San Juan and Raton Basins; Eocene basin-fill successions throughout central and northern New Mexico and southern Colorado.

Stage 5—Waning Laramide deformation continues during widespread, intermediate-composition volcanism. Non-volcanic detritus from active Laramide uplifts locally intercalated with andesitic volcaniclastic deposits. Persistence of Laramide basin geometries and subsidence patterns.
EXAMPLE: Upper Eocene (40–36 Ma) volcaniclastic deposits of the lower Datil Group in west-central New Mexico (Cather, 1990).

Stage 6—End of Laramide orogeny. Beginning of extensional tectonism causes bimodal volcanism and incipient structural inversion of Laramide uplifts, several of which will eventually invert to form basins of the Rio Grande rift by middle Miocene.
EXAMPLE: Volcanotectonic transition in west-central New Mexico at 36 Ma (Cather, 1990).

FIGURE 15. Criteria utilized in this study to delineate sequential stages of uplift development.

are derived from the sedimentary record in adjacent basins. These criteria help answer such questions as: When did incipient Laramide intraforeland deformation begin? When were Paleozoic and Proterozoic rocks initially exposed on rising Laramide uplifts? When did Laramide crustal shortening end and extensional deformation begin?

Because of the relative completeness of their Laramide stratigraphic records, the San Juan and Raton Basins contain the greatest amount of information about their adjacent uplifts. Although diagnostic criteria for uplift development are lacking for some

Laramide positive areas, a reasonably complete, composite evolutionary history is discernible.

San Juan Uplift

The San Juan Uplift (Needle Uplift of some workers) lies north of the San Juan Basin in southwestern Colorado (Fig. 1). A domal feature that is elongated to the northeast, the San Juan Uplift appears to be divided from the Archuleta Anticlinorium and the San Juan Sag by the northeastward projection of the Hogback monocline. The northern part of the uplift is largely obscured by the mid-Tertiary San Juan volcanic field.

Structural relief between the San Juan Uplift and the deepest part of the San Juan Basin is at least 6100 m (Kelley, 1955). An unknown part of this relief may be the result of igneous doming in the San Juan Uplift (Kelley, 1955; Larsen and Cross, 1956). Laramide igneous activity occurred between ~74–60 Ma in the Four Corners area (Mutschler et al., 1987; Semken and McIntosh, 1997).

The structural development of the San Juan Uplift is not well constrained. The Laramide uplift formed along the southwest margin of the Uncompahgre Uplift of late Paleozoic age. Initial Laramide development probably began with northwest shortening across the Hogback monocline (Erslev, 1997; Ruf, 2000) in the late Campanian. Magmatism in the southwestern part of the Colorado Mineral Belt began at about the same time. Siliceous pebbles in the basal McDermott Member of the volcaniclastic Animas Formation may indicate exposure of the Dakota Sandstone or Burro Canyon Formation during the Late Cretaceous (Dickinson et al., 1968) (Fig. 15, stage 3). Detrital input from Paleozoic and Proterozoic sources during deposition of the Naashoibito Member (uppermost Cretaceous) of the Ojo Alamo Sandstone (Baltz et al., 1966; Lehman, 1985), Animas Formation (Upper Cretaceous-Paleocene), and the lower Paleocene Kimbeto Member of the Ojo Alamo Sandstone (Lehman, 1985; Sikkink, 1987) is indicative of deep erosion north and northwest of the San Juan Basin (Fig. 15, stage 4).

Archuleta Anticlinorium

The Archuleta Anticlinorium (or Gallina-Archuleta arch) trends north-northwest and presently divides the San Juan Basin from the San Juan Sag. The Archuleta Anticlinorium is asymmetrical; its steep southwestern limb faces the San Juan Basin. Structural relief on the Dakota Sandstone between the Archuleta Anticlinorium and the deep part of the San Juan Basin is ~2450 m (Craigg et al., 1989, fig. 6). Structural relief between these same areas measured on the top of Proterozoic basement, however, is significantly greater (Brister and Chapin, 1994, fig. 6) because the Archuleta Anticlinorium formed part of the Uncompahgre Uplift of late Paleozoic age.

Superimposed on the Archuleta Anticlinorium are numerous lesser folds and faults. Many of the folds are asymmetrical; some have been demonstrated to be basement-cored by drilling (Baltz, 1967, p. 78–80). It is unclear whether the Archuleta Anticlinorium terminates against, or folds, the Hogback monocline to the northwest. To the southeast, the Archuleta Anticlinorium and its subsidiary faults and folds end near the Salado-Cumbres discontinuity of Baltz (1967, fig. 26) (Fig. 16). Proprietary industry seismic data described by Taylor and Huffman (1998) suggest that the Archuleta Anticlinorium is at least locally underlain by southwest-directed thrust faults.

Initial Laramide structural development of the Archuleta Anticlinorium began ~78–75 Ma, as shown by the previously described seaward thinning of the Lewis Shale between the San Juan Basin and San Juan Sag (Fig. 15, stage 1) and the stratigraphic omission of the Pictured Cliffs Sandstone along the southwest limb of the southern part of the anticlinorium (Baltz, 1967; p. 19). Major uplift, however, did not occur until Paleocene and Eocene time. Uplift continued following deposition of the lower Eocene San Jose and Blanco Basin Formations, as both units are folded on the flanks of the anticlinorium (Dunn, 1964, fig. 8). Structural development of the Archuleta Anticlinorium ceased prior to deposition of the volcaniclastic Conejos Formation in the late Eocene-early Oligocene (Brister and Chapin, 1994).

Nacimiento Uplift

The Nacimiento Uplift is a north-trending, east-tilted basement block that bounds the southeast part of the San Juan Basin (Fig. 16; Woodward, 1987). Structural relief on Proterozoic basement from the high part of the uplift to the adjacent San Juan Basin is at least 3050 m, although a significant part of this is attributable to a late Paleozoic precursor, the Peñasco Uplift (Woodward, 1996). Steeply dipping to overturned beds as young as Eocene occur in the eastern limb of a syncline adjacent to the faulted western margin of the uplift. An en echelon series of northwest-plunging growth folds that may have begun in the Late Cretaceous (Baltz, 1967, p. 85), but mostly developed synchronously with Paleocene-Eocene sedimentation, occur west of the uplift (Kelley, 1955; Baltz, 1967) and are indicative of dextral components of slip on the range-bounding Nacimiento fault.

The earliest stratigraphic evidence for Laramide uplift of the Sierra Nacimiento is the thinness or absence of the late Campanian (~75 Ma) Pictured Cliffs Sandstone in the steeply dipping to overturned eastern limb of the basin-margin syncline that parallels the Nacimiento fault (Baltz, 1967; Fassett and Hinds, 1971; Woodward, 1987). By early Eocene time, south-flowing paleorivers were focused in a belt west of, and parallel to, the Nacimiento fault (Smith, 1992b). The oldest AFT cooling age in the Nacimiento Uplift is Campanian (80.8 ± 7.5 Ma); most of the remaining cooling ages are Paleocene and Eocene (Kelley et al., 1992).

The western boundary fault system of the Nacimiento Uplift has been interpreted by some workers (Woodward, 1987; Woodward et al., 1992; Woodward, 1996) to consist of two faults (Pajarito and Nacimiento faults) that are separated along strike by a gap in which unfaulted Permian strata are exposed. Recent mapping, however, has demonstrated that faulting is continuous through this gap (Pollock et al., *in press*). The term Nacimiento fault is used herein to denote the continuous western boundary structure of the Nacimiento Uplift (Fig. 16). The Nacimiento fault is contiguous with the Sand Hill fault to the south (Santos, 1975; Kelley, 1977; Cather et al., 1997; Cather, 1999a).

In surficial exposures, the Nacimiento fault is generally steep to subvertical, although the structurally higher parts of the fault may locally flatten to gentle or subhorizontal dips (Woodward, 1987; Pollock et al., *in press*). Alternatively, the low-angle fault may represent the slip surface of a younger landslide (E. H. Baltz, written commun., 2001). The general steepness and linear trace of the Nacimiento fault has led many previous workers (including the writer) to assume that horizontal shortening across the range front was minor. Gravity modeling and construction of balanced cross-sections across the western range front and adjacent parts of the San Juan Basin by Pollock et al. (*in press*), however, have pro-

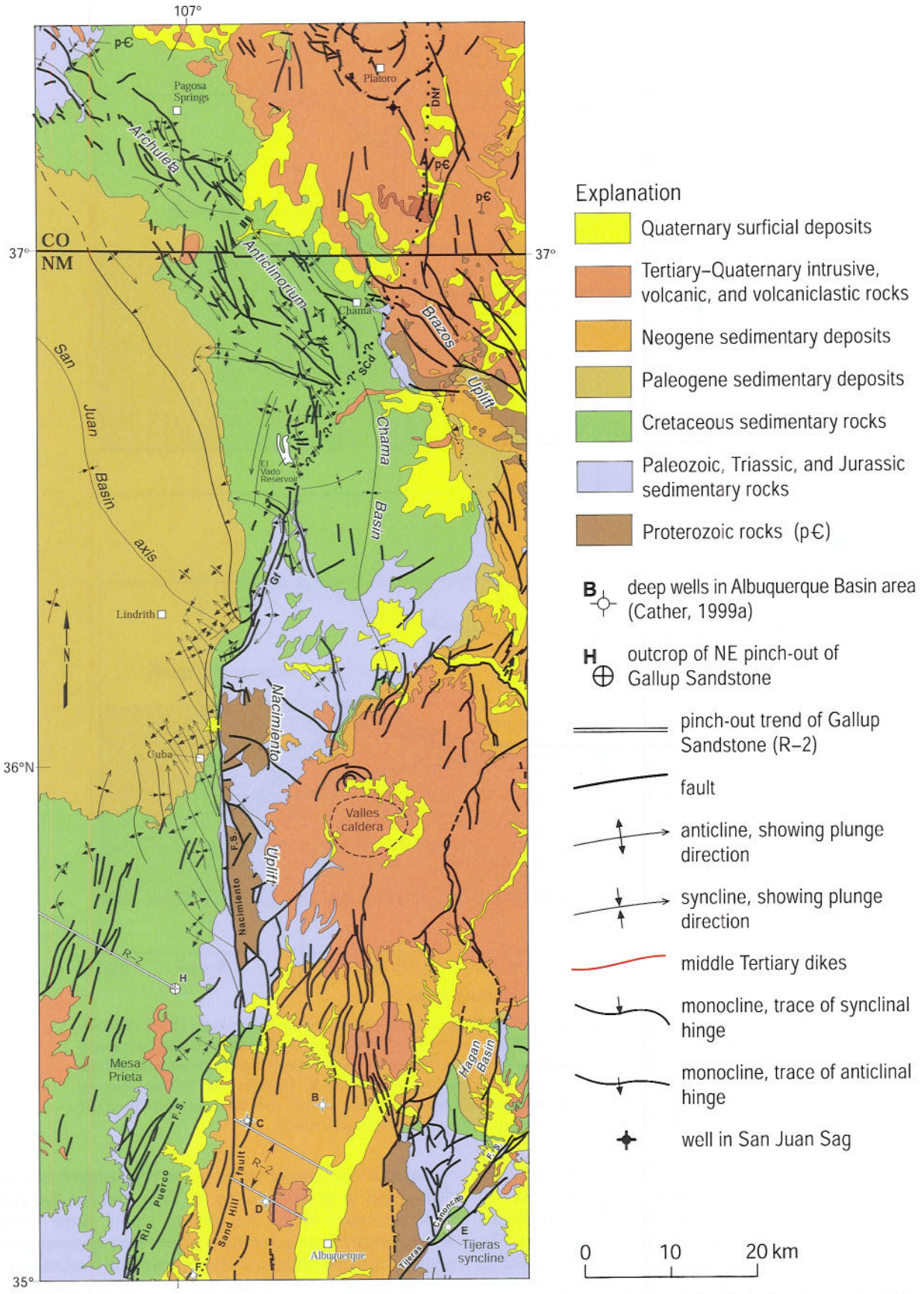

FIGURE 16. Simplified geologic map of the eastern San Juan Basin, Nacimiento Uplift, Archuleta Anticlinorium, and adjoining areas. **Gf**, Gallina fault; **SCd**, Salado-Cumbres discontinuity, **DNf**, Del Norte fault. Modified from Steven et al. (1974), Baltz (1967), and Cather (1999a).

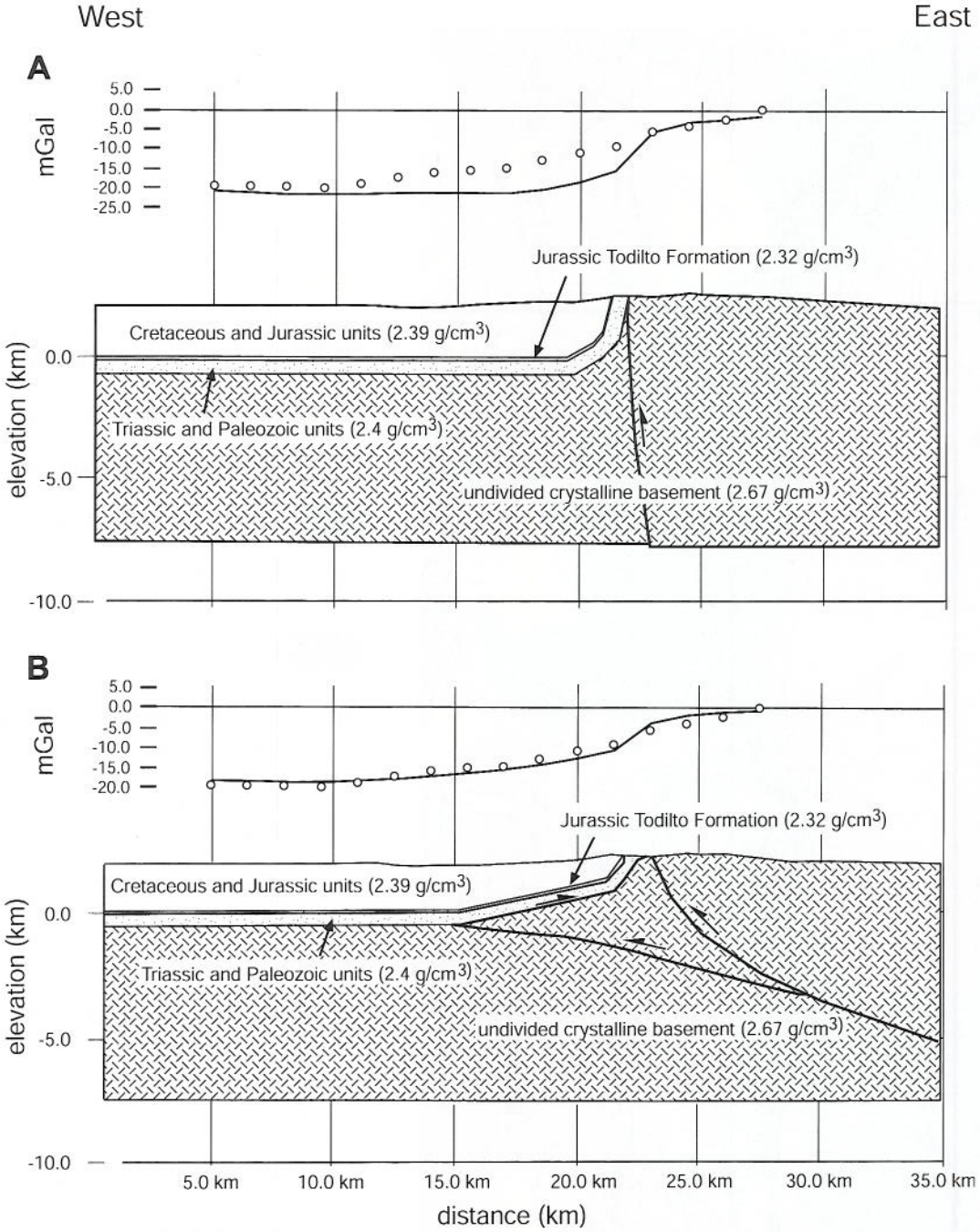

FIGURE 17. Gravity and structural models of the eastern San Juan Basin and the Nacimiento Uplift (Pollock et al., *in press*). **A**, Upthrust interpretation of Woodward (1987). Note poor fit between measured complete Bouguer anomaly values (circles) and calculated complete Bouguer anomaly profile (solid line) and the lack of structural balance in the cross section. East-west shortening is minimal. **B**, Triangle-zone interpretation of Pollock et al. (*in press*). Note good fit between observed (circles) and calculated (solid line) complete Bouguer anomaly values. This model requires approximately 7 km of east-west shortening.

duced some intriguing new concepts: (1) the Nacimiento fault system may sole downward into an east-dipping master thrust, the tip of which is blind and lies beneath the Phanerozoic strata of the San Juan Basin about 8 km west of the Nacimiento fault trace (Fig. 17); and (2) a west-tilted basement wedge between these faults is responsible for the observed lack of a steep gravity gradient along the Sierra Nacimiento front. Based on their model, Pollock et al. (*in press*) calculate an east-west (range-normal) component of shortening of about 7 km (Fig. 17).

Based on en echelon folds in the southeastern San Juan Basin that appear to be cross-cut by the tight syncline that parallels the western border of the Nacimiento Uplift, some workers have inferred that Laramide strike-slip preceded shortening and development of major structural relief across the Nacimiento fault system (Woodward, 1987; Pollock et al., *in press*), despite the fact that the en echelon folds formed relatively late in the Laramide. In a contrasting analysis, Erslev (2001) used Laramide minor fault data to interpret that east-northeast shortening occurred first, followed

by more oblique (northeast) shortening. Erslev's observations are in accord with interpretations of sequential Laramide deformation elsewhere in New Mexico (Chapin and Cather, 1981, 1983; Erslev, 1999, 2001). A third possibility, favored by the writer, is that the en echelon folds formed contemporaneously with the development of major structural relief on the range front during middle and late Laramide deformation. This interpretation is supported by the synchroneity of three events: (1) a development of greater shortening of the San Juan Basin-Archuleta Anticlinorium relative to the Nacimiento Uplift-Chama Basin area, which requires dextral slip between these regions (Baltz, 1967) during the Paleogene; (2) dextral slip on the Nacimiento fault, as shown by en echelon folds that exhibit growth relationships with Paleocene and early Eocene strata (Baltz, 1967), was largely Paleogene; and (3) the dominance of Paleocene-Eocene AFT cooling ages in the Nacimiento Uplift (Kelley et al., 1992) indicate that most of the structural relief was attained in the Paleogene.

The magnitude of the dextral strike-slip along the western margin of the Nacimiento Uplift has been a topic of much debate. Baltz (1967) used the apparent offset of en echelon folds to estimate 5 km of dextral displacement along the Nacimiento fault. Woodward et al. (1992) argued that such correlation of fold axes is ambiguous and therefore cannot be used to estimate lateral offset. Woodward et al. (1992) instead preferred the <2 km offset estimate of Slack and Campbell (1976) for the Rio Puerco fault system, a series of en echelon normal faults bounded on the east by the Sand Hill fault (Fig. 16), a southward continuation of the Nacimiento fault system (Cather, 1999a). The estimate of Slack and Campbell (1976), however, was based on the summation of heave across en echelon faults of the Rio Puerco fault system. Their technique did not evaluate the potential for dextral slip on the Rio Puerco faults or the through-going Sand Hill-Nacimiento fault system. Karlstrom and Daniel (1993) estimated ~25 km dextral offset of aeromagnetic anomalies across the Nacimiento fault system, which they attributed largely to Laramide deformation. Cather (1999a) noted that the seaward regressive limit of the Turonian Gallup Sandstone is deflected dextrally 20–33 km across the Sand Hill-Nacimiento fault system, and argued that the deflection was the result of Laramide strike-slip. Pollock et al. (*in press*) interpreted 3–15 km of dextral separation of Proterozoic lithologies across the Nacimiento fault, which they regarded as the net product of Proterozoic, late Paleozoic, and early Laramide displacements.

To the north, the Nacimiento fault bends to the north-northeast to become the Gallina fault. The Gallina fault is subvertical and alternates from west-down to east-down along its trace (Baltz, 1967; Woodward et al., 1992). It was interpreted by Baltz (1967) to be a dextral strike-slip fault with small but unspecified displacement. Linkage between the Nacimiento and Gallina faults, and the fact that the Gallina fault is not strongly contractional or extensional, implies that the Gallina fault is subparallel to the convergence direction between the San Juan Basin and the Nacimiento Uplift. The Gallina fault is subparallel to the interpreted net Laramide relative motion vector between the Colorado Plateau and cratonic North America of Chapin and Cather (1981, 1983) and Cather (1999a), and is in the correct orientation for dextral shear relative to the dominant northeast shortening direction as shown by the orientation of folds in the eastern San Juan Basin and in the Archuleta Anticlinorium (Fig. 16).

The Gallina fault appears to terminate northward in the area south of El Vado reservoir (Fig. 17), where it splays into a closely spaced, polygonal set of small-displacement faults (Landis and Dane, 1967). The north-northeastward projection of the Gallina fault in the El Vado-Chama area corresponds to an enigmatic and poorly exposed segment of what Baltz (1967) termed the Salado-Cumbres discontinuity. Passages of the excellent original description of the discontinuity (Baltz, 1967, p. 83–84) are quoted below, along with comments by the writer in brackets.

"*The Nacimiento and Gallina faults and the eastern margin of the Archuleta anticlinorium mark parts of a major regional structural discontinuity. The two faults themselves are sharp and easily recognized as a discontinuity, but north of the surface termination of the Gallina fault there is no equivalent single structural feature that delineates the discontinuity. However, the patterns of deformation are considerably different on either side of a slightly curved line projected north-northeastward from the northern termination of the Gallina fault. The folds and faults of the Archuleta anticlinorium do not terminate abruptly at the north-northeast-trending* [dotted and queried boundary on Figure 16] *shown as the east boundary of the anticlinorium north of the Gallina fault; nevertheless, many of the structural features do terminate very near this boundary, and the structural grain of the Chama basin at the southeast is dissimilar to that of the anticlinorium.*

The line or band of discontinuity can be projected north-northeast past the northwest-plunging end of the Brazos uplift and the southeast end of the San Juan sag, but it is lost beneath the Tertiary rocks of the San Juan Mountains volcanic field in the vicinity of Cumbres Pass north of the Colorado boundary. The total length of the discontinuity from the vicinity of the place where the Rio Salado crosses the south end of the Nacimiento uplift to the vicinity of Cumbres Pass is almost 110 miles [175 km]. *The structural discontinuity is here called the Salado-Cumbres structural discontinuity. . . .The San Juan sag and the northern part of the Brazos uplift in Colorado are buried beneath the San Juan Mountains volcanic field, and it is not known how far the discontinuity persists to the northeast from Cumbres Pass. Precambrian rocks lying directly beneath the Tertiary Potosi Volcanic Group* [Conejos Formation] *are exposed at a few places along the Conejos River in T. 33 N., Rs. 5 and 6E. (Larsen and Cross, 1956, pl. 1), northeast of Cumbres Pass in Colorado. These Precambrian rocks may be in the buried northern part of the Laramide Brazos uplift. Therefore, the discontinuity might persist, beneath the volcanic rocks, at least as far northeast as the westernmost outcrops of Precambrian rocks on the Conejos River.* [Subsequent drilling has shown (Brister and Chapin, 1994) that the discontinuity, represented by the Del Norte fault, resumes a northerly strike and delineates the eastern boundary of the San Juan Sag at least as far north as the latitude of Saguache, Colorado (Fig. 18).] . . .

The differences in amount of shortening between the northwest-alined San Juan basin and the north-alined Nacimiento and French Mesa-Gallina uplifts were accommodated mainly by right shift on the Nacimiento and Gallinas faults. The folding and crumpling of the Archuleta anticlinorium that caused a small amount of shortening in a northeasterly direction seem to imply some right shift between the anticlinorium and the Chama basin. If the shift took place along a deep-seated shear zone in the basement rocks, the overlying sedimentary blanket would have been twisted and dragged above the shear zone . . ."

The subsurface geometry of the Nacimiento fault system, and the extent of its regional interconnectivity with other Laramide faults, has major implications with regard to the allowable magnitude of strike slip on the Nacimiento fault system. Many previous workers (the writer included) considered that the apparent steep dip of the Nacimiento fault system was compatible with only minor amounts of fault-normal contraction. Such a geometry

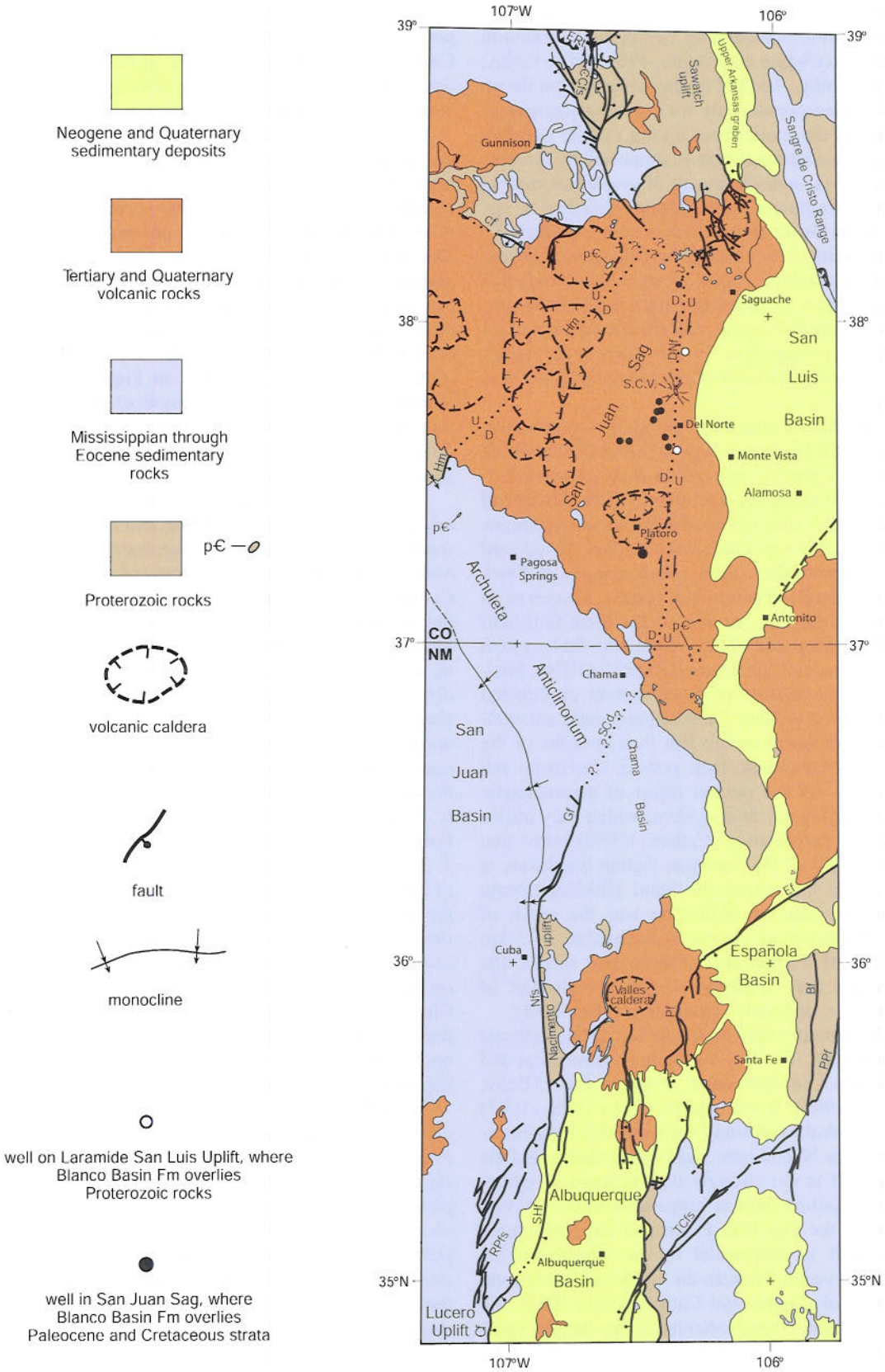

FIGURE 18. Simplified geologic map showing possible linkage between Del Norte fault (**DNF**), Salado-Cumbres discontinuity (**SCd**), Gallina fault (**Gf**), Nacimiento fault system (**Nfs**), and Sand Hill fault (**SHf**). Other abbreviations are **ERt**, Elk Range thrust; **CCfs**, Castle Creek fault system; **Hm**, Hogback monocline; **S.C.V.**, Summer Coon volcano; **Cf**, Cimarron fault; **Ef**, Embudo fault; **Bf**, Borrego fault; **Pf**, Pajarito fault; **TCfs**, Tijeras-Cañoncito fault system; **RPfs**, Rio Puerco fault system. Well control in eastern San Juan Sag from Brister and Chapin (1994).

would dictate that any major horizontal relative motion between the eastern San Juan Basin and the Nacimiento Uplift necessarily would be nearly parallel to the north-striking Nacimiento fault. As correctly pointed out by Baltz (1967, fig. 21), dextral strike-slip on the Nacimiento fault would create extension where the Nacimiento fault bends north-northeast to become the Gallina fault (Fig. 16). Although there are numerous normal faults scattered throughout the Nacimiento Uplift (Woodward, 1987), the cumulative heave on these faults is not large and therefore cannot balance more than modest amounts of strike-slip dilation at a releasing bend at the north end of the uplift.

The results of Pollock et al. (*in press*) have important implications for regional tectonics. If their estimate of ~7 km for the east-west component of shortening between the eastern San Juan Basin and western Nacimiento Uplift is resolved into a vector parallel to the north-northeast striking Gallina fault, ~16.5 km of dextral separation would be predicted for the Gallina fault and ~15 km dextral separation for the Nacimiento fault (Fig. 19). The dextral separation estimate for the Nacimiento fault (15 km) is compatible with the range of net offset given by Proterozoic lithologies (3–15 km; Pollock et al., *in press*), but is somewhat less than the deflection of the Gallup Sandstone pinchout (20–33 km; Cather, 1999a) and the offset of basement aeromagnetic anomalies (~25 km, Karlstrom and Daniel, 1993). The biggest problem with this construction is that the predicted dextral offset along the Gallina fault (~16.5 km) is too large to be balanced by shortening northwest of the fault, if the fault ends near El Vado Reservoir (Fig. 16). If, on the other hand, there is strike-slip linkage along the Salado-Cumbres discontinuity with the Del Norte fault in southern Colorado, then the construction may be viable. Despite poor exposure, it seems unlikely that a single, throughgoing shear exists in surficial exposures along the discontinuity in the El Vado-Chama area. It is possible, however, that the Salado-Cumbres discontinuity in this area may have accommodated broadly distributed dextral wrenching. Perhaps the polygonal pattern of faults described by Landis and Dane (1967) near the termination of the Gallina fault results from regional detachment, interstratal shear and vertical axis rotations above a basement strike-slip fault. If so, such rotations should be testable through paleomagnetic analysis. Detachment may have been facilitated by thick (>30 m) gypsum of the Todilto Formation in the subsurface near the termination of the Gallina fault (Ash, 1958; Cather, 1999a, fig. 5).

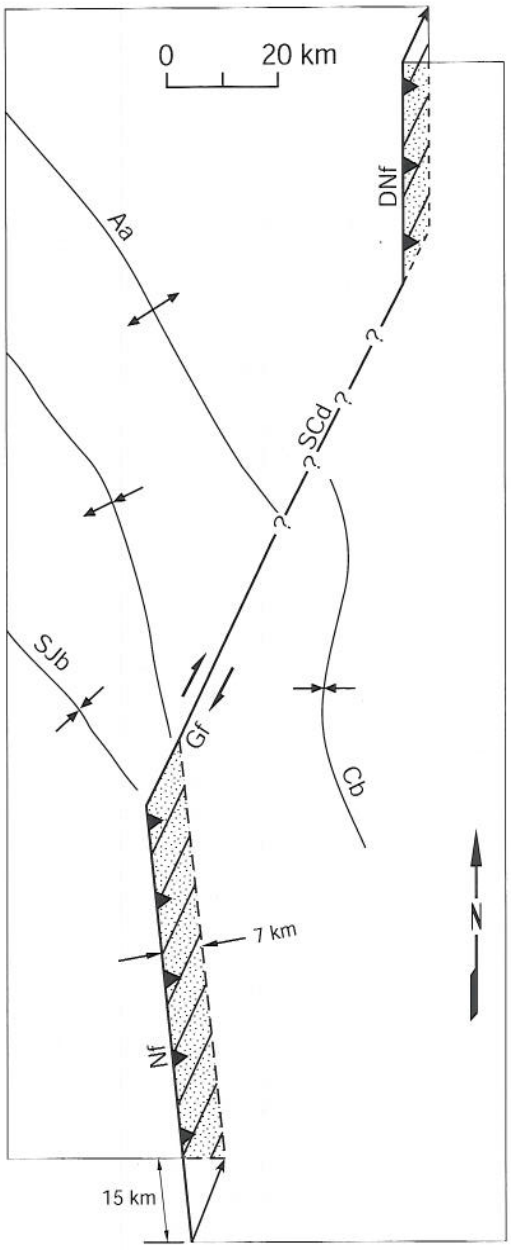

FIGURE 19. Simplified tectonic model for Laramide development of Nacimiento Uplift-Archuleta Anticlinorium area (see text). **DNf**, Del Norte fault; **Aa**, Archuleta Anticlinorium; **SCd**, Salado-Cumbres discontinuity; **SJb**, axis of San Juan Basin; **Gf**, Gallina fault; **Cb**, Chama Basin; **Nf**, Nacimiento fault.

The greater San Luis Uplift

The greater San Luis Uplift was a broad Laramide highland in northern New Mexico and southern Colorado that consisted of the San Luis, Brazos and Pajarito Uplifts (Fig. 1). Remnants of this uplift are exposed in northern New Mexico and include the Tusas Mountains, the Santa Fe Range, and the Picuris Mountains. Other parts of the greater San Luis Uplift have been structurally inverted during middle and late Tertiary extension to form the San Luis Basin (Baltz, 1965; Sales, 1983; Brister and Gries, 1994), the Española Basin (Cather, 1992), and the Peñasco embayment of the Rio Grande rift. The greater San Luis Uplift generally coincides with the southeast part of the Uncompahgre Uplift of late Paleozoic age.

The greater San Luis Uplift is bounded on the east by the Picuris-Pecos fault. A related highland east of the Picuris-Pecos fault, the Sangre de Cristo Uplift, has a distinct Laramide denudational history (e.g., Kelley and Chapin, 1995) and structural style, and is thus considered separately. Nearly all workers (Miller et al., 1963; Mallory, 1972; Baars and Stevenson, 1984; Casey, 1980; Chapin, 1983; Cather, 1999a) have interpreted the Picuris-Pecos fault to continue northward along strike to form the faulted, eastern margin of the Neogene San Luis Basin (Taos fault, Sangre de Cristo fault). In contrast, Baltz and Myers (1999) considered the Picuris-Pecos fault to bend to the northwest to accommodate their preferred interpretation that the southeast part of the San Luis Basin near Taos, New Mexico, was a buried extension of the late Paleozoic Taos trough. The gravity low near Taos that they cite as evidence for this extension, however, probably represents Neogene rift sediments (Cordell and Keller, 1984; G. R. Keller, oral commun., 2001).

The southwestern termination of the Laramide greater San Luis Uplift is not well defined because of post-Laramide sedimentary

and volcanic cover. The uplift ends southwestward against the Galisteo-El Rito Basin, but the location and nature of the uplift margin there are in dispute. Biehler et al. (1991) and Ferguson et al. (1995) have argued using seismic data that the deep western part of the Española half graben is underlain by Mesozoic and Paleozoic strata, and thus was not part of a Laramide highland. Cather (1992) utilized regional stratigraphy, provenance and paleocurrents of Eocene deposits, and limited well-bore data to argue that the Pajarito fault system that presently bounds the Española half-graben was formerly a Laramide west-down range-bounding fault for a Laramide highland (Pajarito Uplift of Cather, 1992) that was subsequently inverted during rifting to form the Española half-graben. See Smith (this volume) for a more detailed assessment of the controversy.

The Laramide uplift and cooling of the southeast part of the greater San Luis Uplift is recorded by AFT data from the Santa Fe Range, about 25 km northeast of Santa Fe, New Mexico (Kelley and Duncan, 1986; Kelley et al., 1992; Kelley, 1995; Kelley and Chapin, 1995). There, AFT ages show the high part of the range cooled ~74 Ma, and the lower elevations by ~44 Ma. Initial uplift and cooling were probably earlier than 74 Ma, however, because the pre-Laramide partial annealing zone that would overlie the earliest Laramide cooling ages has been eroded from the top of the range. Analysis of mean track lengths suggests moderate cooling rates (4°C/m.y.) ~74–55 Ma, with slow cooling rates (1°C/m.y.) thereafter (Kelley, 1990).

The uplift history of the northern San Luis Uplift (now subsided to form the San Luis Basin of the rift; Sales, 1983; Brister and Gries, 1994) is constrained by the Laramide stratigraphic record of the Raton Basin. Point-sourced sedimentary supply of the Trinidad Sandstone (Fig. 12) indicates control of drainages by the rising San Luis Uplift by 72–71 Ma (Fig. 15, stage 2). The first exposure of Dakota Sandstone on the uplift (stage 3) is recorded by siliceous pebbles and quartzose sandstones in the overlying Vermejo Formation (Flores and Tur, 1981, p. 36; Flores, 1987, p. 263; Flores and Pillmore, 1987, p. 311). Voluminous detritus derived from Paleozoic and Proterozoic sources is present in the upper Poison Canyon, Cuchara, Huerfano, and Farasita Formations (Johnson and Wood, 1956), indicating deep erosion of the San Luis Uplift during middle(?) Paleocene to early Eocene time (stage 4).

The northwestern part of the San Luis Uplift foundered and became a depocenter in middle(?) Eocene time in response to reactivation and postulated wrenching along the eastern margin of the San Juan Sag (Del Norte fault) during late Laramide time (Brister and Chapin, 1994). This created the poorly understood Monte Vista Basin in which red beds of the Blanco Basin Formation are as much as 960 m thick and overlie Proterozoic rocks (Brister and Chapin, 1994). The end of Laramide deformation along the western margin of the Brazos Uplift is locally constrained where the upper Blanco Basin Formation onlaps and buries basin-margin faults (Brister, 1992, fig. 10). Although the Blanco Basin Formation is not well dated, it is older than the upper Eocene-lower Oligocene Conejos Formation that overlies it.

The long-standing interpretation that the Neogene San Luis Basin has been broadly inverted from a precursor Laramide uplift recently has been challenged by Hoy and Ridgway (2002). In support of their interpretation, Hoy and Ridgway cite recently documented fault-bounded outcrops of Mesozoic strata that are present on the western flank of the northern Sangre de Cristo Mountains (Watkins et al., 1995; Shirley, 1995) and possibly within the Sangre de Cristo fault zone that forms the eastern margin of the Neogene San Luis Basin (Morel and Watkins, 1997). It is plausible that similar such faulted inliers of Mesozoic rocks are preserved locally beneath the Tertiary fill of the San Luis Basin. Contrary to the hypothesis of Hoy and Ridgway (2002), however, widespread preservation of Mesozoic strata beneath the basin seems improbable, based on many lines of evidence including deep drilling (Brister and Gries, 1994; Brister and McIntosh, *in press*), seismic reflection surveys (Kluth and Shaftenaar, 1994; Tandon et al., 1999), and provenance data for Laramide sediments derived from the San Luis Uplift (Johnson and Wood, 1956; Baltz, 1965; Merin et al., 1988).

Sangre de Cristo Uplift

The Sangre de Cristo structural uplift as defined here lies east of the Picuris-Pecos fault and west of the Raton Basin. The Sangre de Cristo Uplift flanks the east side of the greater San Luis Uplift but differs from it in several ways. Insofar as is known, the faults that bound and occur within the San Luis Uplift are steep to moderately dipping, north-striking faults that in some cases have important dextral separations of controversial origin (Fig. 1; see below). Rise of the Laramide San Luis Uplift began in the Late Cretaceous, as shown by both AFT data and sedimentological evidence in the Raton Basin, causing deep erosion that stripped off most Mesozoic and Paleozoic strata prior to the early Eocene.

In contrast, the Sangre de Cristo Uplift is characterized by gently to moderately dipping, generally east-directed thrust faults (some are reactivated late Paleozoic structures; Baltz and Myers, 1999) and associated tight fault-propagation folds commonly with overturned limbs (Johnson, 1959; Lindsay, 1998). These folds involve rocks as young as the Huerfano and Farasita Formations (Johnson, 1959) of late Wasatchian-early Bridgerian age (~53–49 Ma) (Robinson, 1966) and thus indicate that the end of thrusting in the Sangre de Cristo Uplift post-dates these units. Initial thrust-loading of the Raton Basin may have begun as early as ~80–75 Ma, as shown by increased stratal accumulation rates at this time (Fig. 3). It is not clear, however, if this initial thrust loading occurred along the present frontal thrusts of the uplift, or along older faults in the Sangre de Cristos to the west of the frontal faults.

While the above relationships indicate that the timing of deformation was approximately the same (late Campanian-Eocene) for both the greater San Luis and the Sangre de Cristo Uplifts, the denudational history and associated AFT cooling were not. In contrast to the greater San Luis Uplift, Paleozoic rocks have not been eroded from much of the Sangre de Cristo Uplift. The Sangre de Cristo Uplift also shows little evidence of early to middle Laramide denudation and subsequent AFT cooling. Most of the eastern part of the uplift cooled in the late Oligocene-early Miocene; the few Laramide cooling ages that are present are mostly late Laramide (Eocene) (Kelley and Chapin, 1995). Although early to middle Laramide deformation must have been occurring in the Sangre de Cristo Uplift as shown by contemporaneous rapid subsidence in the Raton Basin and the presence of numerous local unconformities along the western basin margin in Poison Canyon and younger strata (e.g., Johnson and Wood, 1956), AFT data indicate such deformation was not accompanied by deep erosion and cooling. As described by Kelley and Chapin (1995), this requires that the Sangre de Cristo Uplift was an area of little or no erosion until the late Laramide. The Sangre de Cristo Uplift, while structurally higher than the adjoining Raton Basin, was probably a shallow structural platform in the western part of this basin throughout much of the early and middle Laramide. Prior to the Eocene, sediment was transported across this platform to the Raton Basin from

the high-standing San Luis Uplift to the west (Merin et al., 1988, p. 174). Lack of deep erosion on the Sangre de Cristo Uplift prior to the late Laramide is also attested by stratigraphic evidence near Eagle Nest Lake, ~30 km northeast of Taos, New Mexico. There, preserved remnants of the Paleocene Poison Canyon Formation perhaps as much as 300 m thick unconformably overlie Upper Cretaceous strata that include the Pierre Shale and the Dakota Sandstone (Clark and Read, 1972).

Stratigraphic and AFT data from the Sangre de Cristo Uplift and provenance data from the Raton Basin thus indicate that the Sangre de Cristo Uplift was not strongly emergent during the early and middle Laramide. These relationships suggest that the evolving thrust faults of the Sangre de Cristo Uplift were probably blind beneath synorogenic sediments during much of the Laramide. Late in the Laramide orogeny, cooling indicated by AFT ages occurred locally in the topographically higher, western part of the uplift; most of the eastern part did not begin to cool until the onset of epeirogenic denudation in the late Oligocene (Kelley and Chapin, 1995).

Defiance Uplift

The north-northwest-trending Defiance Uplift is asymmetrical, with its steep eastern flank (the Defiance monocline) facing the Gallup Sag and the San Juan Basin (Fig. 1). With the exception of a few small outcrops of Proterozoic quartzite, the majority of the exposures on the Defiance Uplift are of Permian and Triassic sedimentary rocks. Structural relief between the highest part of the uplift and the Gallup Sag is at least 2150 m (Kelley, 1955). The Laramide Defiance Uplift encompasses part of the broader Defiance-Zuni Highland of late Paleozoic age (e.g., Ross and Ross, 1986, fig. 8). The structural controls on this earlier highland, however, are very poorly understood.

The central Defiance monocline appears to be contiguous with the Hogback monocline to the northeast, although the southern part of the Hogback monocline is weakly developed. The central part of the Defiance monocline is highly sinuous due to the presence of a series of en echelon, southeast-plunging anticlines and synclines that modify the southeastern part of the uplift (Fig. 20; Kelley and Clinton, 1960). These en echelon folds are suggestive of right-slip along the central Defiance monocline, and Kelley (1967) has proposed approximately 13 km of dextral deflection of Jurassic facies and pinchouts in this area. The Ute dome that adjoins the Hogback monocline northwest of Farmington (Fig. 20) also shows evidence of minor dextral deformation (Ralser and Hart, 1999). The timing of dextral wrenching along the Defiance-Hogback system is unclear; it probably post-dates northwest shortening of the Hogback monocline (late Campanian-early Maastrichtian) and may be coeval with major Paleocene-Eocene northeast shortening in the San Juan Basin.

The presence of a series of en echelon shortening structures to the northwest of the central Defiance monocline-Hogback monocline system, the most prominent of which is the northern Defiance monocline (Fig. 20), and the absence of such structures to the southeast of the monocline system, seemingly require significant lateral slip along the monocline system. Local differential shortening across the monocline system, however, is probably significantly less than the 13 km offset value estimated by Kelley (1967). If Kelley's estimate is correct, then dextral strike-slip on the basement faults that underlie the monocline system may accommodate deformation on a much larger scale (for example, perhaps transferring slip to the San Juan Uplift to the northeast). If this is the case, then the fact that central Defiance-Hogback monocline system does not appear to be broken by an exposed, throughgoing fault implies that significant components of strike-slip on the underlying basement fault would necessarily be accommodated by a broad zone of detachment, interstratal shear, and vertical-axis rotation in the overlying Phanerozoic sedimentary rocks (e.g., Jones, 2000). Such wrench deformation, if present, should be discernible with paleomagnetic analysis. The central Defiance monocline is dextrally separated from the southern Defiance monocline by the Wide Ruins fault (Fig. 20). This separation is about 8 km and suggests that the Wide Ruins fault may have dextral components of slip.

Zuni Uplift

The Zuni Uplift trends northwest and is markedly asymmetrical; its northeastern flank dips gently into the San Juan Basin, whereas its southwestern flank (the Nutria monocline) dips steeply toward the Baca Basin and exhibits as much as 1400 m of structural relief (Edmunds, 1961). The majority of the exposures on the Zuni Uplift consist of sedimentary rocks of Permian to Triassic age. Proterozoic granite, metarhyolite, gneiss, schist, and metaquartzite (Fitzsimmons, 1967; Goddard, 1966) crop out along the crest of the uplift. The structurally low area between the Zuni and Defiance Uplifts was termed the Gallup Sag by Kelley (1955) (Fig. 20). More than 2450 m of structural relief exists between the highest part of the Zuni Uplift and the Gallup Sag. Structural relief between the Zuni Uplift and the deepest part of the San Juan Basin is more than 4000 m (Kelley, 1955). The Laramide Zuni Uplift occupies part of the broader, late Paleozoic Zuni-Defiance Uplift (Ross and Ross, 1986). Chamberlin and Anderson (1989) attributed the Laramide structural development of the Zuni Uplift to indentation-extrusion tectonics caused by impingement of an indenter block from the southwest.

The timing of Laramide deformation in the Zuni Uplift is not well constrained. A major deltaic depocenter existed during deposition of the Pictured Cliffs Sandstone in the southwestern San Juan Basin (Flores and Erpenbeck, 1981) in the late Campanian (*Baculites scotti* zone of Fassett, 2000; dated 75.89 ± 0.72 Ma by Obradovich, 1993). This deltaic depocenter was localized down depositional dip (northeast) of the Gallup Sag, which suggests that the structural differentiation of the Defiance Uplift-Gallup Sag-Zuni Uplift area may have begun to control fluvial patterns by this time (Fig. 15, stage 2). Metaquartzite-bearing pebbly sandstones in the east-central Baca Basin were derived from the Zuni Uplift (Johnson, 1978; Cather and Johnson, 1984, 1986) and imply exposure of Proterozoic basement occurred prior to, or during, the middle Eocene (stage 4).

Lucero Uplift

The Lucero Uplift lies to the southeast of the Zuni Uplift and flanks the southwest side of the Neogene Albuquerque Basin (Fig. 1). The Lucero Uplift was formerly thought to be entirely Laramide in origin (Kelley and Clinton, 1960; Chapin and Cather, 1981, 1983; Cather and Johnson, 1984, 1986). It now seems more likely that the Lucero Uplift is, at least in part, a Neogene feature that reflects isostatic footwall uplift resulting from extension in the southwest Albuquerque Basin (e.g., Lewis and Baldridge, 1994). Compressional and transpressional features along faults that mark the eastern boundary of the Lucero Uplift (Comanche fault, Saiz fault) record Laramide deformation (Callender and Zillinski, 1976; Hammond, 1987; Cabezas, 1991; cf. Lewis and Baldridge, 1994), possibly related to mild uplift of what is now the southern

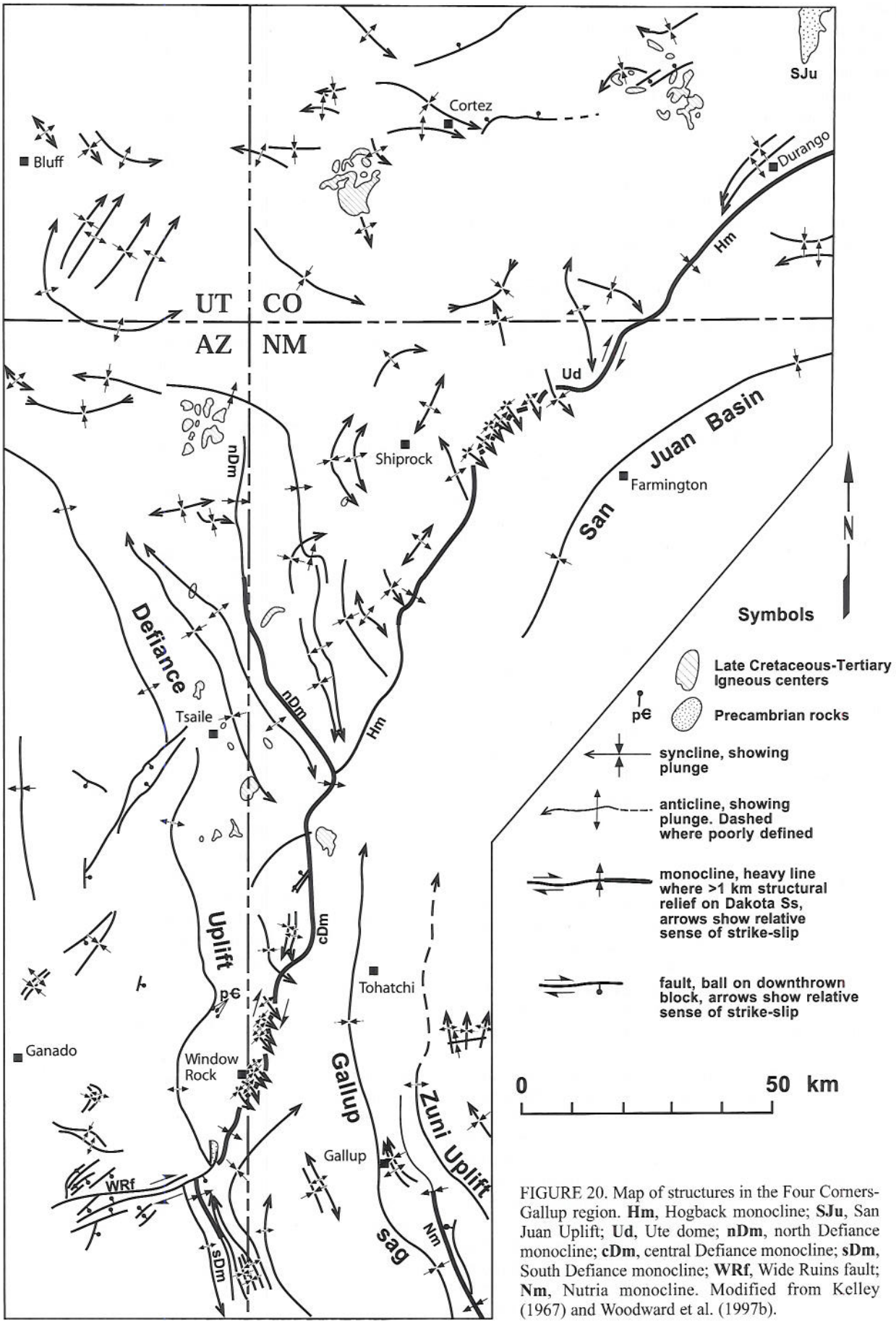

FIGURE 20. Map of structures in the Four Corners-Gallup region. **Hm**, Hogback monocline; **SJu**, San Juan Uplift; **Ud**, Ute dome; **nDm**, north Defiance monocline; **cDm**, central Defiance monocline; **sDm**, South Defiance monocline; **WRf**, Wide Ruins fault; **Nm**, Nutria monocline. Modified from Kelley (1967) and Woodward et al. (1997b).

Albuquerque Basin. Such uplift would explain the lack of Laramide sedimentary deposits in the subsurface of the southern Albuquerque Basin (Lozinsky, 1988, 1994; Russell and Snelson, 1994; Cather, 1992) and might provide the necessary damming element to produce Eocene lacustrine deposits in the eastern Baca Basin (Cather and Johnson, 1984, 1986).

Montosa Uplift

The existence of a Laramide positive area in the vicinity of the modern Sandia, Manzano and Los Pinos Mountains has been proposed by several workers (Eardley, 1962; Kelley and Northrop, 1975; Kelley, 1977). This uplift was termed the Sandia Uplift by Chapin and Cather (1981) and Cather and Johnson (1984, 1986), a name that is now a misnomer (Cather, 1992) because it appears that the modern Sandia Mountains were probably not strongly involved in the Laramide uplift. Although Laramide contractile structures of modest structural relief exist in the range (Karlstrom et al., 1999), the Sandia Mountains exhibit no evidence of Laramide cooling (Kelley and Duncan, 1986) and stratigraphic evidence from the Placitas area in the northern part of the range favors only mild pre-Eocene erosion as shown by preservation of the Campanian Menefee Formation (Fig. 2B; Connell et al., 1995). In the Manzano and Los Piños Mountains to the south, however, fission-track cooling ages indicate Paleocene-Eocene uplift (Kelley et al., 1992), probably related to dextral oblique convergence along the Montosa fault system (Fig. 1; Hayden, 1991; Behr, 1999). Because of these relations, the term Montosa Uplift was proposed (Cather, 1992) to encompass that part of the former Laramide Sandia Uplift to the south of the Tijeras-Cañoncito fault system. East of Belen (Fig. 1), conglomerates possibly correlative with the Baca Formation on the Hubble bench are dominated by fragments of the Permian Abo Formation, indicating moderately deep erosion on the Laramide Montosa Uplift to the east (Cather and Johnson, 1984, 1986). Correlation of these conglomerates with the Baca Formation, however, has been questioned by Lozinsky (1988, p. 128), who regarded them as possibly Santa Fe Group.

Sierra Uplift

Eardley (1962) proposed the existence of a Laramide positive area adjacent to the eastern margin of the Colorado Plateau in southern New Mexico and termed it the Sierra Uplift. Sedimentologic data from the Baca Formation indicate that the uplift extended northward into the Socorro vicinity, approximately 70 km beyond the northern boundary of the uplift as depicted by Eardley (Cather, 1983b; Cather and Johnson, 1984, 1986). Large portions of this uplift subsided to form basins of the Rio Grande rift during middle and late Tertiary time.

Baca Formation sediments derived from the northern part of the Sierra Uplift are arkosic and contain locally abundant clasts of Precambrian granite, schist, and metaquartzite. Only a few small exposures of Precambrian rocks, however, are present today along the Rio Grande rift near Socorro. Thus, Precambrian detritus in the Baca Formation in this area must have been derived largely from source terranes that were subsequently down-faulted and buried in the rift. In the Chupadera Mountains, the southern part of an intrarift horst adjacent to the Socorro Basin, Proterozoic rocks are locally overlain by upper Eocene volcanic and volcaniclastic deposits (Eggleston, 1982), indicating at least 1.5 km of Laramide uplift and erosional stripping in that area. Clasts of Proterozoic and Paleozoic rocks from the Baca Formation in the northern and southern parts of the Carthage-La Joya Basin have yielded AFT cooling ages of 57–45 Ma (Kelley et al., 1997) and thus provide a record of Laramide cooling in the northern Sierra Uplift. The Sierra Uplift continued to rise and shed arkosic detritus during the early part of mid-Tertiary volcanism (~40–36 Ma), implying a continuance of active Laramide-style tectonism (Fig. 15, stage 5). The beginning of structural inversion of the Sierra Uplift and the onset of bimodal (basaltic andesite-rhyolite) volcanism at 36 Ma marked the end of Laramide deformation and the beginning of incipient mid-Tertiary extension (Fig. 15, stage 6) (Cather, 1989, 1990).

Morenci Uplift

The probable existence of a Laramide drainage divide along the southeastern margin of the Baca Basin, which was subsequently obscured by thick accumulations of mid-Tertiary volcanic rocks of the Datil-Mogollon field, was pointed out to the author by C. E. Chapin (1980, oral commun.). The presence of large exposures of Laramide volcanic and plutonic rocks in southwestern New Mexico and adjacent Arizona and the nearly complete lack of volcaniclastic detritus in the eastern part of the Baca outcrop belt (Cather, 1980) imply the existence of an intervening uplift that prohibited input of volcanic detritus into the eastern part of the Baca Basin. The Morenci lineament (Chapin et al., 1978) provides a possible site along which such a drainage divide may have developed. Laramide structural relief along the Morenci Uplift is impossible to estimate at present, although it must have been appreciable, because significant amounts of Precambrian detritus are present in Baca Formation deposits derived from this uplift (Cather, 1980).

A series of en echelon, northeast-trending fault zones and grabens, the largest of which is the San Agustin Basin (Fig. 1), may represent portions of the Morenci Uplift that collapsed during middle and late Tertiary extension. The en echelon pattern of late Tertiary extensional structures in this area, if inherited from a Laramide compressional precursor, are consistent with dextral wrenching along the Morenci lineament during the Laramide orogeny. In their analysis of unpublished industry seismic data, Kopacz et al. (1989) and Garmezy et al. (1990) interpreted Laramide dextral deformation along the Morenci lineament.

Tularosa Uplift

The Tularosa Basin (Fig. 1) of the Rio Grande rift may have been inverted from an earlier Laramide uplift, the Tularosa Uplift. Evidence for such an uplift is scant. In the Sacramento Mountains that form the eastern border of the Tularosa Basin, east-directed thrust faults and associated folds occur in a localized zone along the western escarpment of the range (Pray, 1961). These faults cut rocks as young as Pennsylvanian and are, in turn, cut by middle Eocene dikes. The east-vergent structures in the western Sacramento Mountains may record a Laramide uplift that encompassed what is now the Tularosa Basin, and this uplift may have been a source of Eocene sediments for the Sierra Blanca Basin to the northeast. Alternatively, these faults may be late Paleozoic structures, although they differ from other Pennsylvanian faults in the area which are typically steeply dipping (Pray, 1961). Testing this inversion hypothesis will probably require deep drilling in the western Tularosa Basin, presently under the auspices of White Sands Missile Range.

THE STRIKE-SLIP CONTROVERSY

A great point of controversy in the southern Rocky Mountains is the magnitude of dextral slip along the eastern Colorado Plateau boundary. The first published inference of such dextral deforma-

tion was by Kelley (1955, p. 66), "[The eastern] *part of the Plateau was principally shortened in a northeasterly direction . . . General shortening of this nature in the eastern part of the Plateau would appear to necessitate right-lateral shift between the Plateau and the Eastern Rockies along their southern boundary and left-lateral shift between the Plateau and the Uinta Uplift at the northern end. Echelon folds at the bases of the Nacimiento and Uinta Uplifts are oriented in ways that suggest these relative shifts.*" Since the pioneering work of Kelley (1955), attempts to quantify the magnitude of Laramide dextral slip along the eastern Colorado Plateau have produced a wide range of values. Chapin and Cather (1981, 1983) estimated 60–120 km of dextral slip, based largely on the magnitude of crustal shortening north of the plateau. The estimates of Karlstrom and Daniel (1993; 100–170 km) and Daniel et al. (1995; 50 km) were based on dextral separation of aeromagnetic anomalies and Proterozoic lithologic and structural features. Isopach patterns and pinch-out trends for Mesozoic strata have been utilized to argue for 5–20 km (Woodward et al., 1997a) and for 33–110 km (Cather, 1999a) of dextral offset.

Hamilton (1981, 1988) variously invoked unspecified moderate to small dextral displacements in the southern Rocky Mountains, based on differing Euler-pole locations and the inferred amounts of Laramide shortening to the north of the Colorado Plateau. Other regional studies that argue for dextral slip of unspecified magnitude in the southern Rocky Mountains are Woodward (1974, 1976), Woodward and Callender (1977), Tikoff and Maxson (2001), and Erslev (2001).

In a recent tectonic analysis of the southern Rocky Mountains, Yin and Ingersoll (1997) proposed little or no Laramide dextral slip (<1 km) across the eastern margin of the Colorado Plateau. They instead interpreted faults to be largely thrusts or back thrusts, and that the narrow, en echelon basins of late Laramide age (Echo Park Basins of Chapin and Cather, 1981, 1983; axial basins of Dickinson et al., 1988) were simple synclinal depressions between paired thrusts and back thrusts. Several aspects of their analysis, however, are questionable. Yin and Ingersoll (1977, fig. 2) depicted the Carthage-La Joya Basin to lie north of Socorro, wholly in the hanging wall of the Montosa fault. Most of the basin, in fact, lies in the footwall of the fault, to the south and southeast, and thus does not occupy a synclinal depression between paired thrusts and back thrusts. They depicted the Galisteo-El Rito Basin to trend northeast, rather than north. Yin and Ingersoll (1997, fig. 2) also showed the Galisteo-El Rito Basin to end northwest of the Tijeras-Cañoncito fault system, and by doing so omitted the deepest part of the basin which lies directly adjacent to this structure (Gorham and Ingersoll, 1979). Much of the purported "Laramide San Luis Basin," as represented by Yin and Ingersoll (1997, fig. 2), was actually part of a Laramide highland (Brister and Gries, 1994); only the northwesternmost part of their basin corresponds to a known basin (the Monte Vista Basin of Brister and Chapin, 1994), and the Monte Vista Basin cannot be readily interpreted to be a simple synclinal sag between linked thrusts and back thrusts. Finally, Yin and Ingersoll do not reconcile the various lines of evidence that have led other workers to postulate dextral components of slip on Laramide faults in the southern Rocky Mountains, but instead have promulgated an essentially one-stage, dip-slip tectonic model that seems at odds with current knowledge of paleostresses (Erslev, 1999, 2001), fault kinematics (Cather, 1999a, Table 1), ancestry of basement structures (Karlstrom et al., 1999), and the diachronous nature of Laramide basin evolution (Chapin and Cather, 1981).

Two classes of piercing lines have been utilized in attempts to delimit the magnitude of Laramide strike-slip in the southern Rocky Mountains: those based on Mesozoic stratigraphy and those based on Proterozoic rock types, structures, and aeromagnetic anomalies. Mesozoic piercing lines have been exhaustively discussed in the recent literature (Woodward et al., 1997a; Cather, 1999; Woodward, 2000; Lucas et al., 2000; Ingersoll, 2000) and will not be described in detail here. Because of the effects of post-Laramide erosion, most potential Mesozoic piercing lines are ambiguous in their significance. Many show dextral deflections, but most of these cannot be conclusively demonstrated to be tectonic in origin. The two best-defined piercing lines that show dextral deflections of probable tectonic origin (the 20–33 km pinch-out deflection of the Gallup Sandstone across the Sand Hill-Nacimiento fault system and the 13 km deflection of Jurassic stratigraphic features across the central Defiance monocline) have been described earlier in this report. There are no Mesozoic piercing lines that argue definitively for little or no Laramide dextral offset in the southern Rocky Mountains, although some of the more poorly constrained piercing lines are permissive of such interpretations (Cather, 1999a).

Proterozoic piercing lines in northern New Mexico have been interpreted to exhibit dextral offsets of between 50 and 170 km (Chapin, 1983; Karlstrom and Daniel, 1993; Daniel et al., 1995; Woodward, 2000). The best-defined of these are along the Picuris-Pecos fault (Fig. 1), which exhibits 37 km of dextral strike separation (Miller et al., 1963) of Proterozoic rock types, ductile faults, and folds. Because Proterozoic rocks juxtaposed across the Picuris-Pecos fault record similar P-T conditions (3.5–4.5 kbar, 500–550°C; Grambling and Williams, 1985; Grambling et al., 1989), the 37 km dextral separation of rock types and structures cannot be explained by dip slip alone (Daniel et al., 1995).

The Picuris-Pecos fault clearly has been repeatedly reactivated (e.g., Miller et al., 1963; Bauer and Ralser, 1995), and the timing of slip events that produced the 37 km net dextral separation is not well constrained. This separation has been interpreted to have originated mostly in the Proterozoic (Miller et al., 1963; Yin and Ingersoll, 1997), predominantly in the late Paleozoic (Woodward et al., 1999; Baltz and Myers, 1999), or mostly in the Late Cretaceous-early Tertiary (Chapin and Cather, 1981, 1983; Chapin, 1983; Karlstrom and Daniel, 1993; Daniel et al., 1995; Bauer and Ralser, 1995; Cather, 1999a). Using a process-of-elimination rationale, Cather (1999a) interpreted the net 52 km dextral separation of Proterozoic features on the Picuris-Pecos fault and Tusas-Picuris fault (Fig. 1) to represent the minimum Laramide displacements, in order to account for the effects of late Paleozoic and Miocene deformations which he argued were largely sinistral. This interpretation has been subsequently invalidated by documentation of probable dextral slip on several north-striking Ancestral Rocky Mountain faults in New Mexico (Baltz and Myers, 1999; Cather, 2000).

Because of gouge development, most of the major Laramide faults in New Mexico and southern Colorado do not display slickenlines that would help constrain their kinematics. As a proxy for direct kinematic data from major faults, Erslev (1999, 2001) and Wawrzyniec (1999) analyzed kinematic data from adjacent minor faults. They used these data to reconstruct local Laramide σ_1 orientations or convergence directions, which then were utilized to constrain the sense of slip on major faults. Erslev (2001) analyzed over 2500 minor faults at 88 localities in northern New Mexico and concluded that an early phase of east to east-northeast contraction was followed by a later phase (early Eocene and younger) of northeast to east-northeast shortening. Based on these relationships,

Erslev (2001) interpreted mostly thrust slip on the dominantly north-striking major faults in northern New Mexico during the early Laramide, followed by limited dextral transpressive deformation beginning in the early Eocene. Erslev argued that the late phase of Laramide dextral strike-slip was not likely to be responsible for the majority of the shortening north of the Colorado Plateau in Wyoming because deformation there was well underway prior to the early Eocene.

In an analysis broadly similar to that of Erslev (2001) but utilizing fewer data points and sample localities, Wawrzyniec (1999) argued for unimodal northeast (054°) Laramide shortening in central and southern Colorado. Combining this with a conservative estimate of 17 km net east-west contraction in central Colorado and a presumption of no-slip partitioning, he calculated 12 km of Laramide northward translation of the Colorado Plateau. Based on paleomagnetic data, Wawrzyniec (1999) also noted the local presence of modest (8–21°), clockwise vertical axis rotations associated with Laramide faults (see also Marshall and Geissman, 2001), and inferred that these rotations were an indication that slip partitioning did not occur.

Implicit in the tectonic models of Erslev (2001) and Wawrzyniec (1999) is the assumption that weak-fault behavior and the partitioning of slip among discrete strike-slip and dip-slip faults did not occur in the Laramide southern Rocky Mountains. Partitioning of slip occurs in fault systems where weak (low frictional resistance to sliding) strike-slip faults cannot sustain large shear stresses, thus causing the near-field maximum principal stress to rotate into near perpendicularity with the strike-slip fault. This, in turn, causes compressional structures to develop subparallel to the strike-slip fault. Slip partitioning in fault systems has been documented in many areas of oblique convergence (Fitch, 1972; McCaffrey, 1992; Dewey and Lamb, 1992; Molnar, 1992; Jones and Tanner, 1995; Bunds, 2001), but is perhaps best documented in the San Andreas fault system of California (Mount and Suppe, 1987; Teyssier and Tikoff, 1998; Tavarnelli, 1998). In her study of minor faults adjacent to the dextral San Andreas fault, Ghisetti (2000) noted the rarity of dextral minor faults parallel to the San Andreas, and concluded that the *". . . orientation and kinematics of weak master faults cannot be predicted by the population of small-scale faults . . ."* (Ghisetti, 2000, p. 42).

Figure 21 depicts idealized fault and fold geometries for end-member examples of high- and low-strength strike-slip faults. For a high-strength fault under high confining pressures, the difference between the strength of the fault and that of the country rock thus may be as little as the relatively small cohesive strength of the country rock (Byerlee, 1978; Davis and Reynolds, 1996, p. 304–311). The illustrated high-strength end member (Fig. 21a) corresponds to the idealized situation where the frictional characteristics of the strike-slip fault and the country rock are *identical*, thus producing no refraction of far-field stresses in the near field, and giving rise to the Andersonian-based, classical en echelon patterns of contractional and extensional structures typically attributed to wrench tectonics (e.g., Wilcox et al., 1973; Harding, 1974). Such idealized high-strength fault behavior is probably rare or non-existent in nature, as shown by the near-universal proclivity of faults to be reactivated. It is this idealized situation, however, where the techniques of Wawrzyniec (1999) and Erslev (2001) are most strictly applicable.

For low-strength faults the frictional resistance to sliding becomes very small. The example depicted in Figure 21b is for an idealized frictionless fault. The inability of the frictionless strike-slip fault to sustain shear stress causes the near-field σ_1 to become

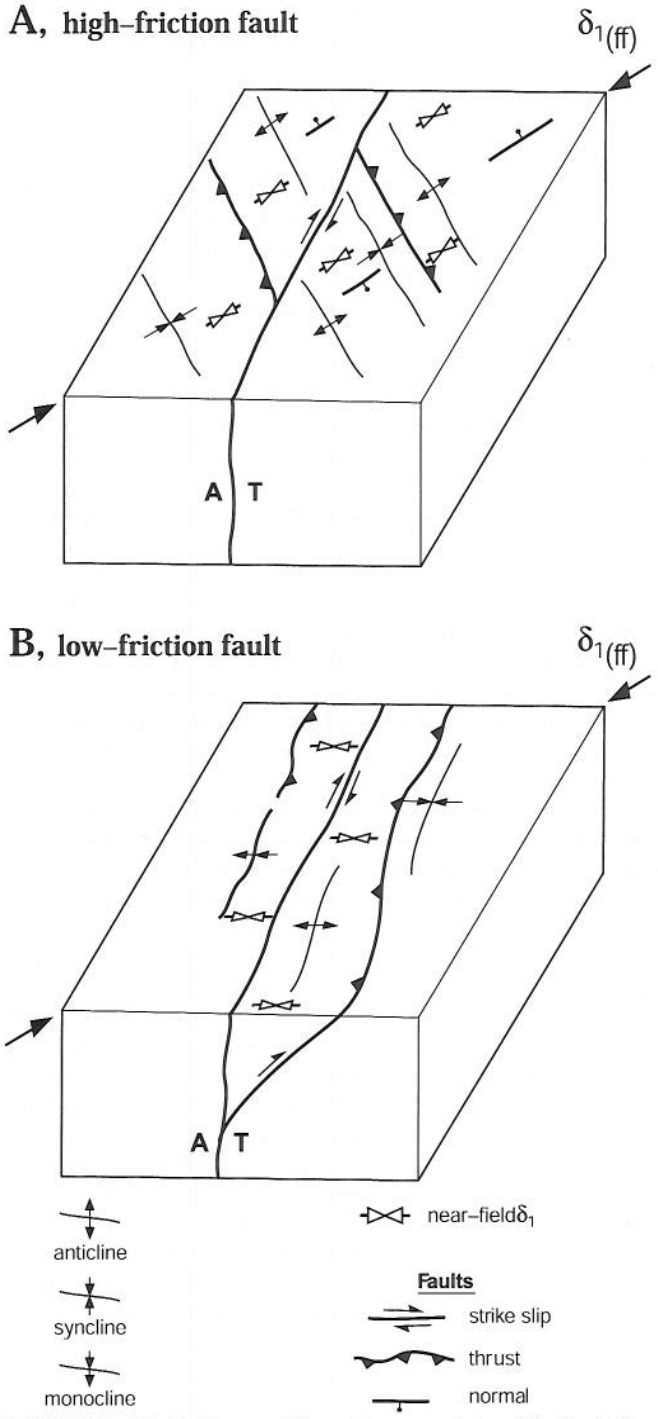

FIGURE 21. Block diagrams illustrating geometries of faults, folds, and far-field maximum principal stress orientations ($\sigma_{1(ff)}$) and near-field stress orientations for end-member examples of **A** (strong) and **B** (weak) strike-slip faults. See text.

perpendicular to the fault, and causes components of convergence to be partitioned into contractile structures that parallel the fault. Although serving as a useful end-member for visualizing the behavior of low-friction faults, the frictionless behavior of the strike-slip fault idealized in Figure 21b is probably unattainable in nature. The absence of shear stress along a frictionless strike-slip fault would produce no vertical-axis rotations in strata adjacent to the fault. The observed presence of vertical-axis rotations associated with Laramide faults in the southern Rocky Mountains

(Wawrzyniec, 1999) is therefore only an argument against frictionless faults, and not against other non-end-member forms of slip partitioning as inferred by Wawrzyniec.

Most natural examples of oblique convergence should fall within a continuum of deformation styles that lie between the end members of Figure 21. The slip behavior of faults that lie near the high-strength end of the spectrum should be predictable, although not precisely, using the minor-fault techniques of Erslev (2001) and Wawrzyniec (1999). Only the high-strength end member, however, should be entirely free of the effects of stress refraction and incipient partitioning. Strike-slip will occur on faults near the low-strength end of the spectrum even though the σ_1 direction, as determined from adjacent minor structures, is nearly perpendicular to the fault (Mount and Suppe, 1987; Tavarnelli, 1990; Ghisetti, 2000). Lateral components of slip on such weak faults would be underestimated using the methods of Erslev (2001) and Wawrzyniec (1999).

Was slip partitioning an important process during Laramide deformation in northern New Mexico and southern Colorado? Several Laramide dextral faults and monoclines in New Mexico are associated with en echelon structures (see Cather, 1999a, table 1) and thus geometrically resemble high-friction wrench structures. The most prominent of these are the previously described Defiance monocline and the Sand Hill-Nacimiento fault system. Only the latter has closely datable en echelon features: the en echelon normal faults of the Rio Puerco fault system adjacent to the Sand Hill fault that involve Eocene deposits (Slack and Campbell, 1976) and the en echelon folds west of the Nacimiento fault that exhibit growth relationships with Paleocene and Eocene strata (Baltz, 1967). The Sand Hill-Nacimiento fault system thus is likely to have been a high-friction wrench structure, although perhaps only in the late Laramide.

In contrast, the deformational style of the greater San Luis and Sangre de Cristo Uplifts seems more compatible with slip partitioning. As described by Cather (1999b), thrust, reverse, and strike-slip faults in this region are mutually subparallel and largely coeval. In contrast to the eastern Colorado Plateau, the near-field σ_1 orientations adjacent to the Picuris-Pecos fault have prominent modes parallel with, or perpendicular to, major faults (Erslev, 2001, fig. 6). Such orientations are expectable near weak faults (Ben-Avraham and Zoback, 1992, fig. 3) because of the inability of weak faults to sustain significant shear stress. Most of the contractile structures west of the southern Rockies on the eastern Colorado Plateau trend northwest (Kelley, 1955). In contrast, structures east of the Picuris-Pecos fault (frontal thrusts of Sangre de Cristo Uplift, La Veta syncline, Anton Chico monocline) trend north. Contractile structures of such orientation would be a predictable consequence of weak strike-slip faults associated with the greater San Luis Uplift. Oblique components of convergence would have been partitioned along weak strike-slip faults, leaving only east-west components of shortening to affect areas to the east. If such a scenario is correct, then the early Laramide east-west σ_1 orientation documented near the Picuris-Pecos and related faults by Erslev (2001) is not necessarily incompatible with large components of early Laramide dextral slip on these faults.

The source of the potential weakness of Laramide faults in the southern Rocky Mountains is unknown, but may have been related to weak, fine-grained fault rocks or to elevated pore-fluid pressures. Fluids may have been derived from dehydration reactions in the upper mantle or lower crust during Laramide shallow subduction, magmatism, and crustal thickening, as has been proposed for Miocene metallogenic fluids in Chile (Kay and Mpodozis, 2001). Overpressurization of pore fluids beneath a seal of low-permeability sediments conceivably may have contributed to fault weakening. At the onset of the Laramide orogeny, a vast region of western North America from southern New Mexico northward into Canada was covered by a world-class aquitard composed of a thick blanket of Mesozoic strata, most of which was mudrock. Mesozoic strata ranged from a thin edge in southern New Mexico to more typical thicknesses of 600–2500 m in northern New Mexico and southern Colorado (Peterson and Smith, 1986). The effectiveness of the Mesozoic seal would have been largely compromised in the later phases of Laramide orogeny, as a result of breaching of the regional aquitard by deep erosion on Laramide uplifts.

The timing of the end of right lateral deformation in the southern Rocky Mountains is problematic and may have been diachronous. In the Chloride fault system of south-central New Mexico (Fig. 1), cross-cutting relationships with dated volcanic units constrain the end of right-lateral deformation to have occurred between 36 and 34.93 Ma (Harrison, 1990; Harrison and Chapin, 1990; Harrison and Cather, *in press*), closely similar to the end of Laramide shortening and the beginning of incipient extension in adjacent areas (Cather, 1989, 1990; Mack et al., 1994). In north-central New Mexico, dextral faults do not cut a 26.55 ± 0.30 Ma dike near Hagan, but elsewhere in northern New Mexico rocks as young as 25 Ma are cut by north-striking, dextral faults (Erslev, 2001). It is not clear if these relationships argue for a diachronous end (younger to the north) to dextral faulting that began in the Laramide, or if they are the result of much younger dextral slip on faults related to recently recognized dextral oblique extension of latest Miocene-Recent age in the Rio Grande rift (Karlstrom et al., 1999, p. 163; Chamberlin, 1999). Such rift-related dextral faulting may have occurred on the Picuris-Pecos fault southwest of Taos where it is intersected by the Embudo fault, a left-lateral transfer fault in the northern Rio Grande rift. There the 34–18 Ma Picuris Formation is cut by strands of the Picuris-Pecos fault that show evidence of dextral slip (Bauer et al., 1999; Erslev, 2001; Bauer et al., *in press*). The reactivation of the Picuris-Pecos fault near the Embudo fault may be due to anticlockwise rotation of domino-like blocks between dextral strands of the Picuris-Pecos fault in response to rift-age sinistral shear on the Embudo fault.

The Oligocene transition from Laramide deformation to rifting is an important but poorly understood period in the kinematic development of the southern Rockies. According to Chapin and Cather (1994), during the main phase of rifting (middle to late Miocene) extension was southwestward, causing sinistral-oblique deformation. In contrast, Wawrzyniec (1999) inferred that rift deformation was characterized by northwest extension and dextral components of slip throughout its development, based on minor fault analyses from six localities in southern Colorado. Several lines of evidence, however, are best explained by sinistral-oblique deformation during Miocene southwest-northeast extension: (1) east-west trending extensional basins north of the Colorado Plateau contain middle to upper Miocene sedimentary rocks and thus require southward components of Colorado Plateau relative motion during this time (Chapin and Cather, 1994); (2) northwest-trending early rift basins near Albuquerque (Hudson et al., 2001) are indicative of northeast-southwest extension; (3) anticlockwise rotation of Oligocene and Miocene rocks in the Española Basin area is most reasonably explained by vertical axis rotations during sinistral shear (Brown and Golombek, 1985, 1986; Salyards et al., 1994); (4) the strike-slip transfer faults, such as the northeast-striking Embudo fault, are typically subparallel to the extension direction (Faulds and Varga, 1998); (5) post-Laramide rocks in several local-

ities in central and southern Colorado contain populations of minor faults that are indicative of southwest-northeast extension (E. A. Erslev, oral commun., 2001; S. M. Cather and C. E. Chapin, *unpubl.*).

SUMMARY

In Late Cretaceous time prior to about 80–75 Ma, stratal accumulation rates (not decompacted) in what were to become the axial parts of the San Juan and Raton Basins were relatively low (18–60 m/m.y.), and there is little evidence of tectonic disturbance along the sites of future Laramide uplifts. Primarily because of the scarcity of control points on the early and middle Campanian parts of stratal accumulation-rate curves (Fig. 3) and because of the relatively imprecise nature of AFT data, it is difficult to state precisely when the Laramide orogeny began in northern New Mexico and southern Colorado. Several lines of evidence converge to suggest it began sometime between about 80 to 75 Ma: (1) Initial Laramide AFT cooling in the Nacimiento Uplift occurred 80.8 ± 7.5 Ma (two-sigma error), and cooling was underway in the Santa Fe Range at least by about 74 Ma; (2) stratal accumulation rates increased greatly in both the San Juan and Raton Basins in the middle Campanian (80–75 Ma); (3) non-deposition or erosion of the Pictured Cliffs Sandstone (~75 Ma) occurred in the eastern limb of the evolving range-margin syncline adjacent to the Nacimiento Uplift and locally adjacent to the Archuleta Anticlinorium; and (4) a two-fold seaward thinning of the middle to late Campanian Lewis Shale between the axial part of the San Juan Basin and the San Juan Sag documents an early episode of northeastward tilting and subsidence in the San Juan Basin that began prior to deposition of the Huerfanito Bentonite Bed (75.76 ± 0.34 Ma; Fassett et al., 1997) (Fig. 5).

In northern New Mexico and southern Colorado, basin subsidence during the Laramide orogeny consisted of three distinct phases, the first two of which are recorded only in the San Juan and Raton Basins. Subsidence phases were approximately synchronous in both basins and were separated by unconformities related to lulls in tectonism. These intervening unconformities, whereas demonstrably not entirely synchronous, overlap temporally between the two basins. In general, episodes of rapid subsidence and sedimentation were characterized by underfilled, mudstone-dominated successions, whereas intervening episodes of decreased accommodation and overfilling produced regional unconformities and associated sandstone- and conglomerate-dominated sedimentary deposits.

The early phase of Laramide subsidence culminated in the late Campanian-early Maastrichtian and is recorded by marine, marginal marine, and coastal plain sedimentation. Northwest tilting of the San Juan Basin occurred ~74–67 Ma and created a depocenter in the northwest part of the basin adjacent to the Hogback monocline. This depocenter may have extended northeastward along the Hogback monocline into the San Juan Sag, which was only weakly differentiated from the San Juan Basin at this time. During deposition of the Kirtland and Fruitland Formations, stratal accumulation rates equaled or exceeded those for continental deposits of any basin in northern New Mexico or southern Colorado during the Late Cretaceous through Eocene. Early Laramide stratal accumulation rates in the Raton Basin peaked during deposition of the upper Pierre-Trinidad-Vermejo interval in a depocenter that straddled the Colorado-New Mexico state line. The first diagnostic detritus from a local uplift, recycled from exposures of the Dakota Sandstone on the San Luis Uplift, appeared in the Raton Basin (Vermejo Formation) in the early(?) Maastrichtian. This detritus indicates at least 1 km of structural relief existed between the San Luis Uplift and the Raton Basin by this time. Cessation of subsidence and accommodation in the middle to late Maastrichtian produced a basin-wide unconformities in both the San Juan and Raton Basins that marked the end of the early phase of Laramide subsidence.

The early phase of Laramide basin development was associated with modest deformation in the northeastern San Juan Basin and the adjoining Archuleta Anticlinorium during deposition of the Lewis Shale and Pictured Cliffs Sandstone, major folding along the Hogback monocline, east-down components of slip on the Picuris-Pecos fault, modest west-down faulting and associated folding along the Nacimiento fault, and thrust faulting (presumably blind) in the Sangre de Cristo Uplift. Other structures in the region also may have been active during the early Laramide, but are difficult to evaluate because they were not located adjacent to the San Juan and Raton depocenters. Strike-slip faulting associated with slip partitioning may have begun in the early Laramide, as is seemingly required by late Campanian-early Maastrichtian shortening north of the Colorado Plateau in the Uinta Uplift (Bryant and Nichols, 1988, p. 421) and the Wind River Uplift (Wiltschko and Dorr, 1983; Cerveny, 1990).

Figure 22 is an interpretation of the paleogeography of northern New Mexico and southern Colorado during the latest Campanian (~72 Ma). It differs from previous paleogeographic syntheses in several ways: (1) the shoreline associated with the retreating Late Cretaceous seaway was strongly embayed due to active uplift and volcanism northwest of the Hogback monocline and the rise of the greater San Luis Uplift; (2) a major depocenter was present in the northwestern San Juan Basin; (3) drainage control by the rising San Luis Uplift caused point-sourcing of sediments to the eastward-prograding upper Pierre-Trinidad-Vermejo shoreline in the Raton Basin; (4) the Sangre de Cristo Uplift was probably a shallow structural bench along the western margin of the deeper, thrust-loaded Raton Basin; and (5) AFT cooling was underway in the southern part of the greater San Luis Uplift and in the Nacimiento Uplift.

The medial phase of Laramide subsidence and accommodation began in the latest Maastrichtian-early Paleocene and continued until early late Paleocene. Sediments, now entirely non-marine, accumulated in depocenters in different locations than those for the early Laramide. In the San Juan Basin, a Paleocene depocenter developed in the northeast part of the basin adjacent to the rising Archuleta Anticlinorium. The medial Laramide depocenter associated with the Raton and Poison Canyon Formations in the Raton Basin moved northward into Colorado. Paleozoic and Precambrian detritus first appeared in late Maastrichtian-early Paleocene Ojo Alamo Sandstone of the San Juan Basin and became widespread in the Raton Basin during deposition of upper part of the Poison Canyon Formation (middle? Paleocene). AFT cooling was in progress during the Paleocene in the Montosa Uplift, and continued in the Nacimiento Uplift and Santa Fe Range (southern San Luis Uplift) (Kelley et al., 1992). En echelon growth folds developed in the eastern San Juan Basin (Baltz, 1967), and the rising Archuleta Anticlinorium began to divide the San Juan Sag from the San Juan Basin. During the late Paleocene a period of decreased subsidence and accommodation may have produced a second episode of basin-wide non-deposition or erosion that marked the end of the medial phase of sedimentary accumulation in both the San Juan and Raton Basins.

The final, late Laramide (Eocene) phase of subsidence and sed-

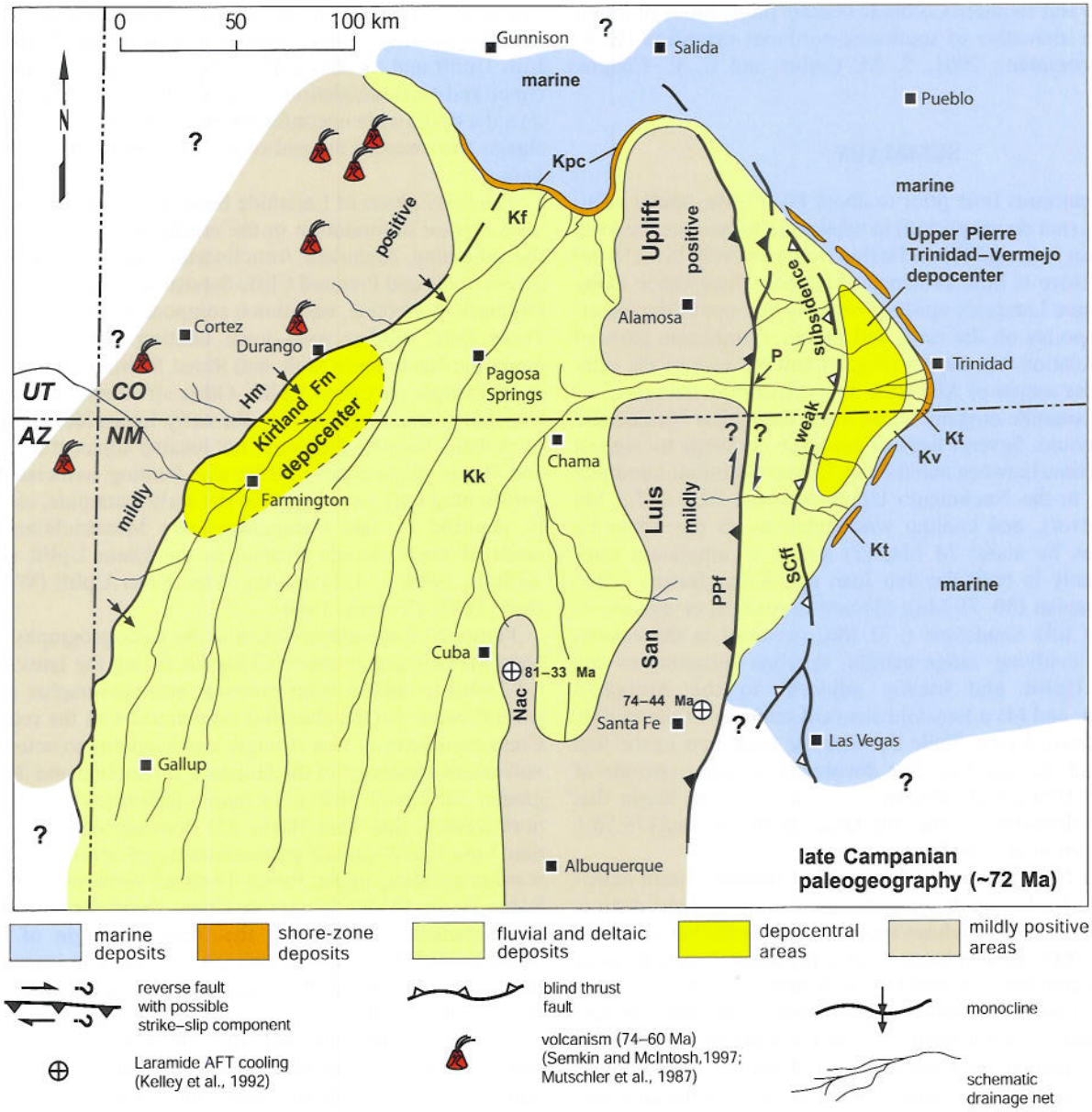

FIGURE 22. Early Laramide (~72 Ma, late Campanian) paleogeographic map showing areas of deposition and mild erosion, shoreline configurations, inferred drainage net, and principal active structures. **Kpc**, Pictured Cliffs Sandstone; **Kf**, Fruitland Formation; **Kk**, Kirtland Formation; **Kt**, Trinidad Sandstone; **Kv**, Vermejo Formation; **Hm**, Hogback monocline; **PPf**, Picuris-Pecos fault; **SCff**, blind(?) frontal faults of the Sangre de Cristo Uplift; **P**, sediment point source for upper Pierre-Trinidad-Vermejo depocenter; **Nac**, Nacimiento Uplift. Map has not been restored palinspastically.

iment accumulation saw the creation of numerous new basins in the Laramide foreland (Chapin and Cather, 1981, 1983). In southern Colorado and central and northern New Mexico, these include the Monte Vista, El Rito, Galisteo, Baca, Carthage-La Joya, and Sierra Blanca Basins (Fig. 23). Sediment accumulation was renewed in the San Juan and northern Raton Basins in the early Eocene. Except in the Galisteo Basin, where sedimentation was initiated in the late Paleocene(?)-early Eocene, sediment accumulation in all other late Laramide basins appears to have begun about 5 m.y. later, in the middle Eocene (Fig. 2). It is not clear if the younger onset of late Laramide sedimentation in these basins records a separate middle Eocene tectonic event, as advocated by Lucas (1984), or if deformation in these new basins began in early Eocene but did not develop sufficiently to begin accumulating sediments until middle Eocene.

In each of the newly formed, late Laramide basins in New Mexico, Eocene strata were deposited with profound unconformity on Upper Cretaceous strata. Only in the Galisteo-El Rito Basin, where Eocene deposits overlie the Campanian Menefee Formation and the Lewis Shale, is the age of the directly underlying strata reasonably well constrained. In the Baca, Carthage-La Joya, and Sierra Blanca Basins to the south, Upper Cretaceous strata (mostly Crevasse Canyon Formation) that lie unconformably beneath basal Eocene beds are poorly dated. It is interesting to note, however, that the Gallup Sandstone occurs at a reasonably constant stratigraphic depth (108–320 m; Fig. 2D, E, F) beneath the Eocene unconformity in all three basins. This relative consistency suggests that the unconformity records mostly non-deposition, as uplift and deep erosion would have likely produced significant paleotopography associated with the unconformity.

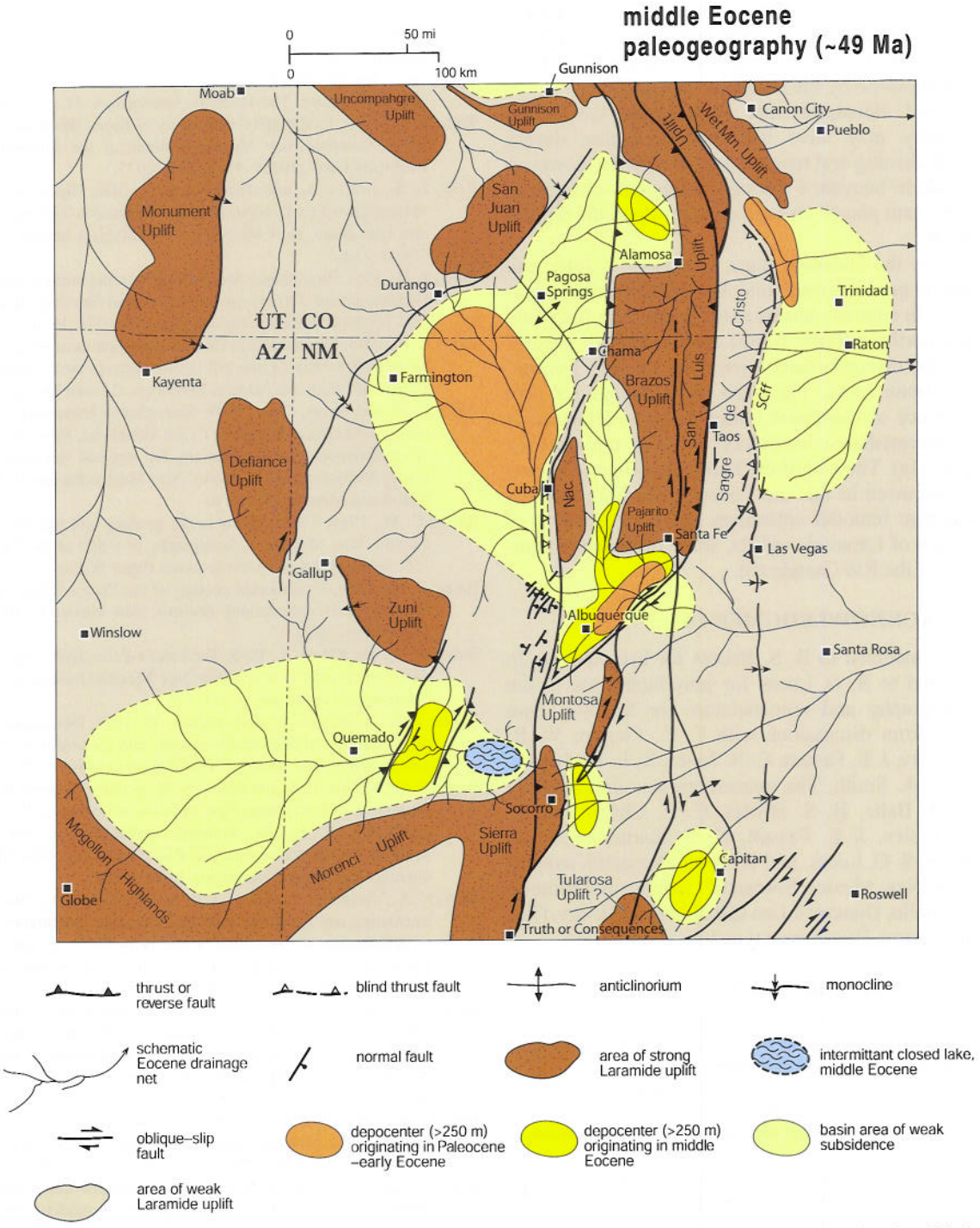

FIGURE 23. Late Laramide (middle Eocene, ~49 Ma) paleogeographic map showing depocenters, uplifts, simplified structures, and inferred drainage net. Names of structures are given on Figure 1. **MVb**, Monte Vista Basin; **Rb**, Raton Basin; **SJb**, San Juan Basin; **SJs**, San Juan Sag; **GERb**, Galisteo-El Rito Basin; **Bb**, Baca Basin; **CLJb**, Carthage-La Joya Basin; **SBb**, Sierra Blanca Basin. Map has not been restored palinspastically.

In the San Juan Basin, late Laramide sedimentation continued to be focused in the northeast part of the basin adjacent to the rising Archuleta Anticlinorium. The Eocene depocenter in the Raton Basin shifted northward to the Spanish Peaks area in Colorado, possibly in response to continued dextral offset of a sediment point source by slip on the Picuris-Pecos fault. A short-lived intra-Wasatchian unconformity developed between the Diamond Tail and Galisteo Formations in the Galisteo Basin. This unconformity corresponds temporally with a local shift from east-northeast to northeast σ_1 orientation (Erslev, 2001).

The numerous basins, uplifts and lesser structures of late Laramide age are best explained by dextral oblique deformation in the southern Rocky Mountains. The magnitude of the dextral slip, however, remains a topic of much contention. AFT cooling began during the Eocene in the Sierra Uplift as well as locally in the Sangre de Cristo Uplift, and AFT cooling continued in the Nacimiento, southern San Luis, and Montosa Uplifts. Widespread erosion of Proterozoic and Paleozoic lithologies was occurring on

most Laramide uplifts throughout the region at this time. A shallow, closed lacustrine system formed in the eastern part of the Baca Basin during the middle Eocene in response to damming of the regional easterly paleoslope by the rising Sierra Uplift.

The high regional elevations that characterize the Rocky Mountain area today may have had their inception during Laramide crustal thickening and magmatism. It is likely, however, that changes in mantle buoyancy during subsequent widespread mid-Tertiary magmatism played an even greater role in the regional epeirogenic uplift.

Eocene deposits in the Galisteo, Baca, Carthage-La Joya, and Sierra Blanca Basins grade upward into late middle Eocene volcaniclastic deposits. In contrast, basins to the north (San Juan Sag, El Rito Basin, and northern Raton Basin) contain Eocene synorogenic strata that are disconformably overlain by late Eocene-Oligocene volcaniclastic rocks. The Baca and Carthage-La Joya Basins record evidence of continued Laramide-style deformation during the early, intermediate-composition phase of mid-Tertiary volcanism (~40–36 Ma). The end of the Laramide orogeny in central New Mexico occurred in the late Eocene (~36 Ma) and was marked by a switch to bimodal volcanism and the beginning of extensional inversion of Laramide uplifts, some of which eventually formed basins of the Rio Grande rift.

ACKNOWLEDGMENTS

I am particularly indebted to B. S. Brister for his expertise in well-log analysis, and to S. G. Lucas for introducing me to the intricacies of stratigraphy and nomenclature for the San Juan Basin. I benefitted from discussions with C. E. Chapin, W. R. Dickinson, E. A. Erslev, J. E. Fassett, C. H. Jones, K. E. Karlstrom, S. A. Kelley, and G. A. Smith. The manuscript was improved by reviews from E. H. Baltz, B. S. Brister, C. E. Chapin, W. R. Dickinson, E. A. Erslev, J. E. Fassett, K. E. Karlstrom, S. A. Kelley, T. F. Lawton, S. G. Lucas, and H. Tobin. Research support was provided by the New Mexico Bureau of Geology and Mineral Resources (P. A. Scholle, Director). Leo Gabaldon and Becky Titus drafted the figures. Lynne Hemenway typed the manuscript.

REFERENCES

Abbott, J. C., 1995, Constraints on the deformational history of the Tijeras-Cañoncito fault system, north-central New Mexico [M.S. thesis]: Socorro, New Mexico Institute of Mining and Technology, 161 p.

Abbott, J. C., Cather, S. M., and Goodwin, L. B., 1995, Paleogene synorogenic sedimentation in the Galisteo Basin related to the Tijeras-Cañoncito fault system: New Mexico Geological Society, 46th Field Conference, Guidebook, p. 271–278.

Abbott, J. C., Goodwin, L. B., and Kelley, S. A., *in press*, The anatomy of a long-lived fault system: Structural and thermochronologic evidence for Laramide to Quaternary activity on the Tijeras fault, New Mexico, *in* Cather, S. M., McIntosh, W. C., and Kelley, S. A., eds., Tectonics, geochronology, and volcanism in the southern Rocky Mountains and the Rio Grande rift: New Mexico Bureau of Geology and Mineral Resources, Bulletin 160.

Ash, H. O., 1958, The Jurassic Todilto Formation of New Mexico [M.S. thesis]: Albuquerque, University of New Mexico, 63 p.

Ash, S. R. and Tidwell, W. D., 1976, Upper Cretaceous and Paleocene floras of the Raton Basin, Colorado and New Mexico: New Mexico Geological Society, 27th Field Conference, Guidebook, p. 197–203.

Ayers, W. B., Jr., and Kaiser, W. R., 1994, Coalbed methane in the Upper Cretaceous Fruitland Formation, San Juan Basin, New Mexico and Colorado: New Mexico Bureau of Mines and Mineral Resources, Bulletin 146, 216 p.

Ayers, W. B., Jr., Kaiser, W. R., Laubach, S. E., Ambrose, W. A., Baumgardener, R. W., Jr., Scott, A. R., Tyler, R., Yeh, J., Hawkins, G. J., Swartz, T. E., Schultz-Ela, D. D., Zellers, S. D., Tremain, C. M., and Whitehead, N. H., III, 1991, Geologic and hydrologic controls on the occurrence and producibility of coalbed methane, Fruitland Formation, San Juan Basin: Gas Research Institute, Topical Report GRI-91/0072, 314 p.

Baars, D. L. and Stevenson, G. M., 1984, The San Luis Uplift—an enigma of the ancestral Rockies: The Mountain Geologist, v. 21, p. 21–42.

Baltz, E. H., 1965, Stratigraphy and history of Raton Basin and notes on San Luis Basin, Colorado-New Mexico: Bulletin of the American Association of Petroleum Geologists, v. 49, p. 2041-2075.

Baltz, E. H., Ash, S. R., and Anderson, R. Y, 1966, History of nomenclature and stratigraphy of rocks adjacent to the Cretaceous-Tertiary boundary, western San Juan Basin, New Mexico: U.S. Geological Survey, Professional Paper 524-D, 23 p.

Baltz, E. H., 1967, Stratigraphy and regional tectonic implications of part of Upper Cretaceous and Tertiary rocks, east-central San Juan Basin, New Mexico, U.S. Geological Survey, Professional Paper 552, 101 p.

Baltz, E. H., 1978, Résumé of Rio Grande depression in north-central New Mexico: Guidebook to Rio Grande rift in New Mexico and Colorado, New Mexico Bureau of Mines and Mineral Resources, Circular 163, p. 210–228.

Baltz, E. H. and Myers, D. A., 1999, Stratigraphic framework of upper Paleozoic rocks, southeastern Sangre de Cristo Mountains, New Mexico with a section on speculations and implications for regional interpretation of ancestral Rocky Mountains paleotectonics: New Mexico Bureau of Mines and Mineral Resources, Memoir 48, 269 p.

Bauer, C. M., 1916, Contributions to the geology and paleontology of San Juan County, New Mexico; 1. Stratigraphy of a part of the Chaco River valley: U.S. Geological Survey, Professional Paper 98-P, p. 271–278.

Bauer, P. W., 1988, Precambrian geology of the Picuris Range, north-central New Mexico [Ph.D. dissertation]: Socorro, New Mexico Institute of Mining and Technology, 280 p.

Bauer, P. W. and Ralser, S., 1995, The Picuris-Pecos fault—repeatedly reactivated from Proterozoic(?) to Neogene: New Mexico Geological Society, 46th Field Conference, Guidebook, p. 111–115.

Bauer, P. W., Kelson, K. I., and Johnson, P., 1999, Development of a major rift transfer zone (Embudo fault): insights into the evolution of the northern Rio Grande rift in New Mexico: New Mexico Geology, v. 21, p. 37.

Bauer, P. W., Kelson, K. I., and Kelley, S. A., *in press*, Tectonic development of the southern San Luis Basin, New Mexico, *in* Cather, S. M., McIntosh, W. C., and Kelley, S. A., eds., Tectonics, geochronology, and volcanism in the southern Rocky Mountains and Rio Grande rift: New Mexico Bureau of Geology and Mineral Resources, Bulletin 160.

Beck, R. A., Vondra, C. F., Filkins, J. E., and Olander, J. D., 1988, Syntectonic sedimentation and Laramide basement thrusting, Cordilleran foreland; Timing of deformation, *in* Schmidt, C. J. and Perry, W. J., Jr., eds., Interaction of the Rocky Mountain foreland and the Cordilleran thrustbelt: Geological Society of America, Memoir 171, p. 465–487.

Beck, W. C. and Chapin, C. E., 1994, Structural and tectonic evolution of the Joyita Hills, central New Mexico: implications of basement control on Rio Grande rift, *in* Keller, G. R. and Cather, S. M., eds., Basins of the Rio Grande rift: Structure, stratigraphy and tectonic setting: Geological Society of America, Special Paper 291, p. 187–205.

Behr, R.-A., 1999, Structure and thermochronologic constraints on the movement history of the Montosa fault, central New Mexico [M.S. thesis]: Socorro, New Mexico Institute of Mining and Technology, 129 p.

Ben-Avraham, Z. and Zoback, M. D., 1992, Transform-normal extension and asymmetric basins: an alternative to pull-apart models: Geology, v. 20, p. 423–426.

Biehler, S., Ferguson, J., Baldridge, W. S., Jiracek, G. R., Aldren, J. L., Martinez, M., Fernandez, R., Romo, J., Gilpin, B., Braile, L. W., Hersey, D. R., Luyendyk, B. P., and Aiden, C. L., 1991, A geophysical model of the Española Basin, Rio Grande rift, New Mexico: Geophysics, v. 56, p. 340–353.

Bingler, E. C., 1968, Geology and mineral resources of Rio Arriba County, New Mexico: New Mexico Bureau of Mines and Mineral Resources, Bulletin 91, 158 p.

Blair, T. C. and Bilodeau, W. L., 1988, Development of tectonic cyclothems in rift, pull-apart, and foreland basins: sedimentary response to episodic tectonism: Geology, v. 16, p. 517–520.

Bodine, M. W., Jr., 1956, Geology of the Capitan coal field, Lincoln County, New Mexico: New Mexico Bureau of Mines and Mineral Resources, Circular 35, 27 p.

Briggs, L. I. and Goddard, E. N., 1956, Geology of Huerfano Park, Colorado, *in*

Guidebook to the geology of the Raton Basin, Colorado: Denver, Rocky Mountain Association of Geologists, p. 40–45.

Brister, B. S., 1992, The Blanco Basin Formation (Eocene), San Juan Mountains region, Colorado and New Mexico: New Mexico Geological Society, 43rd Field Conference, Guidebook, p. 321–331.

Brister, B. S. and Chapin, C. E., 1994, Sedimentation and tectonics of the Laramide San Juan Sag, southwestern Colorado: The Mountain Geologist, v. 31, no. 1, p. 2–18.

Brister, B. S. and Gries, R. R., 1994, Tertiary stratigraphy and tectonic development of the Alamosa Basin (northern San Luis Basin), Rio Grande rift, south-central Colorado, *in* Keller, G. R. and Cather, S. M., eds., Basins of the Rio Grande rift: Structure, stratigraphy, and tectonic setting: Geological Society of America, Special Paper 291, p. 39–58.

Brister, B. S. and McIntosh, W. C., *in press*, Identification and correlation of Oligocene ignimbrites in well bores, Alamosa Basin (northern San Luis Basin, Colorado), by single-crystal laser-fusion $^{40}Ar/^{39}Ar$ geochronology of well cuttings, *in* Cather, S. M., McIntosh, W. C., and Kelley, S. A., eds., Tectonics, geochronology, and volcanism in the southern Rocky Mountains and Rio Grande rift: New Mexico Bureau of Geology and Mineral Resources, Bulletin 160.

Brown, L. L. and Golombek, M. P., 1985, Tectonic rotations within the Rio Grande rift; evidence from paleomagnetic studies: Journal of Geophysical Research, v. 90, p. 790–802.

Brown, L. L. and Golombek, M. P., 1986, Block rotations in the Rio Grande rift, New Mexico: Tectonics, v. 5, p. 423–438.

Bryant, B. and Nichols, D. J., 1988, Late Mesozoic and early Tertiary reactivation of an ancient crustal boundary along the Uinta trend and its interaction with the Sevier orogenic belt, *in* Schmidt, C. J. and Perry, W. J., eds., Interaction of the Rocky Mountain Foreland and the Cordilleran thrust belt: Geological Society of America, Memoir 171, p. 411–430.

Bunds, M. P, 2002, Fault strength and transpressional tectonics along the Castle Mountain strike-slip fault, southern Alaska: Geological Society of America Bulletin, v. 113, p. 908–919.

Byerlee, J. D., 1978, Friction of rocks: Pure and Applied Geophysics, v. 116, p. 615–626.

Cabezas, P., 1991, The southern Rocky Mountains in west-central New Mexico—Laramide structures and their impact on the Rio Grande rift extension: New Mexico Geology, v. 13, p. 25–37.

Callender, J. F. and Zilinski, R. E., 1976, Kinematics of Tertiary and Quaternary deformation along the eastern edge of the Lucero Uplift, central New Mexico, *in* Woodward, L. A. and Northrop, S. A., eds., Tectonics and mineral resources of southwestern North America, New Mexico Geological Society, Special Publication 6, p. 53–61.

Casey, J. M., 1980, Depositional systems and basin evolution of the late Paleozoic Taos Trough, northern New Mexico [Ph.D. dissertation]: Austin, The University of Texas, 253 p.

Cather, S. M., 1980, Petrology, diagenesis, and genetic stratigraphy of the Eocene Baca Formation, Alamo Navajo Reservation and vicinity, Socorro County, New Mexico [M.A. thesis]: Austin, The University of Texas, 242 p.

Cather, S. M., 1983a, Laramide Sierra Uplift: evidence for major pre-rift uplift in central and southern New Mexico: New Mexico Geological Society, 34th Field Conference, Guidebook, p. 99–101.

Cather, S. M., 1983b, Lacustrine deposits of the Eocene Baca Formation, western Socorro County, New Mexico: New Mexico Geological Society, 34th Field Conference, Guidebook, p. 179–185.

Cather, S. M., 1983c, Arroyo-fill facies of Baca Formation: New Mexico Geological Society, 34th Field Conference, Guidebook, p. 27.

Cather, S. M., 1989, Post-Laramide tectonic and volcanic transition in west-central New Mexico: New Mexico Geological Society, 40th Field Conference, Guidebook, p. 91–97.

Cather, S. M., 1990, Stress and volcanism in the northern Mogollon-Datil field, New Mexico: effects of the post-Laramide tectonic transition: Geological Society of America Bulletin, v. 102, p. 1447–1458.

Cather, S. M., 1991, Stratigraphy and provenance of Upper Cretaceous and Paleogene strata of the western Sierra Blanca Basin, New Mexico: New Mexico, New Mexico Geological Society, 42nd Field Conference, Guidebook, p. 265–275.

Cather, S. M., 1992, Suggested revisions to the Tertiary tectonic history of north-central New Mexico: New Mexico Geological Society, 43rd Field Conference, Guidebook, p. 109–122.

Cather, S. M., 1999a, Implications of Jurassic, Cretaceous, and Proterozoic piercing lines for Laramide oblique-slip faulting in New Mexico and rotation of the Colorado Plateau: Geological Society of America Bulletin, v. 111, p. 849–868.

Cather, S. M., 1999b, Laramide faults in the southern Rocky Mountains; a role for strain partitioning and low frictional strength strike-slip faults? (abs.): Geological Society of America, Abstracts with programs, v. 31, p. 186–187.

Cather, S. M., 2000, Preliminary analysis of the Fresnal fault system; a major dextral normal fault of late Pennsylvanian age in south-central New Mexico (abs.): American Association of Petroleum Geologists Bulletin, v. 84, p. 1237.

Cather, S. M. and Johnson, B. D., 1984, Eocene tectonics and depositional setting of west-central New Mexico and eastern Arizona: New Mexico Bureau of Mines and Mineral Resources, Circular 192, 33 p.

Cather, S. M. and Johnson, B. D., 1986, Eocene depositional systems and tectonics in west-central New Mexico and eastern Arizona, *in* Peterson, J. A., ed., Paleotectonics and sedimentation in the Rocky Mountain region, United States: American Association of Petroleum Geologists, Memoir 41, p. 623–652.

Cather, S. M., Connell, S. D., and Black, B. A., 2000, Geology of the San Felipe Pueblo NE 7.5-minute quadrangle, New Mexico: New Mexico Bureau of Mines and Mineral Resources, Open-file Digital Geologic Map OF-DM 37, scale 1:24,000.

Cather, S. M., Connell, S. D., Lucas, S. G., Picha, M. G., and Black, B. A., 2002, Preliminary geologic map os the Hagan 7.5-minute quadrangle, Sandoval County, New Mexico: New Mexico Bureau of Geology and Mineral Resources, Open-file Geologic Map GM-50, scale 1:24,000.

Cather, S. M., Chamberlin, R. M., and Ratté, J. C., 1994, Tertiary stratigraphy and nomenclature for western New Mexico and eastern Arizona: New Mexico Geological Society, 45th Field Conference, Guidebook, p. 259–266.

Cather, S. M., Connell, S. D., Heynekamp, and Goodwin, L. B., 1997, Geologic map of the Sky Village SE 7.5-minute quadrangle, New Mexico: New Mexico Bureau of Mines and Mineral Resources, Open-file Digital Geologic Map OF-DM 9, scale 1:24,000.

Cather, S. M., McIntosh, W. C., and Chapin, C. E., 1987, Stratigraphy, age, and rates of deposition of the Datil Group (upper Eocene-lower Oligocene), west-central New Mexico: New Mexico Geology, v. 9, p. 50–54.

Cather, S. M., Peters, L., Dunbar, N. W., and McIntosh, W. C., *in press*, Genetic stratigraphy, provenance, and new age constratins for the Chuska Sandstone, New Mexico-Arizona: New Mexico Geological Society, 54th Field Conference, Guidebook.

Cerveny, P. F., III, 1990, Fission-track thermochronology of the Wind River Range and other basement-cored uplifts in the Rocky Mountain foreland [Ph.D dissertation]: Laramie, University of Wyoming, 199 p.

Chamberlin, R. M., 1999, Partitioning of dextral slip in an incipient transverse shear zone of Neogene age, northwestern Albuquerque Basin, Rio Grande rift, New Mexico (abs.): Geological Society of America, Abstracts with Programs, v. 31, p. 113.

Chamberlin, R. M. and Anderson, O. J., 1989, The Laramide Zuni Uplift, southeastern Colorado Plateau; a microcosm of Eurasian-style indentation-extrusion tectonics?: New Mexico Geological Society, 40th Field Conference, Guidebook, p. 81–90.

Chapin, C. E. and Cather, S. M., 1981, Eocene tectonics and sedimentation in the Colorado Plateau-Rocky Mountain area, *in* Dickinson, W. R. and Payne, W. D., eds., Relations of tectonics to ore deposits in the southern Cordillera, Arizona Geological Society Digest, p. 173–198.

Chapin, C. E. and Cather, S. M., 1983, Eocene tectonics and sedimentation in the Colorado Plateau; Rocky Mountain area, *in* Lowell, J. D., ed., Rocky Mountain foreland basins and uplifts: Denver, Rocky Mountain Association of Geologists, p. 33–56.

Chapin, C. E. and Cather, S. M., 1994, Tectonic setting of the axial basins of the northern and central Rio Grande rift, *in* Keller, G. R. and Cather, S. M., eds., Basins of the Rio Grande rift: Structure, stratigraphy and tectonic setting: Geological Society of America, Special Paper 291, p. 5–26.

Chapin, C. E., Chamberlin, R. M., Osburn, G. R., Sanford, A. R., and White, D. L., 1978, Exploration framework of the Socorro geothermal area, New Mexico, *in* Chapin, C. E. and Elston, W. E., eds., Field guide to selected cauldrons and mining districts of the Datil-Mogollon volcanic field, New Mexico: New Mexico Geological Society, Special Publication 7, p. 115–129.

Cobban, W. A., 1956, The Pierre Shale and older Cretaceous rocks in southeastern Colorado, *in* Geology of the Raton Basin: Denver, Rocky Mountain Association of Geologists Guidebook, p. 25–27.

Connell, S. D., Cather, S. M., Karlstrom, K. E., Read, A., Ilg, B., Menne, B., Andronicus, C., Bauer, P., and Anderson, O. J., 1995, Geology of the Placitas 7.5-minute quadrangle, Sandoval County, New Mexico: New Mexico Bureau of Mines and Mineral Resources, Open-file Digital Geologic Map OF-DM 2, scale 1:12,000.

Craigg, S. D., Dam, W. L., Kernodle, J. M., and Levings, G. W., 1989, Hydrology of the Dakota Sandstone in the San Juan structural Basin, New Mexico, Colorado, Arizona, and Utah: U.S. Geological Survey, Atlas HA-720-I, various scales, 2 sheets.

Cumella, S. P., 1983, Relation of Upper Cretaceous regressive sandstone units of the San Juan Basin to source area tectonics, *in* Reynolds, M. W. and Dolly, E. D., eds., Mesozoic paleogeography of the west-central United States: Rocky Mountain Section, Society of Economic Paleontologists and Mineralogists, p. 189–199.

Daniel, C. G., Karlstrom, K. E., Williams, M. L., and Pedrick, J. N., 1995, The reconstruction of a middle Proterozoic orogenic belt in north-central New Mexico, U.S.A.: New Mexico Geological Society, 46th Field Conference, Guidebook, p. 193–200.

Davis, G. H. and Reynolds, S. J., 1996, Structural geology of rocks and regions, 2nd ed.: New York, John Wiley and Sons, 776 p.

Dewey, J. F. and Lamb, S. H., 1992, Active tectonics of the Andes: Tectonophysics, 205, p. 79–95.

Dickinson, R. G., Leopold, E. B., and Marvin, R. F., 1968, Late Cretaceous uplift and volcanism on the north flank of the San Juan Mountains, Colorado: Colorado School of Mines, Quarterly, v. 63, p. 125–148.

Dickinson, W. R., Klute, M. A., Hayes, M. J., Janecke, S. U., Lundin, E. R., McKittrick, M. A., and Olivares, M. D., 1988, Paleogeographic and paleotectonic setting of Laramide sedimentary basins in the central Rocky Mountain region: Geological Society of America Bulletin, v. 100, p. 1023–1039.

Dilworth, O. L., 1960, Upper Cretaceous Farmington Sandstone of northeastern San Juan County, New Mexico [M.S. thesis]: Albuquerque, University of New Mexico, 96 p.

Dolly, E. D. and Meissner, F. F., 1977, Geology and gas exploration potential, Upper Cretaceous and lower Tertiary strata, northern Raton Basin, Colorado, *in* Veal, H. K., ed., Exploration frontiers of the central and southern Rockies: Denver, Rocky Mountain Association of Geologists, p. 247–270.

Dunn, D. E., 1964, Evolution of the Chama Basin and Archuleta Anticlinorium, eastern Archuleta County, Colorado [Ph.D. dissertation]: Austin, The University of Texas, 114 p.

Eardley, A. J., 1962, Structural geology of North America, 2nd ed.: New York, Harper and Row, 743 p.

Edmunds, R. J., 1961, Geology of the Nutria monocline, McKinley County, New Mexico [M.S. thesis]: Albuquerque, University of New Mexico, 100 p.

Eggleston, T. L., 1982, Geology of the central Chupadera Mountains, Socorro County, New Mexico [M.S. thesis]: Socorro, New Mexico Institute of Mining and Technology, 161 p.

Erslev, E. A., 1997, Multi-directional Laramide compression in the Durango area—why?, *in* Close, J. C. and Casey, T. N., eds., Natural fracture systems in the southern Rocky Mountains: Four Corners Geological Society, Guidebook, p. 1–6.

Erslev, E. A., 1999, Multistage, multidirectional horizontal compression during Laramide and mid-Tertiary deformation east of the Rio Grande rift, north-central New Mexico: New Mexico Geological Society, 50th Field Conference, Guidebook, p. 22–23.

Erslev, E. A., 2001, Multistage, multidirectional Tertiary shortening and compression in north-central New Mexico: Geological Society of America Bulletin, v. 113, p. 63–74.

Fassett, J. E., 1976, What happened during Late Cretaceous time in the Raton and San Juan Basins—with some thoughts about the area in between: New Mexico Geological Society, 27th Field Conference, Guidebook, p. 185-190.

Fassett, J. E., 1985, Early Tertiary paleogeography and paleotectonics of the San Juan Basin area, New Mexico and Colorado, *in* Flores, R. M. and Kaplan, S. S., eds., Cenozoic paleogeography of the west-central United States: Denver, Rocky Mountain Section, Society of Economic Paleontologists and Mineralogists, p. 317–334.

Fassett, J. E., 2000, Geology and coal resources of the Upper Cretaceous Fruitland Formation, San Juan Basin, New Mexico and Colorado, *in* Kirschbaum, M. A., Roberts, L. N. R., and Biewick, L. R. H., eds., Geologic assessment of coal in the Colorado Plateau: Arizona, Colorado, New Mexico and Utah: U.S. Geological Survey, Professional Paper 1625-B, p. Q1–Q132.

Fassett, J. E. and Hinds, J. S., 1971, Geology and fuel resources of the Fruitland Formation and Kirtland Shale of the San Juan Basin, New Mexico and Colorado: U.S. Geological Survey, Professional Paper 676, 76 p.

Fassett, J. E. and Lucas, S. G., 2000, Evidence for Paleocene dinosaurs in the Ojo Alamo Sandstone, San Juan Basin, New Mexico, *in* Lucas, S. G. and Heckert, A. B., eds., Dinosaurs of New Mexico: New Mexico Museum of Natural History and Science, Bulletin 17, p. 221–230.

Fassett, J. E. and Steiner, M. B., 1997, Precise age of C33N-C32R magnetic-polarity reversal, San Juan Basin, New Mexico and Colorado: New Mexico Geological Society, 48th Field Conference, Guidebook, p. 239–247.

Fassett, J. E., Cobban, W. A., and Obradovich, J. D., 1997, Biostratigraphic and isotopic age of the Huerfanito Bentonite Bed of the Upper Cretaceous Lewis Shale at an outcrop near Regina, New Mexico: New Mexico Geological Society, 48th Field Conference, Guidebook, p. 229–232.

Fassett, J. E., Lucas, S. G., and O'Neill, F. M., 1987, Dinosaurs, pollen and spores, and the age of the Ojo Alamo Sandstone, San Juan Basin, New Mexico, *in* Fassett, J. E. and Rigby, J. K., Jr., eds., The Cretaceous-Tertiary boundary in the San Juan and Raton Basins, New Mexico and Colorado: Geological Society of America, Special Paper 209, p. 17–34.

Fassett, J. E., Zielinski, R. A., and Budahn, J. R., 2002, Dinosaurs that did not die: Evidence for Paleocene dinosaurs in the Ojo Alamo Sandstone, San Juan Basin, New Mexico, *in* Koerberl, C. and MacLeod, K. G., eds., Catastrophic events and mass extinctions: Impacts and beyond: Geological Society of America, Special Paper 356, p. 307–336.

Faulds, J. E. and Varga, R. J., 1998, The role of accommodation zones and transfer zones in the regional segmentation of extended terranes, *in* Faulds, J. E. and Stewart, J. H., eds., Accommodation zones and transfer zones; the regional segmentation of the Basin and Range Province: Geological Society of America, Special Paper 323, p. 1–45.

Ferguson, J. F., Baldridge, W. S., Braile, L. W., Biehler, S., Gilpin, B., and Jiracek, G. R., 1995, Structure of the Española Basin, Rio Grande rift, New Mexico, from SAGE seismic and gravity data: New Mexico Geological Society, 46th Field Conference, Guidebook, p. 105–110.

Fitch, T. J., 1972, Plate convergence, transcurrent faults, and internal deformation adjacent to southeast Asia and the western Pacific: Journal of Geophysical Research, v. 77, p. 4432–4460.

Fitzsimmons, J. P., 1967, Precambrian rocks of the Zuni Mountains: New Mexico Geological Society, 18th Field Conference, Guidebook, p. 119–121.

Flores, R. M., 1987, Sedimentology of Upper Cretaceous and Tertiary siliciclastics and coals in the Raton Basin: New Mexico Geological Society, 38th Field Conference, Guidebook, p. 255–264.

Flores, R. M. and Erpenbeck, M. F., 1981, Differentiation of delta-front and barrier lithofacies of the Upper Cretaceous Pictured Cliffs Sandstone, southwest San Juan Basin, New Mexico: The Mountain Geologist, v. 18, p. 23–34.

Flores, R. M. and Pillmore, C. L., 1987, Tectonic control on alluvial paleoarchitecture of the Cretaceous and Tertiary Raton Basin, Colorado and New Mexico, *in* Ethridge, F. G., Flores, R. M., Harvey, M. D., and Weaver, J. N., eds., Recent developments in fluvial sedimentology: Society of Economic Paleontologists and Mineralogists, Special Publication 39, p. 311–320.

Flores, R. M. and Tur, S. M., 1982, Characteristics of deltaic deposits in the Cretaceous Pierre Shale, Trinidad Sandstone, and Vermejo Formation, Raton Basin, Colorado: The Mountain Geologist, v. 19, p. 25–40.

Garmezy, L., Zarrow, L., and Stillman, N. W., 1990, Strike-slip deformation along the southeastern margin of the Colorado Plateau (abs.): Geological Society of America, Abstracts with Programs, v. 22, p. 276.

Ghisetti, F., 2000, Slip partitioning and deformation cycles close to major faults in southern California; evidence from small-scale faults: Tectonics, v. 19, p. 25–43.

Goddard, E. N., 1966, Geologic map and sections of the Zuni Mountains fluorspar district, Valencia County, New Mexico: U.S. Geological Survey, Miscellaneous Investigations Map I-454, scale 1:31,680.

Goff, F., Gardner, J. N., and Valentine, G., 1990, Geology of the St. Peter's Dome area, Jemez Mountains, New Mexico: New Mexico Bureau of Mines and Mineral Resources, Geologic Map 69, scale 1:24,000.

Gorham, T. W., 1979, Geology of the Galisteo Formation, Hagan Basin, New Mexico [M.S. thesis]: Albuquerque, University of New Mexico, 136 p.

Gorham, T. W. and Ingersoll, R. V., 1979, Evolution of the Eocene Galisteo Basin, north-central New Mexico: New Mexico Geological Society, 30th Field Conference, Guidebook, p. 219–224.

Grambling, J. A. and Williams, M. L., 1985, The effects of Fe3+ and Mn3+ on aluminum silicate phase relationships in north-central New Mexico, U.S.A.:

Journal of Petrology, v. 26, p. 324–354.
Grambling, J. A., Williams, M. L., Smith, R. F., and Mawer, C. K., 1989, The role of crustal extension in the metamorphism of Proterozoic rocks in New Mexico: Geological Society of America, Special Paper 235, p. 87–110.
Gries, R. R., Clayton, J. L., and Leonard, C., 1997, Geology, thermal maturation, and source rock geochemistry in a volcanic covered basin: San Juan Sag, south-central Colorado: American Association of Petroleum Geologists Bulletin, v. 81, p. 1133–1160.
Hammond, C. M., 1987, Navajo Gap area between the Ladron Mountains and Mesa Sarca, Socorro County, NM; structural analysis [M.S. thesis]: Socorro, New Mexico Institute of Mining and Technology, 212 p.
Harding, T. P., 1974, Petroleum traps associated with wrench faults: American Association of Petroleum Geologists Bulletin, v. 58, p. 1290–1304.
Harrison, R. W., 1990, Cenozoic stratigraphy, structure, and epithermal mineralization of the north-central Black Range, in the regional geologic framework of south-central New Mexico [Ph.D. dissertation]: Socorro, New Mexico Institute of Mining and Technology, 359 p.
Harrison, R. W. and Cather, S. M., *in press*, The Hot Springs fault system: evidence in south-central New Mexico for northward translation of the Colorado Plateau during the Laramide orogeny, *in* Cather, S. M., McIntosh, W. C., and Kelley, S. A., eds., Tectonics, volcanism, and geochronology in the southern Rocky Mountains and Rio Grande rift: Socorro, New Mexico Bureau of Geology and Mineral Resources, Bulletin 160.
Harrison, R. W. and Chapin, C. E., 1990, A NNE-trending, dextral wrench-fault zone of Laramide age in southern New Mexico (abs): Geological Society of America, Abstracts with Programs, v. 22, p. 327.
Hayden, S. N., 1991, Dextral oblique-slip deformation along the Montosa fault zone at Abo Pass, Valencia and Socorro Counties, New Mexico (abs.): New Mexico Geology, v. 13, p. 64.
Hoy, R. G. and Ridgway, K. D., 2002, Syndepositional thrust-related deformation and sedimentation in an Ancestral Rocky Mountains basin, central Colorado trough, Colorado, USA: Geological Society of America Bulletin, v. 114, p. 804–828.
Hudson, M. R., Minor, S. A., and Grauch, V. J. S., 2001, Fault framework for the Albuquerque Basin, Rio Grande rift (abs.): Geological Society of America, Abstracts with Programs, v. 33, no. 5, p. A47.
Hunt, A. P. and Lucas, S. G., 1992, Stratigraphy, paleontology and age of the Fruitland and Kirtland Formations (Upper Cretaceous), San Juan Basin, New Mexico: New Mexico Geological Society, 43rd Field Conference, Guidebook, p. 217–239.
Ingersoll, R. V., 2000, Implications of Jurassic, Cretaceous, and Proterozoic piercing lines for Laramide oblique-slip faulting in New Mexico and rotation of the Colorado Plateau; discussion and reply: Geological Society of America Bulletin, v. 112, p. 796–798.
Ingersoll, R. V., Cavazza, W., Baldridge, W. S., and Shafiqullah, M., 1990, Cenozoic sedimentation and paleotectonics of north-central New Mexico; implications for initiation and evolution of the Rio Grande rift: Geological Society of America Bulletin, v. 102, p. 1280–1296.
Johnson, B. D., 1978, Genetic stratigraphy and provenance of the Baca Formation, New Mexico, and the Eagar Formation, Arizona [M.A. thesis]: Austin, The University of Texas, 150 p.
Johnson, R. B., 1959, Geology of the Huerfano Park area, Huerfano and Custer Counties, Colorado: U.S. Geological Survey, Bulletin 1071-D, p. C87–C119.
Johnson, R. B. and Wood, G. H., Jr., 1956, Stratigraphy of Upper Cretaceous and Tertiary rocks of Raton Basin, Colorado, and New Mexico: Bulletin of the American Association of Petroleum Geologists, v. 40, p. 707–721.
Jones, C. H., 2000, Horizontal folds as both contractional and strike-slip shear zones? (abs.): Geological Society of America, Abstracts with Programs, v. 32, p. 29.
Jones, R. R., Holdsworth, R. E., and Tanner, P. W. G., 1995, Strain partitioning in transpression zones: Journal of Structural Geology, v. 17, p. 793–802.
Karlstrom, K. E. and Daniel, C. G., 1993, Restoration of Laramide right-lateral strike slip in northern New Mexico by using Proterozoic piercing points: Tectonic implications from the Proterozoic to the Cenozoic: Geology, v. 21, p. 1193–1142.
Karlstrom, K. E., Cather, S. M., Kelley, S. A., Heizler, M. T., Pazzaglia, F. J., and Roy, M., 1999, Sandia Mountains and Rio Grande rift; ancestry of structures and history of deformation: New Mexico Geological Society, 50th Field Conference, Guidebook, p. 155–166.
Kay, S. M. and Mpodozis, C., 2001, Central Andean ore deposits linked to evolving shallow subduction systems and thickening crust: GSA Today, v. 11, no. 3, p. 4–9.
Kelley, S. A., 1990, Late Mesozoic to Cenozoic cooling history of the Sangre de Cristo Mountains, Colorado and New Mexico: New Mexico Geological Society, 41st Field Conference, Guidebook, p. 123–132.
Kelley, S. A., 1995, Evidence for post-Laramide displacement on the Picuris-Pecos fault: New Mexico Geological Society, 46th Field Conference, Guidebook, p. 32–33.
Kelley, S. A. and Chapin, C. E., 1995, Apatite fission-track thermochronology of Southern Rocky Mountain-Rio Grande rift-western High Plains provinces: New Mexico Geological Society, 46th Field Conference, Guidebook, p. 87–96.
Kelley, S. A. and Duncan, I. J., 1986, Late Cretaceous to middle Tertiary tectonic history of the northern Rio Grande rift: Journal of Geophysical Research, v. 91, p. 6246–6262.
Kelley, S. A., Chapin, C. E., Cather, S. M., and Person, M., 1997, Paleohydrology and thermal history of the eastern margin of the Socorro Basin, New Mexico (abs.): Geological Society of America, Abstracts with Programs, v. 29, p. 17.
Kelley, S. A., Chapin, C. E., and Corrigan, J., 1992, Late Mesozoic to Cenozoic cooling histories of the flanks of the northern and central Rio Grande rift, Colorado and New Mexico: New Mexico Bureau of Mines and Mineral Resources, Bulletin 145, 39 p.
Kelley, V. C., 1955, Regional tectonics of the Colorado Plateau and relationships to the origin and distribution of uranium: Albuquerque, University of New Mexico Publications in Geology, no. 5, 120 p.
Kelley, V. C., 1967, Tectonics of the Zuni-Defiance region, New Mexico and Arizona: New Mexico Geological Society, 18th Field Conference, Guidebook, p. 28–31.
Kelley, V. C., 1977, Geology of the Albuquerque Basin, New Mexico: New Mexico Bureau of Mines and Mineral Resources, Memoir 33, 60 p.
Kelley, V. C. and Clinton, N. J., 1960, Fracture systems and tectonic elements of the Colorado Plateau: Albuquerque, University of New Mexico Press, 104 p.
Kelley, V. C. and Northrop, S. A., 1975, Geology of the Sandia Mountains and vicinity, New Mexico, New Mexico Bureau of Mines and Mineral Resources, Memoir 29, 136 p.
Klute, M. A., 1986, Sedimentology and sandstone petrography of the upper Kirtland Shale and Ojo Alamo Sandstone, Cretaceous-Tertiary boundary, western and southern San Juan Basin, New Mexico: American Journal of Science, v. 286, p. 463–488.
Kluth, C. F. and Shaftenaar, C. H., 1994, Depth and geometry of the northern Rio Grande rift in the San Luis Basin, south-central Colorado, *in* Keller, G. R. and Cather, S. M., eds., Basins of the Rio Grande rift: Structure, stratigraphy and tectonic setting: Geological Society of America, Special Paper 291, p. 27–37.
Kopacz, M. A., Zarrow, L., and Garmezy, L., 1989, The Mogollon: subvolcanic frontier play: 28th International Geological Congress, Abstracts, New York, Springer-Verlag, p. 2–213.
Landis, E. R. and Dane, C. H., 1967, Geologic map of Tierra Amarilla quadrangle, Rio Arriba County, New Mexico: New Mexico Bureau of Mines and Mineral Resources, Geologic Map 19, scale 1:62,500.
Larsen, E. S., Jr., and Cross, C. W., 1956, Geology and petrology of the San Juan region, southwestern Colorado: U.S. Geological Survey, Professional Paper 258, 303 p.
Lawton, 1988, Tectonic setting of Mesozoic sedimentary basins, Rocky Mountain region, United States, *in* Caputo, M. V., Peterson, J. A., and Franczyk, K. J., eds., Mesozoic systems of the Rocky Mountain region, USA: Denver, Society of Economic Paleontologists and Mineralogists, p. 1–25.
Leckie, R. M., Kirkland, J. I., and Elder, W. P., 1997, Stratigraphic framework and correlation of a principal reference section of the Mancos Shale (Upper Cretaceous), Mesa Verde, Colorado: New Mexico Geological Society, 48th Field Conference, Guidebook, p. 163–189.
Leeder, M. R. and Gawthorpe, R. L., 1987, Sedimentary models for extensional tilt-block/half graben basins: London, Geological Society of London, Special Publication 28, p. 139–152.
Lehman, T. M., 1985, Depositional environments of the Naashoibito Member of the Kirtland Shale, Upper Cretaceous, San Juan Basin, New Mexico, *in* Wolberg, D. L., compiler, Contributions to Late Cretaceous paleontology and stratigraphy of New Mexico: New Mexico Bureau of Mines and Mineral Resources, Circular 195, p. 55–79.
Lewis, C. J. and Baldridge, W. S., 1994, Crustal extension in the Rio Grande rift, New Mexico; half-grabens, accommodation zones, and shoulder uplifts in the Ladron Peak-Sierra Lucero area, *in* Keller, G. R. and Cather, S. M., eds., Basins of the Rio Grande rift: Structure, stratigraphy, and tectonic setting,

Geological Society of America, Special Publication 291, p. 135–155.
Lindsay, D. A., 1998, Laramide structure of the central Sangre de Cristo Mountains and adjacent Raton Basin, southern Colorado: The Mountain Geologist, v. 35, p. 55–70.
Lisenbee, A. L., Woodward, L. A., and Connolly, J. R., 1979, Tijeras-Canoncito fault system—a major zone of recurrent movement in north-central New Mexico: New Mexico Geological Society, 30th Field Conference, Guidebook, p. 89–99.
Logsdon, M. J., 1981, A preliminary basin analysis of the El Rito Formation (Eocene), north-central New Mexico: Geological Society of America Bulletin, v. 92, p. 968–975.
Lozinsky, R. P., 1988, Stratigraphy, sedimentology, and sand petrology of the Santa Fe Group and pre-Santa Fe Tertiary deposits in the Albuquerque Basin, central New Mexico [Ph.D. dissertation]: Socorro, New Mexico Institute of Mining and Technology, 298 p.
Lozinsky, R. P., 1994, Cenozoic stratigraphy, sandstone petrology, and depositional history of the Albuquerque Basin, central New Mexico, *in* Keller, G. R. and Cather, S. M., eds., Basins of the Rio Grande rift: Structure, stratigraphy, and tectonic setting: Geological Society of America, Special Paper 291, p. 73–81.
Lucas, S. G., 1982, Vertebrate paleontology, stratigraphy, and biostratigraphy of Eocene Galisteo Formation, north-central New Mexico: New Mexico Bureau of Mines and Mineral Resources, Circular 186, 34 p.
Lucas, S. G., 1984, Correlation of Eocene rocks of the northern Rio Grande rift and adjacent areas: Implications for Laramide tectonics: New Mexico Geological Society, 35th Field Conference, Guidebook, p. 123–128.
Lucas, S. G., 1990, Middle Eocene mammal from the base of the Baca Formation, west-central New Mexico: New Mexico Journal of Science, v. 30, p. 35–39.
Lucas, S. G. and Sullivan, R. M., 2000, Stratigraphy and vertebrate biostratigraphy across the Cretaceous-Tertiary boundary, Betonnie Tsosie Wash, San Juan Basin, New Mexico, *in* Lucas, S. G. and Heckert, A. B., eds., Dinosaurs of New Mexico: New Mexico Museum of Natural History and Science, Bulletin 17, p. 95–103.
Lucas, S. G. and Williamson, T. E., 1993a, Late Cretaceous to early Eocene vertebrate biostratigraphy and biochronology of the San Luis Basin, New Mexico, *in* Lucas, S. G. and Zidek, J., eds., Vertebrate paleontology in New Mexico: New Mexico Museum of Natural History and Science Bulletin 2, p. 93–104
Lucas, S. G. and Williamson, T. E., 1993b, Eocene vertebrates and late Laramide stratigraphy of New Mexico, *in* Lucas, S. G. and Zidek, J., eds., Vertebrate paleontology in New Mexico: New Mexico Museum of Natural History and Science Bulletin 2, p. 145–158.
Lucas, S. G., Anderson, O. J., and Black, B. A., 2000, Implications of Jurassic, Cretaceous, and Proterozoic piercing lines for Laramide oblique-slip faulting in New Mexico and rotation of the Colorado Plateau; discussion and reply: Geological Society of America Bulletin, v. 112, p. 789–795.
Lucas, S. G., Cather, S. M., Abbott, J. C., and Williamson, T. E., 1997, Stratigraphy and tectonic implications of Paleogene strata in the Laramide Galisteo Basin, north-central New Mexico: New Mexico Geology, v. 19, p. 89–95.
Lucas, S. G., Cather, S. M., Sealey, P., and Hutchison, J. H., 1989, Stratigraphy, paleontology, and depositional systems of the Eocene Cub Mountain Formation, Lincoln County, New Mexico; a preliminary report: New Mexico Geology, v. 11, p. 11–17.
Mack, G. H., Nightengale, A. L., Seager, W. R., and Clemons, R. E., 1994, The Oligocene Goodsight-Cedar Hills half graben near Las Cruces and its implications to the evolution of the Mogollon-Datil volcanic field and to the southern Rio Grande rift: New Mexico Geological Society, 45th Field Conference, Guidebook, p. 135–142.
Mallory, W. W., 1972, Pennsylvanian arkose and the ancestral Rocky Mountains, *in* Mallory W. W., ed., Geologic atlas of the Rocky Mountain region: Denver, Rocky Mountain Association of Geologists, p. 131–132.
Marshall, K. A. and Geissman, J. W., 2001, Paleomagnetism of Upper Pennsylvanian to Lower Permian Sangre de Cristo Formation strata: evaluation of Late Cretaceous to early Tertiary deformation in the Sangre de Cristo Mountains, southern Colorado (abs.): Geological Society of America, Abstracts with Programs, v. 33, p. 46.
Matuszczak, R. A., 1969, Trinidad Sandstone interpreted, evaluated, in Raton Basin, Colorado-New Mexico: The Mountain Geologist, v. 6, p. 119–124.
McCaffrey, R., 1992, Oblique plate convergence, slip vectors, and forearc deformation: Journal of Geophysical Research, v. 97, no. B6, p. 8905–8915.
Merin, I. S., Everett, J. R., and Rose, P. R., 1988, *in* Sloss, L. L., ed., Sedimentary cover-North American craton: U.S.: Geological Society of America, The Geology of North America, v. D-2, p. 171–179.
Miller, J. P., Montgomery, A., and Sutherland, P. K., 1963, Geology of part of the southern Sangre de Cristo Mountains, New Mexico: New Mexico Bureau of Mines and Mineral Resources, Memoir 11, 106 p.
Molenaar, C. M., 1983, Major depositional cycles and regional correlations of Upper Cretaceous rocks, southern Colorado Plateau, and adjacent areas, *in* Reynolds, M. W. and Dolly, E. D., eds., Mesozoic paleogeography of west-central United States: Denver, Society of Economic Paleontologists and Mineralogists, p. 201–224.
Molnar, P., 1992, Brace-Goetze strength profiles, the partitioning of strike-slip and thrust faulting at zones of oblique convergence, and the stress-heat flow paradox of the San Andreas fault, *in* Evans, B. and Wong, T.-F., eds., Fault mechanics and transport properties of rocks: London, Academic Press, p. 435–459.
Morel, J. and Watkins, T. A., 1997, More data point to potential in S. Colorado subbasin: Oil and Gas Journal, v. 95, no. 35, p. 78–80.
Mount, V. S. and Suppe, J., 1987, State of stress near the San Andreas fault; implications for wrench tectonics: Geology, v. 15, p. 1143–1146.
Muehlberger, W. R., 1967, Geology of Chama quadrangle, New Mexico: New Mexico Bureau of Mines and Mineral Resources, Bulletin 89, 114 p.
Muehlberger, W. R., 1968, Geologic map, cross sections, and structure contour and tectonic map of the Brazos Peak fifteen-minute quadrangle, New Mexico and Colorado: New Mexico Bureau of Mines and Mineral Resources, Geologic Map GM-22, scale 1:48,000.
Mutschler, F. E., Larson, E. E., and Bruce, R. M., 1987, Laramide and younger magmatism in Colorado—new petrologic and tectonic variations on old themes, *in* Drexler, J. W. and Larson, E. E., eds., Cenozoic volcanism in the southern Rocky Mountains updated: A tribute to Rudy C. Epis—Part 1: Golden, Colorado School of Mines Quarterly, v. 82, p. 1–47.
Newman, K. R., 1987, Biostratigraphic correlation of Cretaceous-Tertiary boundary rocks, Colorado to San Juan Basin, New Mexico, *in* Fassett, J. E. and Rigby, J. K., Jr., eds., The Cretaceous-Tertiary boundary in the San Juan and Raton Basins, New Mexico and Colorado: Geological Society of America, Special Paper 209, p. 151–164.
Obradovich, J. D., 1993, A Cretaceous time scale, *in* Caldwell, W. G. E. and Kauffman, E. G., eds., Evolution of the Western Interior Basin: Geological Association of Canada, Special Paper 39, p. 379–396.
Paola, C., Heller, P. L., and Angevine, C. L., 1992, The large-scale dynamics of grain-size variation in alluvial basins, 1: Theory: Basin Research, v. 4, p. 73–90.
Peirce, H. W., Damon, P. E., and Shafiqullah, M., 1979, An Oligocene (?) Colorado Plateau edge in Arizona: Tectonophysics, v. 61, p. 1–24.
Peters, L., 2001, $^{40}Ar/^{39}Ar$ geochronology results from the upper coal member of the Menefee Formation: New Mexico Bureau of Geology and Mineral Resources, New Mexico Geochronology Research Laboratory, Internal Report NMGRL-IR-246, 8 p.
Peterson, J. A. and Smith, D. L., 1986, Rocky Mountain paleogeography through geologic time, *in* Peterson, J. A., ed., Paleotectonics and sedimentation in the Rocky Mountain region, United States: American Association of Petroleum Geologists, Memoir 41, p. 3–19.
Pillmore, C. L., 1969, Geology and coal deposits of the Raton coal field, Colfax County, New Mexico: The Mountain Geologist, v. 6, p. 125–142.
Pillmore, C. L., 1976, The York Canyon coal bed: New Mexico Geological Society, 27th Field Conference, Guidebook, p. 249-251.
Pillmore, C. L., 1990, Cretaceous and Paleocene rocks of the Raton Basin, New Mexico and Colorado; stratigraphic-environmental framework: New Mexico Geological Society, 41st Field Conference, Guidebook, p. 333–336.
Pillmore, C. L. and Flores, R. M., 1987, Stratigraphy and depositional environments of the Cretaceous-Tertiary boundary clay and associated rocks, Raton Basin, New Mexico and Colorado, *in* Fassett, J. E. and Rigby, J. K., Jr., eds., The Cretaceous-Tertiary boundary in the San Juan and Raton Basins, New Mexico and Colorado: Geological Society of America, Special Paper 209, p. 111–130.
Pillmore, C. L. and Flores, R. M., 1990, Cretaceous and Paleocene rocks of the Raton Basin, New Mexico and Colorado—Stratigraphic-environmental framework: New Mexico Geological Society, 41st Field Conference, Guidebook, p. 333–336.
Pillmore, C. L., Tschudy, R. H., Orth, C. J., Gilmore, J. S., and Knight, J. D., 1984, Geologic framework of nonmarine Cretaceous-Tertiary boundary sites, Raton Basin, New Mexico and Colorado: Science, v. 223, p. 1180–1182.
Pollock, C. J., Stewart, K. G., Hibbard, J. P., Wallace, L., and Giral, R. A., *in press*, Thrust-wedge tectonics and strike-slip faulting in the Sierra Nacimiento, *in*

Cather, S. M., McIntosh, W. C., and Kelley, S. A., eds., Tectonics, geochronology, and volcanism in the southern Rocky Mountains and Rio Grande rift: Socorro, New Mexico Bureau of Geology and Mineral Resources, Bulletin 160.

Potochnik, A. R., 1989, Depositional style and tectonic implications of the Mogollon Rim Formation (Eocene), east-central Arizona: New Mexico Geological Society, 40th Field Conference, Guidebook, p. 107–118.

Potochnik, A. R., 2001, Cenozoic structural and paleogeographic evolution of the transition zone, central Arizona [Ph.D. dissertation]: Tempe, Arizona State University, 173 p.

Powell, J. S., 1972, The Gallegos Sandstone (formerly Ojo Alamo Sandstone) of the San Juan Basin, New Mexico [M.S. thesis]: Tucson, University of Arizona, 131 p.

Powell, J. S., 1973, Paleontology and sedimentation models of the Kimbeto Member of the Ojo Alamo Sandstone, *in* Fassett, J. E., ed., Cretaceous and Tertiary rocks of the southern Colorado Plateau: Four Corners Geological Society, Memoir, p. 111–122.

Pray, L. C., 1961, Geology of the Sacramento Mountains escarpment, Otero County, New Mexico: New Mexico Bureau of Mines and Mineral Resources, Bulletin 35, 144 p.

Prothero, D. R. and Lucas, S. G., 1996, Magnetic stratigraphy of the Duchesnean part of the Galisteo Formation, New Mexico, The terrestrial Eocene-Oligocene transition in North America, *in* Prothero, D. R. and Emry, R. J., eds., The terrestrial Eocene-Oligocene transition in North America: Cambridge, University Press, p. 200–205.

Ralser, S. and Hart, B., 1999, Structural evolution of Ute Dome, NW New Mexico; implications for the development of the Hogback monocline (abs.): Geological Society of America, Abstracts with Programs, v. 31, p. 131.

Reeside, J. B., Jr., 1924, Upper Cretaceous and Tertiary formations of the western part of San Juan Basin, Colorado, and New Mexico: U.S. Geological Survey, Professional Paper 134, 70 p.

Roberts, L. N. R. and Kirschbaum, M. A., 1995, Paleogeography of the Late Cretaceous of the western interior of middle North America: coal distribution and sediment accumulation: U.S. Geological Survey, Professional Paper 1561, 115 p.

Robinson, P., 1966, Fossil mammalia of the Huerfano Formation, Eocene of Colorado: New Haven, Yale University, Peabody Museum of Natural History, Bulletin 21, 95 p.

Ross, C. A. and Ross, J. R. P., 1986, Paleozoic paleotectonics and sedimentation in Arizona and New Mexico, *in* Peterson, J. A., ed., Paleotectonics and sedimentation in the Rocky Mountain region, United States: American Association of Petroleum Geologists, Memoir 41, p. 653–668.

Ruf, J. C., 2000, Origin of Laramide to Holocene fractures in the northern San Juan Basin, Colorado and New Mexico [M.S. thesis]: Fort Collins, Colorado State University, 167 p.

Russell, L. R. and Snelson, S., 1994, Structure and tectonics of the Albuquerque Basin segment of the Rio Grande rift: Insights from seismic reflection data, *in* Keller, G. R. and Cather, S. M., eds., Basins of the Rio Grande rift: Structure, stratigraphy, and tectonic setting, Geological Society of America, Special Publication 291, p. 83–112.

Sales, J. K., 1983, Collapse of Rocky Mountain basement uplifts, *in* Lowell, J. D. and Gries, R. R., eds., Rocky Mountain foreland basins and uplifts: Denver, Rocky Mountain Association of Geologists, p. 79–97.

Salyards, S. L., Ni, J. F., and Aldrich, M. J., Jr., 1994, Variation in paleomagnetic rotations and kinematics of the north-central Rio Grande rift, New Mexico, *in* Keller, G. R. and Cather, S. M., eds., Basins of the Rio Grande rift: Structure, stratigraphy, and tectonic setting: Geological Society of America, Special Paper 291, p. 59–71.

Santos, E. S., 1975, Lithology and uranium potential of Jurassic formations in the San Ysidro-Cuba and Majors Ranch areas, northwestern New Mexico, U.S. Geological Survey, Bulletin 1329, 22 p.

Scott, G. R. and Cobban, W. A., 1963, Apache Creek Sandstone Member of the Pierre Shale of southeastern Colorado: Geological Survey, Professional Paper 475-B, p. 99–101.

Seager, W. R. and Clemons, R. E., 1975, Middle to late Tertiary geology of the Cedar Hills-Selden Hills area, Doña Ana County, New Mexico: New Mexico Bureau of Mines and Mineral Resources, Circular 133, 23 p.

Semken, S. C. and McIntosh, W. C., 1997, $^{40}Ar/^{39}Ar$ age determinations for the Carrizozo Mountains laccolith, Navajo Nation, Arizona: New Mexico Geological Society, 48th Field Conference, Guidebook, p. 75–80.

Shirley, K. and Caldwell, K. R., 1990, An oil find that was good as gold; utilizing several geophysical techniques helps: American Association of Petroleum Geologists Explorer, v. 16, p. 7–9.

Shoemaker, E. M., Pillmore, C. L., and Peacock, E. W., 1987, Remanent magnetization of rocks of latest Cretaceous and earliest Tertiary age from drill core at York Canyon, New Mexico, *in* Fassett, J. E. and Rigby, J. K., Jr., eds., The Cretaceous-Tertiary boundary in the San Juan and Raton Basins, New Mexico and Colorado: Geological Society of America, Special Paper 209, p. 131–150.

Sikkink, P. G. L., 1987, Lithofacies relationships and depositional environment of the Tertiary Ojo Alamo Sandstone and related strata, San Juan Basin, New Mexico and Colorado, *in* Fassett, J. E. and Rigby, J. K., Jr., eds., The Cretaceous-Tertiary boundary in the San Juan and Raton Basins, New Mexico and Colorado: Geological Society of America, Special Paper 209, p. 81–104.

Silver, C., 1950, The occurrence of gas in the Cretaceous rocks of the San Juan Basin, New Mexico and Colorado: New Mexico Geological Society, 1st Field Conference, Guidebook, p. 109–123.

Silver, C., 1951, Cretaceous stratigraphy of the San Juan Basin: New Mexico Geological Society, 2nd Field Conference, Guidebook, p. 104–118.

Simpson, G. G., 1935, The Tiffany fauna, upper Paleocene: American Museum Novitates, no. 795, 19 p.

Sirrine, G. K., 1956, Geology of the Springerville-St. Johns area, Apache County, Arizona [Ph.D. dissertation]: Austin, University of Texas, 248 p.

Slack, P. B. and Campbell, J. A., 1976, Structural geology of the Rio Puerco fault zone and its relationship to central New Mexico tectonics, *in* Woodward, L. A. and Northrop, S. A., eds., Tectonics and mineral resources of southwestern North America: New Mexico Geological Society, Special Publication 6, p. 46–52.

Smith, H. T. U., 1938, Tertiary geology of the Abiquiu quadrangle, New Mexico: Journal of Geology, v. 46, p. 933–965.

Smith, L. N., 1992a, Upper Cretaceous and Paleogene stratigraphy and sedimentation adjacent to the Nacimiento Uplift, southeastern San Juan Basin, New Mexico: New Mexico Geological Society, 43rd Field Conference, Guidebook, p. 251–264.

Smith, L. N., 1992b, Stratigraphy, sediment dispersal and paleogeography of the lower Eocene San Jose Formation, San Juan Basin, New Mexico and Colorado: New Mexico Geological Society, 43rd Field Conference, Guidebook, p. 297–309.

Smith, L. N. and Lucas, S. G., 1991, Stratigraphy, sedimentology, and paleontology of the lower Eocene San Jose Formation in the central portion of the San Juan Basin, northwestern New Mexico: New Mexico Bureau of Mines and Mineral Resources, Bulletin 126, 44 p.

Smith, R. L., Bailey, R. A., and Ross, C. S., 1970, Geologic map of the Jemez Mountains, New Mexico: U.S. Geological Survey, Miscellaneous Geologic Investigations Map I-571, scale 1:125,000.

Speer, W. R., 1976, Oil and gas exploration in the Raton Basin: New Mexico Geological Society, 27th Field Conference, Guidebook, p. 217–226.

Spiegel, Z., 1961, Geology of the lower Jemez River area, New Mexico, New Mexico Geological Society, 12th Field Conference, Guidebook, p. 132–138.

Spradlin, E. J., 1976, Stratigraphy of Tertiary volcanic rocks, Joyita Hills area, Socorro County, New Mexico [M.S. thesis]: Albuquerque, University of New Mexico, 73 p.

Stearns, C. E., 1943, The Galisteo Formation of north-central New Mexico: Journal of Geology, v. 51, p. 301–319.

Stearns, C. E., 1953, Upper Cretaceous rocks of the Galisteo-Tonque area, north-central New Mexico: American Association of Petroleum Geologists Bulletin, v. 37, p. 961–974.

Steven, T. A., Lipman, P. W., Hail, W. J., Jr., Barker, F., and Luedke, R. G., 1974, Geologic map of the Durango quadrangle, southwestern Colorado: U.S. Geological Survey, Miscellaneous Investigations Map I-764, scale 1:250,000.

Tavarnelli, E., 1998, Tectonic evolution of the northern Salinian block, California, USA: paleogene to recent shortening in a transform fault-bounded continental fragment, *in* Holdsworth, R. E., Strachan, R. A. and Dewey, J. F., eds., Continental transpressional and transtensional tectonics: London, Geological Society, Special Publication 135, 107–118.

Taylor, D. J. and Huffman, A. C., Jr., 1998, Map showing inferred and mapped basement faults, San Juan Basin and vicinity, New Mexico and Colorado: U.S. Geological Survey, Geologic Investigations Series I-2641, scale 1:500,000.

Teyssier, C. and Tikoff, B., 1998, Strike-slip partitioned transpression of the San Andreas fault system: a lithospheric-scale approach, *in* Holdsworth, R. E.,

Strachan, R. A., and Dewey, J. F., eds., Continental transpressional and transtensional tectonics: London, Geological Society, Special Publication 135, p. 143–158.

Tikoff, B. and Maxson, J., 2001, Lithospheric buckling of the Laramide foreland during Late Cretaceous and Paleogene, western United States: Rocky Mountain Geology, v. 36, p. 13–35.

Tonking, W. H., 1957, Geology of the Puertecito quadrangle, Socorro County, New Mexico: New Mexico Bureau of Mines and Mineral Resources, Bulletin 41, 67 p.

Tschudy, R. H., 1973, The Gasbuggy core: a palynological perspective: Four Corners Geological Society, Memoir, p. 131–143.

Tyler, R., Kaiser, W. R., Scott, A. R., Hamilton, D. S., and Ambrose, W. A., 1995, Geologic and hydrologic assessment of natural gas from coal: greater Green River, Piceance, Powder River, and Raton Basins, western United States: Texas Bureau of Economic Geology, Report of Investigations no. 228, 291 p.

Watkins, T. A., Belcher, J. S., Gries, R. R., and Longacre, M. B., 1995, "Black gold" leads to new structural interpretation, northern Sangre de Cristo Mountains, northeast San Luis Basin (abs.): American Association of Petroleum Geologists Bulletin, Rocky Mountain section meeting, v. 79, no. 6, p. 926.

Wawrzyniec, T. F., 1999, Dextral transcurrent deformation of the eastern margin of the Colorado Plateau (USA) and the mechanics of footwall uplift along the Simplon normal fault (Switzerland/Italy) [Ph.D. dissertation]: Albuquerque, University of New Mexico, 249 p.

Weber, R. H., 1964, Geology of the Carrizozo quadrangle, New Mexico: New Mexico Geological Society, 15th Field Conference, Guidebook, p. 100–109.

Wilcox, R. E., Harding, T. P., and Seely, D. R., 1973, Basic wrench tectonics: American Association of Petroleum Geologists Bulletin, v. 57, p. 74–96.

Williamson, T. E., 1996, The beginning of the age of mammals in the San Juan Basin, New Mexico: Biostratigraphy and evolution of Paleocene mammals of the Nacimiento Formation: Albuquerque, New Mexico Museum of Natural History and Science, Bulletin 8, 141 p.

Williamson, T. E. and Lucas, S. G., 1992, Stratigraphy and mammalian biostratigraphy of the Paleocene Nacimiento Formation, southern San Juan Basin, New Mexico: New Mexico Geological Society, 43rd Field Conference, Guidebook, p. 265–296.

Wilpolt, R. H., MacAlpin, A. J., Bates, R. L., and Vorbe, G., 1946, Geologic map and stratigraphic sections of Paleozoic rocks of Joyita Hills, Los Pinos Mountains, and northern Chupadera Mesa, Valencia, Torrance, and Socorro Counties, New Mexico: U.S. Geological Survey, Oil and Gas Investigations, Preliminary Map 61.

Wiltschko, D. V. and Dorr, J. A., Jr., 1983, Timing of deformation in overthrust belt and foreland of Idaho, Wyoming, and Utah: American Association of Petroleum Geologists Bulletin, v. 67, p. 1304–1322.

Woodburne, M. O. and Swisher, C. C., III, 1995, Land mammal high-resolution geochronology, intercontinental overland dispersals, sea levels, climate, and vicariance: Society of Economic Paleontologists and Mineralogists, Special Paper 54, p. 335–364.

Woodward, L. A., 1974, Tectonics of central-northern New Mexico: New Mexico Geological Society, 25th Field Conference, Guidebook, p. 123–129.

Woodward, L. A., 1976, Laramide deformation of the Rocky Mountain foreland: Geometry and mechanics: New Mexico Geological Society, Special Publication 6, p. 11–17.

Woodward, L. A., 1984, Potential for significant oil and gas fracture reservoirs in Cretaceous rocks of Raton Basin, New Mexico: American Association of Petroleum Geologists Bulletin, v. 68, p. 628–636.

Woodward, L. A., 1987, Geology and mineral resources of Sierra Nacimiento and vicinity, New Mexico: New Mexico Bureau of Mines and Mineral Resources, Memoir 42, 84 p.

Woodward, L. A., 1996, Paleotectonics of the late Paleozoic Peñasco Uplift, Nacimiento region, northern New Mexico: New Mexico Geological Society, 47th Field Conference, Guidebook, p. 107–113.

Woodward, L. A., 2000, Implications of Jurassic, Cretaceous, and Proterozoic piercing lines for Laramide oblique-slip faulting in New Mexico and rotation of the Colorado Plateau; discussion and reply: Geological Society of America Bulletin, v. 112, p. 783–788.

Woodward, L. A. and Callender, J. F., 1977, Tectonic framework of San Juan Basin: New Mexico Geological Society, 28th Field Conference, Guidebook, p. 209–212.

Woodward, L. A., Anderson, O. J., and Lucas, S. G., 1997a, Mesozoic stratigraphic constraints on Laramide right slip on the east side of the Colorado Plateau: Geology, v. 25, p. 843–846.

Woodward, L. A., Anderson, O. J., and Lucas, S. G., 1997b, Tectonics of the Four Corners region of the Colorado Plateau: New Mexico Geological Society, 48th Field Conference, Guidebook, p. 57–64.

Woodward, L. A., Anderson, O. J., and Lucas, S. G., 1999, Late Paleozoic right-slip faults in the ancestral Rocky Mountains: New Mexico Geological Society, 50th Field Conference, Guidebook, p. 149–154.

Woodward, L. A., Hultgren, M. C., Crouse, D. L., and Merrick, M. A., 1992, Geometry of the Nacimiento-Gallina fault system, northern New Mexico: New Mexico Geological Society, 43rd Field Conference, Guidebook, p. 103–108.

Wright, H. E., 1956, Origin of the Chuska Sandstone, Arizona-New Mexico: A structural and petrographic study of a Tertiary eolian sediment: Geological Society of America Bulletin, v. 67, p. 413–434.

Yin, A. and Ingersoll, R. V., 1997, A model for evolution of Laramide axial basins in the southern Rocky Mountains, USA: International Geology Review, v. 39, p. 1113–1123.